

April 2014

Optical Emission Study of a Pulsed Plasma Thruster

Justin Ryan White

Worcester Polytechnic Institute

Luis Alexander Gonzalez

Worcester Polytechnic Institute

Narimane Khaled

Worcester Polytechnic Institute

Timothy Peter Theriot

Worcester Polytechnic Institute

Follow this and additional works at: <https://digitalcommons.wpi.edu/mqp-all>

Repository Citation

White, J. R., Gonzalez, L. A., Khaled, N., & Theriot, T. P. (2014). *Optical Emission Study of a Pulsed Plasma Thruster*. Retrieved from <https://digitalcommons.wpi.edu/mqp-all/89>

This Unrestricted is brought to you for free and open access by the Major Qualifying Projects at Digital WPI. It has been accepted for inclusion in Major Qualifying Projects (All Years) by an authorized administrator of Digital WPI. For more information, please contact digitalwpi@wpi.edu.


Optical Emission Study of a Pulsed Plasma Thruster

A Major Qualifying Project Report
Submitted to the Faculty of the
WORCESTER POLYTECHNIC INSTITUTE
in Partial Fulfillment of the Requirements for the
Degree of Bachelor of Science
in Aerospace Engineering

by



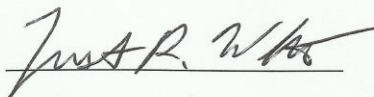
Luis Gonzalez



Narimane Khaled




Peter Theriot



Justin White

April 25, 2014

Approved by:



Professor John J. Blandino, Advisor
Aerospace Engineering Program
Mechanical Engineering Department, WPI

ABSTRACT

A Pulsed Plasma Thruster (PPT) is a type of electric propulsion considered for use on spacecraft flying in formation. The use of a PPT near other spacecraft requires characterization of the light emission when fired. This project's goal was to measure the emission spectra from an Aerojet Corp. laboratory model PPT. Prior to testing, gas leaks in the used vacuum chamber were located and repaired. A PPT mount and plume baffle were also designed and fabricated to support the PPT and protect the chamber walls from exhaust plume carbon deposition. Moreover, custom cabling for both command and telemetry were assembled, tested and installed in the vacuum chamber. Finally, a LabVIEW program was designed, tested, and incorporated in the test setup to allow computer controlled, automated operation.

"Certain materials are included under the fair use exemption of the U.S. Copyright Law and have been prepared according to the fair use guidelines and are restricted from further use."

Table of Contents

ABSTRACT	i
LIST OF FIGURES	iv
LIST OF TABLES	vi
ACKNOWLEDGEMENTS	vii
TABLE OF AUTHORSHIP	viii
EXECUTIVE SUMMARY	ix
CHAPTER 1. INTRODUCTION	1
CHAPTER 2. BACKGROUND	4
2.1 Pulsed Plasma Thrusters (PPT)	4
2.1.1 Principles of Operation.....	4
2.1.2 Aerojet Corp. Modular Test Unit (MTU).....	7
2.1.3 PPT Mission Application.....	13
2.1.4 PPT Contamination.....	18
2.1.5 Toxicity Reports and Precautions.....	28
2.2 Vacuum System Technology	29
2.2.1 Vacuum Pumps.....	29
2.2.2 Vacuum Measurement.....	34
2.2.3 WPI Vacuum Test Facility (VTF) Tank 4 (T4).....	35
2.3 Optical Spectroscopy	38
2.3.1 Theory.....	38
2.3.2 Ocean Optics High Resolution Spectrometer HR4000	39
CHAPTER 3. METHODOLOGY	42
3.1 Vacuum Chamber Leak Detection and Recommissioning	42
3.2 PPT Mount and Plume Baffle Design and Construction	51
3.3 MTU Integration	54
3.4 Spectrometer Integration and Data Acquisition	59
3.5 LabVIEW Integration and Implementation	60
CHAPTER 4. EXPERIMENTAL RESULTS AND DISCUSSION	69
4.1 Test Plan	69
4.2 Sensitivity of Spectra to Pulse Energy and Repetition Rate	72

4.3 Discussion of Results	72
CHAPTER 5. CONCLUSIONS AND RECOMMENDATIONS	83
5.1 Conclusions	83
5.2 Recommendations for Future Work	87
REFERENCES	89
APPENDICES	93
A.1 T4 System Modified Pump Down and Back Venting Procedure	93
A.2 T4 Leak Detection Procedure and Data Sheet	96
A.3 MTU Operational and Safety Procedures	100
A.4 CAD Drawing of PPT Mount and Plume Baffle	116
A.5 LabVIEW VI Instructions to Control PPT Pulse Energy and Repetition Rate	117
A.6 Wiring Diagram for the LabVIEW VI	119

LIST OF FIGURES

Figure 1: Ablative Teflon Pulsed Plasma Thruster Schematic ^[1] . Copyright 2000 AIAA.....	1
Figure 2: Electric Propulsion Systems	4
Figure 3: Ablative Pulsed Plasma Thruster ^[4] . Copyright 2010 Acta Astronautica.	5
Figure 4: PPT Thrust Generation Flow ^[5]	6
Figure 5: Front of the MTU	8
Figure 6: Left and Right Sides of the MTU (left and right images respectively).....	9
Figure 7: Back of MTU (left), Bottom Access Panel (middle) and Inner Electronics (right)	10
Figure 8: Faraday Cage with Brackets.....	10
Figure 9: MTU Interface Box (left) with Power Input Connectors (right).....	11
Figure 10: Power Supply (left) and Contactor Box (middle) with Power Input (right)	12
Figure 11: Capacitor, Teflon Wafers, Used Fuel Bar, and Spare Spark Plug.....	13
Figure 12: Fourth Lincoln Experimental Satellite (LES4) ^[8] . Copyright 1996 Gunter's Space Page.....	14
Figure 13: Engineering Test Satellite (ETS-IV) ^[9] . Copyright 1996 Gunter's Space Page.	15
Figure 14: EO-1 Pulsed Plasma Thruster ^[10] . Copyright 2001 NASA Mission Technology Forum.....	16
Figure 15: A Deployed CubeSat ^[12] . Copyright 2002 Amateur Funk.....	17
Figure 16: Envisioned PPT Technology Development at NASA ^[10] . Copyright 2001 NASA Mission Technology Forum.....	17
Figure 17: Simple Deposition Model Plume Geometry ^[14] . Copyright 1997 AIAA.....	20
Figure 18: Example collimator with Quartz Sample (far left) ^[16] . Copyright 2000 AIAA.	22
Figure 19: Orthogonal (left) and Parallel (right) Planes ^[16] . Copyright 2000 AIAA.	23
Figure 20: Orthogonal Plane Transmittance ^[16] . Copyright 2000 AIAA.	26
Figure 21: Orthogonal (top) and Parallel (bottom) Reflectance ^[16] . Copyright 2000 AIAA.	27
Figure 22: Mechanical Pump ^[2] . Copyright 2011 Sebastian Ryan.....	30
Figure 23: Diagram of Mechanical Pump ^[21] . Copyright 2001 Ideal Vacuum Products.	30
Figure 24: Pumping Speed vs. Pressure of Mechanical Pump ^[21] . Copyright 2001 Ideal Vacuum Products.....	31
Figure 25: Turbomolecular Pump ^[2] . Copyright 2011 Sebastian Ryan.....	32
Figure 26: Turbine of a Turbomolecular Pump ^[22] . Copyright 2009 Cambridge University Press.....	32
Figure 27: Turbotronik Controller ^[2] . Copyright 2011 Sebastian Ryan.....	33
Figure 28: Physical Electronics 640 I/s Ion Pump.....	33
Figure 29: Schematic of T4 Vacuum System ^[2] . Copyright 2011 Sebastian Ryan.	34
Figure 30: T4 Internal Dimensions ^[2] . Copyright 2011 Sebastian Ryan.....	36
Figure 31: T4's Collar and Hoist Assembly	36
Figure 32: PPT Emission as a Function of Discharge Energy and Time ^[20] . Copyright 1997 AIAA.....	39
Figure 33: HR4000 Spectrometer with Components ^[26] . Copyright 2008 Ocean Optics.	40

Figure 34: Cleaning and Greasing T4's Collar and O-ring.....	43
Figure 35: Aluminum Metal Seal with T4's Port #4 Electrical Feedthrough.....	44
Figure 36: CombiVac Displaying Chamber Pressure of 90 mTorr (11/08/2013 @ 10:40 AM) ..	44
Figure 37: Turbopump Valve with Components from Nor-Cal	46
Figure 38: 572 Ion Gauge (left) and BA2 Front Panel with Ion Gauge Pressure Display (right)	47
Figure 39: Determining Starting Pressure for TurboVac 361 Graph ^[28] . Copyright 2006 Leybold Vacuum.....	50
Figure 40: Connection between the Crossbars and the Legs	51
Figure 41: PPT Mount	52
Figure 42: PPT Mount with the MTU.....	52
Figure 43: Plume Baffle around the MTU	53
Figure 44: T4's 15-Pin Double Sided Sub-D Feedthrough, outside (left) and inside (right)	54
Figure 45: Sub-D Connection between the Interface Box and T4's Feedthrough	57
Figure 46: T4's Single Ended, Grounded Shield Coaxial Feedthrough, outside (left) and inside (right)	57
Figure 47: Screenshot of SpectraSuite Software User Interface.....	59
Figure 48: LabVIEW VI Front Panel.....	62
Figure 49: MTU Interface Box	63
Figure 50: Test of VI with Oscilloscope, single pulse (above) and pulse train (below).....	66
Figure 51: LabVIEW Flowchart	68
Figure 52: Block Diagram of the Experimental Setup.....	69
Figure 53: Single-Shot MTU Emission Light.....	71
Figure 54: LabVIEW VI Results	73
Figure 55: Spectra from Test 1	75
Figure 56: Spectra from Test 2.1	76
Figure 57: Spectra from Test 2.2	77
Figure 58: Spectra from Test 3.1	78
Figure 59: Spectra from Test 3.2	79

LIST OF TABLES

Table 1: Mass Deposited on Combiner and Film Thickness ^[14]. Copyright 1997 AIAA. 21

Table 2: Ion Present in the PPT Plumes and their Contamination Risk ^{[16] [19] [20]} 28

Table 3: Description of T4's Collar Ports 37

Table 4: HR4000 Components ^[26]. Copyright 2008 Ocean Optics. 40

Table 5: ROR Measurements after the Initial Leak Fix (11/7/13-11/11/13) 45

Table 6: Post Turbopump Recommissioning ROR Measurements (initial pressure = atmosphere)
..... 47

Table 7: T4's 15-Pin Double Sided Sub-D Feedthrough Pin Assignments..... 54

Table 8: 15 to 25 Sub-D Connection Pin Assignments. 55

Table 9: Assignment List of DAQ Pins to Interface Box BNC Connections 58

Table 10: 50% Duty Cycle..... 64

Table 11: Variable Duty Cycle 64

Table 12: Test Conditions and SpectraSuite Settings 74

Table 13: A Full timeline of the Pulse Cycle..... 79

Table 14: Plume Species Identified by Spectral Peak ^[20] 81

ACKNOWLEDGEMENTS

The team would like to first thank Aerojet Corp. for providing a laboratory model PPT, and NASA for loaning WPI the vacuum testing chamber, T4. The team would also like to thank David Andrew Ephraim, the Washburn Laboratory Manager, for assisting with the construction and machining of project related tasks; as well as Barbara Furhman, the Mechanical Engineering Administrative Assistant, for maintaining project purchase orders and budget, and Adriana Hera, the Academic Computing Applications Scientist, for assisting with LabVIEW VI troubleshooting. In addition, the team appreciates Zachary R. Taillefer for providing first hand insights on problems faced throughout the project. Zachary is a PhD candidate and lab manager for WPI's Fluids Labs including HL016, and his experience and knowledge helped accelerate project milestones. Most importantly, the team thanks Professor John J. Blandino, the project advisor, for all the support and guidance he provided. He helped the team manage the project and overcome obstacles.

TABLE OF AUTHORSHIP

Section	Author
<i>ABSTRACT</i>	LG, NK, PT, JW
<i>ACKNOWLEDGEMENT</i>	NK, JW
<i>EXECUTIVE SUMMARY</i>	NK
<i>INTRODUCTION</i>	LG, NK, PT, JW
<i>BACKGROUND</i>	
2.1.1, 2.1.3	NK
2.1.2, 2.1.4	JW
2.1.5, 2.2.1, 2.2.2, 2.2.3	PT
2.3.1, 2.3.2	LG
<i>METHODOLOGY</i>	
3.1	JW
3.2, 3.3	NK
3.4	PT
3.5	LG
<i>EXPERIMENTAL RESULTS AND DISCUSSION</i>	
4.1	JW
4.2	PT
4.3	LG, PT
<i>CONCLUSIONS AND RECOMMENDATIONS</i>	
5.1	JW
5.2	NK, JW
<i>APPENDICES</i>	
A.1	JW
A.2	JW
A.3	NK
A.4	NK
A.5	LG
A.6	LG

EXECUTIVE SUMMARY

The goal of this project was to investigate the optical emission spectra of a Teflon-fueled, ablative pulse plasma thruster (PPT) operating under vacuum. An Aerojet Corp. breadboard modular testing unit (MTU) and WPI's T4 vacuum tank were used in this project. Windows on the outside of the T4 provided proper viewing angles for the optical spectroscopic measurements when combined with a correctly integrated PPT mount to elevate the MTU. Measurements of optical emission were made with an Ocean Optics HR4000 High Resolution Spectrometer, and a LabVIEW VI was used to control the pulse rate and test duration of the MTU.

Previous work conducted as part of a “directed research” study at WPI described the details and operational procedure of the T4 facility, including the identification of a leak in the system ^[2]. This leak had to be fixed before any testing could occur, because the investigation of optical emission spectra requires a vacuum tank facility capable of pumping to moderately high vacuum ($< 10^{-4}$ Torr). The team developed a Rate-of-Rise (ROR) time measurement procedure, complete with data sheet, for the T4 vacuum chamber leak detection and recommissioning process. The Rate-of-Rise is an effective metric for characterizing vacuum system technology performance. The ROR evaluation led to the discovery of the first major leak source, which was fixed by replacing aluminum metal seals with elastomer seals in the T4 collar ports. A second milestone was the discovery of an uncovered valve port on the turbopump, which required a simple component order from Norcal. Ultimately the T4 vacuum system was recommissioned to a usable state for experimentation. The pump-down procedure, modified from the original version provided in the directed research report, was revised several times before it was complete enough for T4 operations to proceed. This required contacting a representative at Leybold for clarification on what pressures were required before the turbopump could be turned on.

In order to provide a proper viewing angle for the optical spectroscopy, the MTU was elevated. The team designed a PPT mount and plume baffle using 1 inch x-channel and related x-channel fasteners and components. Before the PPT mount and plume baffle were constructed, they were modeled in SolidWorks. With the help of the Washburn Shops` staff, the team was able to manufacture the needed components.

The integration of the MTU with the T4 vacuum system and the Interface Box required substantive construction and assembly of wire bundles, components and custom connections. The team soldered and ordered necessary components from vendors. Then, the team had to complete the checkout and set-up of these connections as part of various procedures in order to verify total system integration. The team developed a modified safety and operational procedure for the MTU, which is based on the original documentation provided by Aerojet Corp. The MTU procedure was the only procedure that all of the group members were expected to be familiar with due to the high voltage and current present when operating the MTU. The initial checkout and set-up procedures were performed with the project advisor, laboratory manager, and some of the team members. In contrast, the single-shot firing of the MTU was performed with all of the MQP team members as well as the project advisor and lab manager.

Autonomous operation to continuously fire the MTU inside T4 was performed using the LabVIEW VI developed for this purpose. This operation required careful design of the VI, and troubleshooting of problems that occurred through the initial checkout and set-up operations. The VI successfully controlled single-shot and autonomous operation of the MTU. The LabVIEW VI also presented the team with a few minor challenges. Also, the SpectraSuite software was installed to use with the Ocean Optics HR4000 High Resolution Spectrometer in order to analyze the data from the MTU. The spectral response of the MTU plume was analyzed effectively using

this software.

CHAPTER 1. INTRODUCTION

Pulsed Plasma Thrusters (PPTs) are one type of electric spacecraft propulsion where a pulse of ionized gas is accelerated electromagnetically to high velocity to provide thrust. There are many types of PPTs in use, but ablative Teflon PPTs are the most common. These type of PPTs use Teflon as a propellant stored as a solid in either a rectangular or cylindrical bar. Figure 1 shows a schematic of an ablative Teflon PPT.

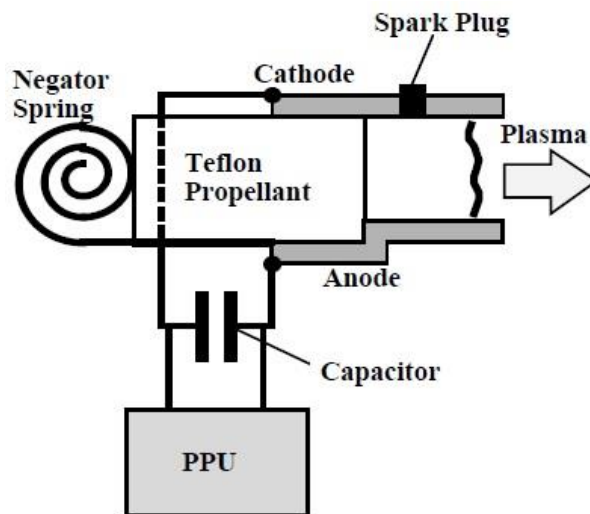


Figure 1: Ablative Teflon Pulsed Plasma Thruster Schematic ^[1]. Copyright 2000 AIAA.

Potential applications of PPTs include deep space exploration, long duration interplanetary missions and close formation flight of multiple spacecraft. Benefits of PPTs are: low thrust, high specific impulse, high propellant mass fraction and correspondingly low propellant structural mass fraction, simple system integration and the elimination of safety and layout complexities associated with fluid propellant propulsion systems. One challenge associated with PPTs is the contamination of spacecraft surfaces due to Teflon ablation. These contamination effects are a result of particulate ejection impinging on and condensation of

Teflon vapor onto spacecraft surfaces. In addition, the close proximity to other spacecraft in formation flight situations brings up the need to investigate whether or not the emitted radiation causes damage to optical sensors ^[1].

This project investigated the optical emission spectra of a rectangular Teflon PPT operating under vacuum. A breadboard modular testing unit (MTU) was provided by Aerojet Corp. and was used for testing. The Aerojet breadboard PPT came with a two page general operating procedure, which means reverse engineering was required to develop documentation and operational procedures related to the electronics circuit and overall capabilities of the system. The investigation of optical emission spectra requires a vacuum tank facility capable of pumping to moderately high vacuum ($< 10^{-4}$ Torr), and the use of optical spectroscopy to characterize the optical radiation being emitted by the MTU under these conditions.

The WPI T4 vacuum tank, which is large enough to house the MTU, was available for use in this project, and is capable of pumping down to the 10^{-4} to 10^{-6} Torr range required for testing. Windows on the outside of T4 also provide proper viewing angles for optical spectroscopic probes when combined with a correctly integrated PPT mount to elevate the MTU. Previous work conducted by a directed research study at WPI describes the details and operational procedure of the T4 facility, including the identification of a leak in the system which must be fixed before any testing can occur ^[2]. A PPT mount and plume baffle had to be designed for integration of the MTU into the T4 vacuum system. This required a modular design which could be adapted for use in T4. In parallel with the design and integration of the MTU mount and baffle, a LabVIEW VI was also required in order to control the energy per pulse and pulse rate of the MTU. Measurements of optical emission were made with an Ocean Optics HR4000 High Resolution Spectrometer.

The results of the optical emission study may lead to future design of optical filters which can be applied to optical sensors for use in formation flight situations such as interferometry arrays. This would make the integration of PPT thrusters into these systems less complex by allowing them to be placed in the most convenient location on the spacecraft, regardless of proximity to optical sensors. In turn the cost of such systems may be driven down with simpler integration of PPT thrusters, but driven up by the optical filter, which may need to be optimized for certain wavelengths depending on energy level and firing rate of the main charging capacitor system.

CHAPTER 2. BACKGROUND

2.1 Pulsed Plasma Thrusters (PPT)

2.1.1 Principles of Operation

Electric Propulsion (EP) systems are categorized by the acceleration method used to produce thrust. There are three types of EP devices: electrothermal, electrostatic, and electromagnetic. Electrothermal thrusters use electrical power to heat a propellant that then expands through a nozzle producing thrust, while electrostatic thrusters use high voltage electrodes to accelerate ions with electrostatic forces. The last category of EP device is electromagnetic, where ionized gases are accelerated using both electric and magnetic fields ^[3].

In this project, the specific type of electromagnetic propulsion device being used is a PPT. PPTs are considered the simplest form of electric spacecraft propulsion, and there are two types: Ablative and Gas-Fed. Both types operate similarly, and only differ in the kind of propellant used. Due to its low rate of outgassing, Ablative PPTs use a solid propellant, typically Polytetrafluoroethylene (PTFE) also known by its commercial name, Teflon; while Gas-Fed PPTs use a gaseous propellant, usually xenon. The diagram in Figure 2 shows how the different types of PPT relate to the different types of EP devices ^[3].

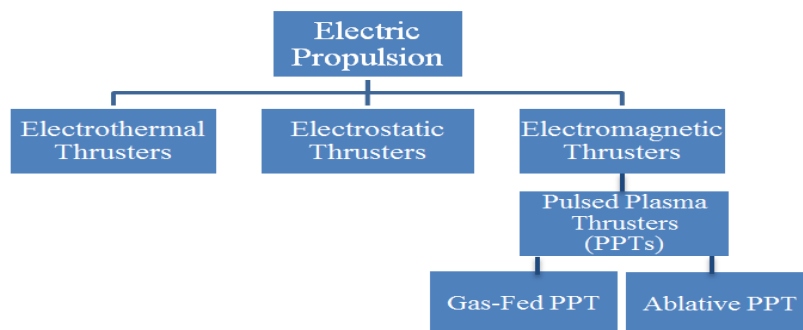


Figure 2: Electric Propulsion Systems

Ablative PPTs have different electrode geometry, and the particular PPT studied in this project is rectangular. As Figure 3 shows, the PPT consists of a capacitor bank connected to two parallel plate electrodes, one of which (cathode) has a spark plug imbedded in its base. A solid propellant Teflon bar is spring fed between the two electrodes ^[4].

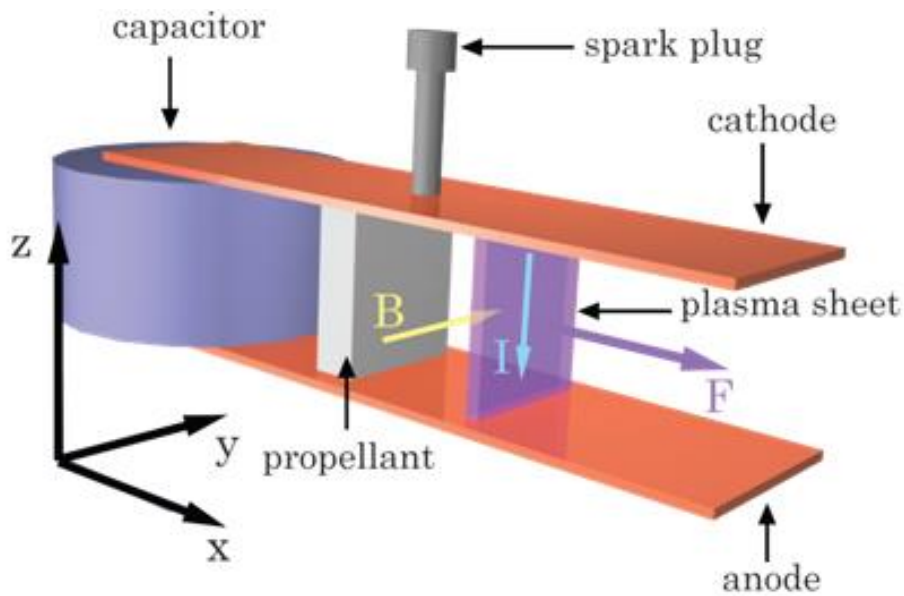


Figure 3: Ablative Pulsed Plasma Thruster ^[4]. Copyright 2010 Acta Astronautica.

In an Ablative PPT, thrust is achieved through three stages: ablation, ionization, and then acceleration of the Teflon propellant vapor electromagnetically. Before operation the capacitor is charged to a desired level of energy. The spark plug is fired and releases a discharge of electrons between the two electrodes. The electrons from this initial discharge in turn provide a current path allowing the primary, high energy discharge to be initiated. This primary discharge ablates and ionizes a small amount (<100 micrograms) of the Teflon solid bar to a state of plasma (ions, electrons, and neutrals). The discharge current flowing between the two electrodes self-induces a magnetic field, which results in a strong Lorentz force ($\mathbf{F} = \mathbf{J} \times \mathbf{B}$) orthogonal to the current vector. The Lorentz force is exerted on the plasma and thus accelerates the plasma sheet out of

the two electrodes exhaust at a high velocity creating thrust. Any neutrals produced from the non-ionized Teflon during ablation are accelerated by gas dynamic expansion [4]. Figure 4 below shows a summary of how thrust is produced in PPTs.

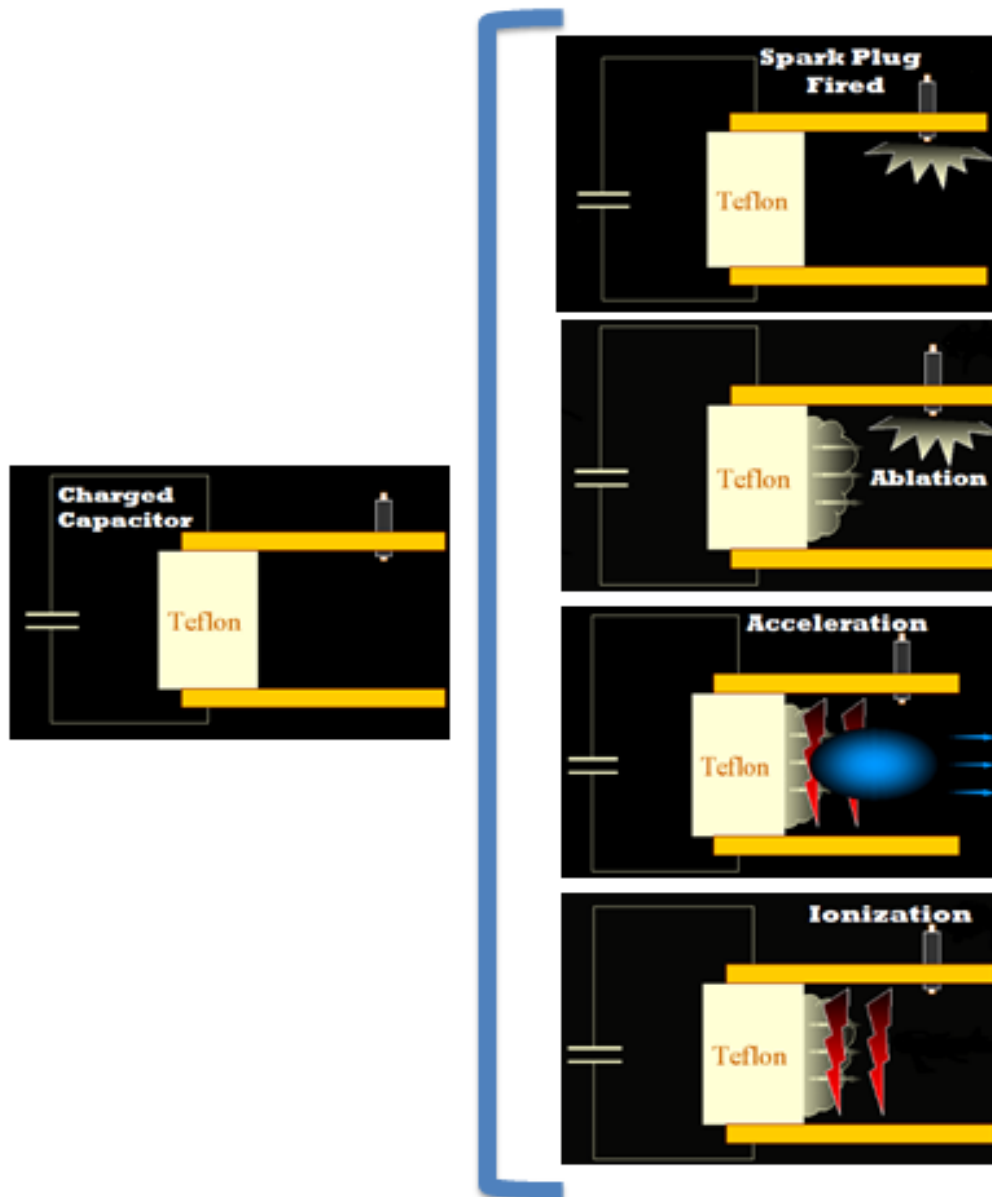


Figure 4: PPT Thrust Generation Flow [5]

The propulsive force is obtained by ejecting the propellant gases at high velocity, and can be directly related to total impulse through $I_t = F * t$ where t is burning time and F is thrust

force. Total impulse is proportional to the total energy released by all of the propellant in a propulsion system ^[6].

An important performance measure in rocket propulsion is the efficiency with which the propulsion system produces a directed impulse. This efficiency is measured in terms of how much propellant is required to generate a certain impulse, or impulse generated per unit weight of propellant. This efficiency is known as “specific impulse,” $I_s = \frac{F}{\dot{m} * g_0} = \frac{F}{\dot{w}}$. Specific Impulse is directly proportional to the propulsive force \mathbf{F} , and inversely proportional to \dot{m} , the total mass flow rate of propellant, and to g_0 , the standard acceleration of gravity at sea level. The product $\dot{m} * g_0$ is the weight flow \dot{w} , so the units of specific impulse in SI units is seconds. The higher I_s value a rocket propulsion device has, the greater the momentum (or velocity change) it will be able to achieve with a given amount of propellant ^[6].

PPTs operate ^[6] by accelerating an ionized gas through electromagnetic forces; thus, they are unable to generate higher thrust at higher power. They can, in principle, attain high specific impulses of 1000s and up.

2.1.2 Aerojet Corp. Modular Test Unit (MTU)

Modular Testing Unit (MTU)

The PPT used in this project is a Modular Testing Unit (MTU) designed by Aerojet Corp. for observing relevant parameters of the ablative PPT propulsion system used in NASA’s Earth Observing 1 (EO-1) mission. The MTU is a breadboard device and is used for prototyping PPT technology and capabilities. Examples of parameters related to contamination are transmittance, reflectance, film composition and film thickness; while physical parameters include thrust, mass per pulse, pulse frequency and pulse energy. The MTU is designed for integration into a 28 volt

system, which is typical of today's satellite systems. It was last tested by an unknown customer of Aerojet Corp. Andrew Hoskins is the Aerojet liaison for this project.

The front side of the MTU is shown in Figure 5 below. Its external connections include a ground and H.V. output. A braided H.V. shield covers the H.V. wires which connect the capacitor to the H.V. output. The capacitor access is also located on this face of the device where the large braided cable joins the circular cover. Standard banana jacks are used for both external connections. The active "thruster head" (i.e. an assembly which includes a fuel bar, spark plug igniter, and electrodes) is located towards the left side and is equipped with a backflow baffle for contamination protection. The MTU was designed to accommodate up to three, independently controllable thruster heads, although only one is installed. The cathode is located on the inner left side of the backflow baffle near the spark plug used to initiate the discharge. The smaller braided H.V. cable is connected to the spark plug, and has a BNC output which connects to the pulse controller interface on the left side of the MTU.



Figure 5: Front of the MTU

There are three BNC connectors on the left side of the MTU as shown in Figure 6, which are used for discharge initiation. DI-1 is labeled “good”, DI-2 “weak”, and DI-3 “bouncy”. It is still unclear why these connections were labeled this way.

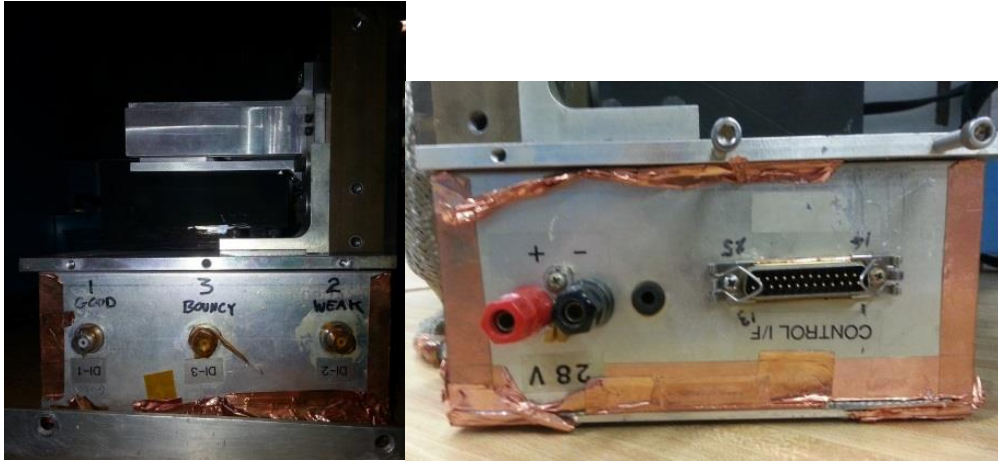


Figure 6: Left and Right Sides of the MTU (left and right images respectively)

The right side of the MTU is shown in Figure 6. There is a 25-pin Sub-D male connector which interfaces with the Interface Box. It also has a 28 volt power input, which uses banana jack connections similar to those found on the back side of the MTU.

The underside of the MTU is shown in Figure 7, and it is the main access panel for reaching the MTU’s electronics, also shown on the right of Figure 7. The back of the MTU shown in Figure 7 has a constant force spring to push the Teflon fuel bar up to the electrode plane, two radiator “fins” for heat removal in vacuum and a central cylindrical enclosure for the main capacitor.



Figure 7: Back of MTU (left), Bottom Access Panel (middle) and Inner Electronics (right)

Faraday Cage

A faraday cage with brackets was included with the MTU assembly as shown in Figure 8 below. It is believed that this cage is used for electromagnetic shielding as well as personnel safety. The large electromagnetic fields generated by the capacitor bank are powerful enough to damage nearby electronics so blocking this electromagnetic radiation is essential. It goes on over the back side of the unit over the capacitor if the radiators have been removed. The cage has a slot cut out which allows the Teflon fuel bar to extend through the cage if necessary. The cage connects to brackets which are connected to the MTU along the top and sides of the unit.

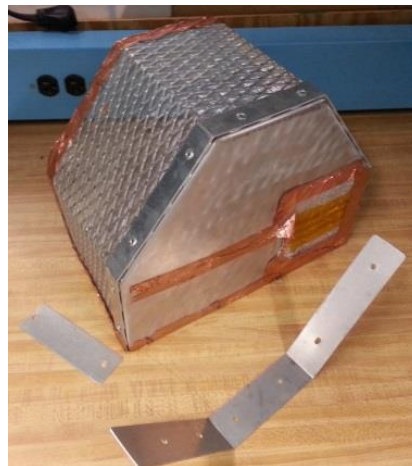


Figure 8: Faraday Cage with Brackets

MTU Interface Box

The Interface Box, shown in Figure 9, controls the charging level of the main capacitor through the use of a 5 V square wave and a manually set, 4-bit resolution control (using four toggle switches). The command to charge and fire the discharge initiator (spark plug) circuit is also provided by an externally supplied, 5 V square wave. When connected to a signal generator, it can also control the pulsing frequency. The Interface Box also provides telemetry on the capacitor and spark plug charge level. Finally, the user can select whether the charging of the spark plug (capacitor) and main capacitor will be controlled independently. The Interface Box utilizes a 25-pin female Sub-D which interfaces with the right side of the MTU. It also requires 5 VDC for input power.



Figure 9: MTU Interface Box (left) with Power Input Connectors (right)

The BIT section of the MTU Interface Box utilizes a 4 bit string, 0000 to 1111, in order to quantize 16 discrete energy levels, including zero, for the main charging capacitor. The TLM telemetry section provides voltage outputs that allow the user to observe how charged the main capacitor and discharge initiation (DI) capacitor are during operation. For example, CHG CAP will output 5 volts when the main capacitor is fully charged (approximately 2 kV), and 0 volts when discharged. “DI VOLT” performs the same function for the discharge initiator spark plug (approximately 0.8 kV when fully charged). The CMD command section controls which

discharge initiator is being used, and relates to the BNC connections for the pre ignition electrode on the left side of the MTU. There is also a switch on the box that allows the user to go from coupled discharge initiator and capacitor commands, to independent commands.

Power Supply and Contactor Box

The power supply and contactor box are pictured below in Figure 10. The power supply, MW 122A, uses direct current (2 A max) and a variable voltage controller. The voltage ranges from 3.5-9.0 volts in 1.5 volt increments, and from 9.0-12.0 in a single increment. Standard banana jacks are used for output interface and the power supply connects to a standard 120 volt wall outlet. The contactor box requires a 28 VDC input power. There are also “in” and “out” female banana jacks on top of the contactor. The contactor came with a male-to-male banana jumper connecting the “in” and “out” jacks. This jumper is equipped with five unknown electronic components under shrink wrap which are of unknown purpose. There is also a “hold” switch on the front cover. The purpose of the contactor box is believed to be related to providing one with the ability to manually fire the capacitor (without the Interface Box) during initial set up and testing.



Figure 10: Power Supply (left) and Contactor Box (middle) with Power Input (right)

Additional MTU Assembly Items

Additional items included with the MTU (when delivered from Aerojet) are a large capacitor (believed to be a spare), two Teflon wafers, an extra Teflon fuel bar piece, and a spare spark plug. All of these items are shown below in Figure 11.



Figure 11: Capacitor, Teflon Wafers, Used Fuel Bar, and Spare Spark Plug

The capacitor is manufactured by Maxwell Components Division of Maxwell Laboratories, Inc. The rated cap is $30.0 + 15.0, -5\%$ micro farad, with a rated voltage of 2.0 kV and a measured capacitance of 33.3 micro farads. The two Teflon wafers are about the same size and measures 1.5 by 1.0 by $3/32$ inches. A label on one of the wafers says 5.19838 grams, but this mass has not been confirmed. The leftover Teflon fuel chunk is about $21/36$ of an inch thick at the 4 corners and roughly $3/8$ of an inch at the center, and has a characteristic curve to it as a result of past ablation. The spare spark plug is about 1.5 in long with an outer diameter of about half an inch.

2.1.3 PPT Mission Application

Research on PPTs started in the early 1960's in the Soviet Union. On November 30, 1964, six PPTs were flown on the Soviet Zond-2 satellite in order to provide positioning for its solar arrays. During the same year in the United States, NASA's Lewis Research Center (Now

NASA Glenn) developed a Space Electric Rocket Test, SERT-1, which was a probe used to test the design of an electrostatic ion thruster. On September 26, 1968, MIT Lincoln Laboratory launched their first Lincoln Experimental Satellite (LES1) using a PPT. LES was a series of satellites (LES1-LES9) designed and tested by MIT. LES4 can be seen in Figure 12. MIT faced many launching issues throughout the duration of the series. The last LES experimental satellite was launched on March 14, 1978 ^[7].

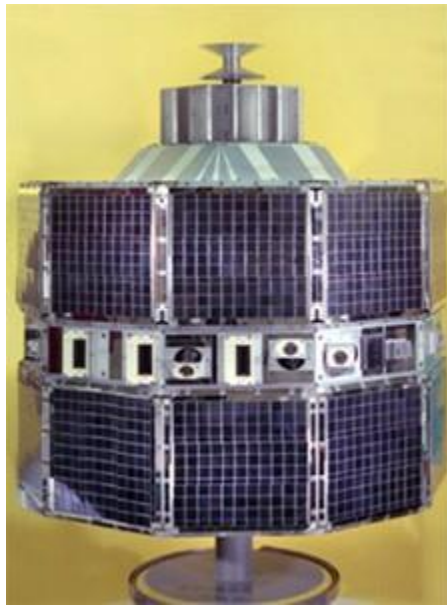


Figure 12: Fourth Lincoln Experimental Satellite (LES4) ^[8]. Copyright 1996 Gunter's Space Page.

In 1975, the United States Navy started using PPTs on their Navy Navigation Satellite System (NAVSAT). The system was primarily used to test the ability of the satellite to provide its correct location for a certain period of time without update from the ground. NAVSAT demonstrated the benefits of using PPTs once designed properly. Research on PPTs continued in different locations around the world into the late 1970's ^[7].

PPTs were used by the National Space Development Agency of Japan in 1981. They were flown on the fourth Engineering Test Satellite (ETS-IV) mission in order to provide attitude control and better performance due to its high specific impulse. ETS-IV can be seen in Figure 13. After the ETS-IV mission, spacecraft propulsion research involved large satellites, which require high power. Thus, the use of PPTs came to a stop as they provide low-power^[7].



Figure 13: Engineering Test Satellite (ETS-IV)^[9]. Copyright 1996 Gunter's Space Page.

PPTs were finally being used again when NASA's Earth Observing 1 (EO-1) mission launched on November 21, 2000. EO-1 used an Ablative PPT shown in Figure 14, which operates similarly to the PPT used in this project. The main technological advances in the EO-1 PPT were the low mass electronics, low cost, and simple structure. The purpose of this mission was to test the PPT's precision attitude control capability, where PPTs would replace the function of one of the pitch wheel/torque bar^[10].

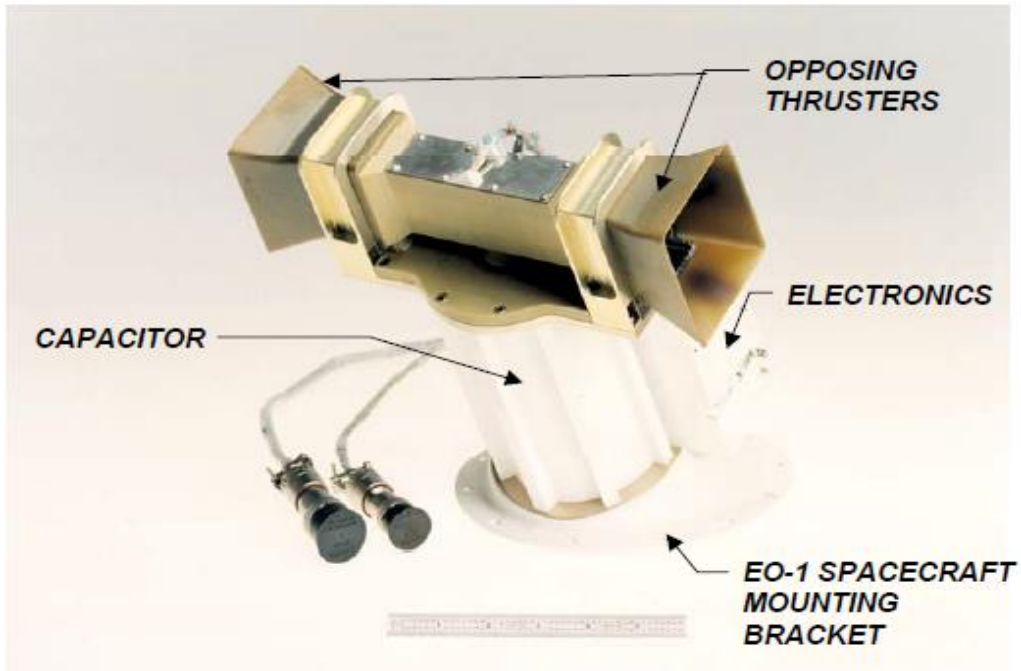


Figure 14: EO-1 Pulsed Plasma Thruster ^[10]. Copyright 2001 NASA Mission Technology Forum.

Since the EO-1 mission, PPTs, especially Ablative PPTs, have seen a resurgence of interest for spacecraft propulsion due to their small impulse bit, low mass, and most importantly their relatively low cost ^[10]. These characteristics make Ablative PPTs ideal for precision attitude control use in small satellites. PPTs have also been considered for use by NASA and the military for communication and interferometry missions. CubeSats such as the one shown in Figure 15 are small, low cost, satellites used for space research ^[11].

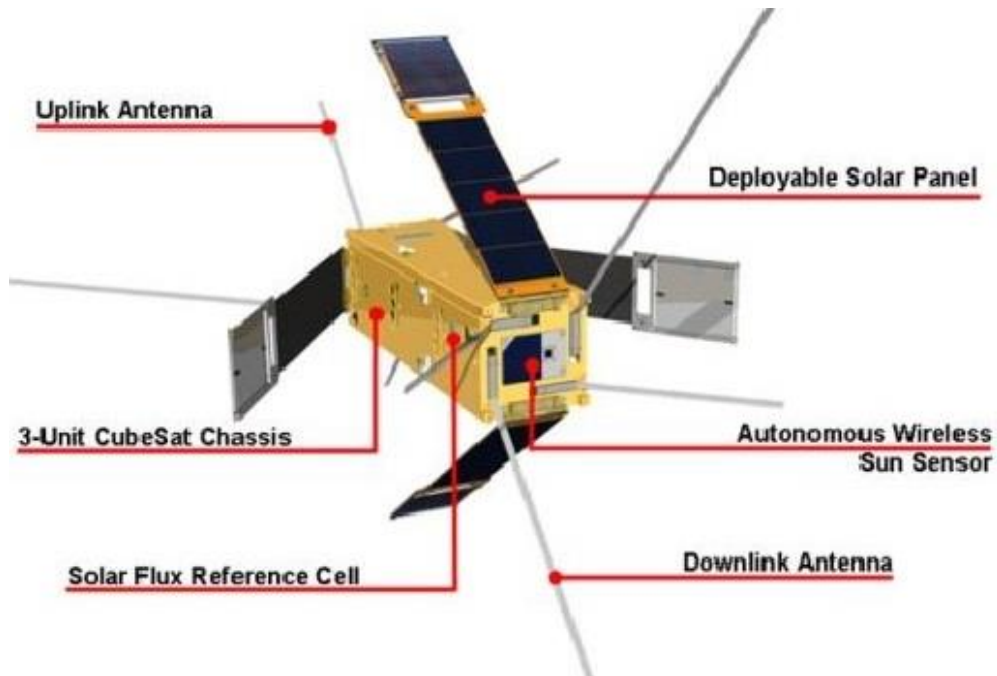


Figure 15: A Deployed CubeSat ^[12]. Copyright 2002 Amateur Funk.

NASA's Glen Research Center is currently working with Unison Industries to design a multi-thruster system with a long life, low mass and volume, provides ease of integration, high specific impulse (compared to chemical), high propellant efficiency, and impulse-bit accuracy. Figure 16 shows NASA's 2001 envisioned PPT technology development and improvement ^[10].



Figure 16: Envisioned PPT Technology Development at NASA ^[10]. Copyright 2001 NASA Mission Technology Forum.

PPTs have the ability to be used in many spacecraft applications due to their superior features compared to other types of electric propulsion. PPTs require no propellant storage tank. The use of a solid propellant reduces the mass and volume of a PPT system due to the elimination of the propellant tanks, lines, and valves. This makes the structure of a PPT simple and increases its reliability. It also saves money in the design and operation of PPTs. PPTs offer many desirable performance abilities, and have only one moving part which is a feed spring for the propellant bar. These benefits make it a really interesting research topic for future space technology ^[13].

On the other hand, PPTs have relatively low thrust efficiency compared with other types of electric thrusters. This is due in part to “late-time ablation” and rapid conductive heat transfer, which results in energy losses from the propellant to the rest of the spacecraft. As of 2011, research on increasing PPT’s thrust efficiency was ongoing at different universities and research centers ^[13].

2.1.4 PPT Contamination

Definition

When a PPT is fired, the solid Teflon fuel is ablated, ionized and accelerated at high velocity in a conical plume with an approximate half-angle of 40 degrees ^[14]. Particulates and other constituents of this plume can have effects on surfaces of the spacecraft on which the ejected mass impinges. This is an important consideration when the surface in question belongs to an optical sensor or other measurement device. Contamination of solar array surfaces is considered negligible due to the 10 year flight experience studies of PPTs on three Navy NOVA spacecraft ^{[15][16]}. Other studies have shown that the plume is not symmetric along the PPT thrust

axis, suggesting that the directionality of effluent contamination can be controlled to some extent [16]. The effects from plume constituents such as ions, atoms and carbon or fluorine molecules on optical surfaces can be broken down into three categories, which are sputtering, deposition, and film condensation [14].

The first effect of contamination is sputtering (i.e. physical removal of material by an incident energetic ion) of optical surfaces and coatings due to high velocity ions. It has shown that these ion velocities are on the order of tens of thousands of meters per second along the plume centerline [15]. The second category is the deposition of particulates onto optical and instrument surfaces. It has been shown that up to 30 percent of propellant mass is ejected in particulate form [17]. The last effect is due to Teflon fuel ablation during discharge of a PPT which causes vaporization of solid fuel particles. These particles condense into a uniform film on surfaces either in the backflow region of the spacecraft or by direct localized impingement on adjacent spacecraft. An example of spacecraft instrument surfaces which could be contaminated are the siderostats and transfer plates considered for use on the NASA ST-3 optical interferometer mission [16].

Simple Direct Flow Model

In order to estimate the flux of contaminant vapor in the direct flow region of the plume, a simple model was used in Ref. 16 to estimate the mass from a single pulse expanding through a conical plume with half angle α [14]. The geometry is shown in Figure 17 below.

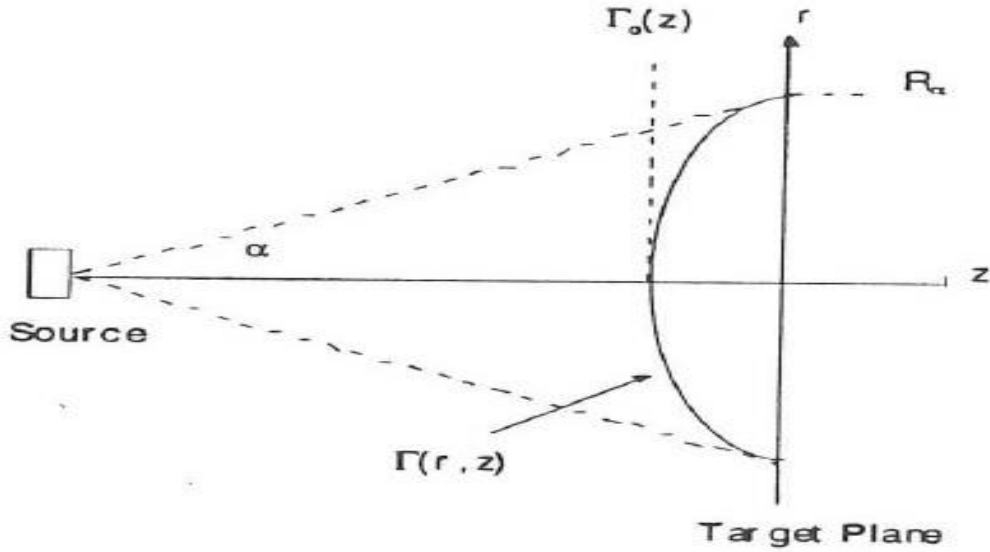


Figure 17: Simple Deposition Model Plume Geometry ^[14]. Copyright 1997 AIAA.

At a given time t , the mass sheet is a distance z from the source plane and has expanded to a radius R_α defined in terms of α as $R_\alpha = z \tan(\alpha)$. One assumption is that the flux density follows a cosine distribution. This flux density is given at any location in the target plane by $\Gamma(r, z) = \Gamma_0(z) \cos\left(\frac{r}{R_\alpha} \frac{\pi}{2}\right)$, where $\Gamma_0(z)$ is the centerline flux density. Assuming that all the mass from the pulse is contained within the plume cone allows one to integrate the following expression: $m_{bit} = \int_0^{R_\alpha} \Gamma(r, z) 2\pi r dr$ in order to determine the centerline flux density in terms of distance z , angle α and mass ablated per pulse, m_{bit} . Solving for the centerline flux density results in the following expression: $\Gamma_0(z) = \left(\frac{\pi}{\pi-2}\right) \left(\frac{m_{bit}}{4z^2 \times \tan^2(\alpha)}\right)$ ^[14].

A specific example of how this model is used for analysis comes from the NASA DS-3 New Millennium Interferometer conference paper ^[14]. In this mission a combiner spacecraft is in formation flight with two collector spacecraft separated by an aperture distance. This aperture distance changes as the collector pair move away from the combiner in an outward radial

direction. The result of this movement is a modified aperture distance for the interferometer measurements, allowing the system of spacecraft to take images of celestial objects at various “baseline” distances. The simple model estimates the amount of contamination which impinges on the combiner as a result of the various thrusting maneuvers performed by both collector crafts. The results of the analysis are presented in Table 1.

Table 1: Mass Deposited on Combiner and Film Thickness ^[14]. Copyright 1997 AIAA.

Pulse Freq (Hz)	Thrust (mN)	Maneuver Time (min)	Deposited Mass (mg)	Film Thickness (nm)
0.5	0.32	10.2	0.075	3.02
1.0	0.70	7.2	0.106	4.27
1.5	1.05	5.9	0.130	5.23
2.0	1.40	5.1	0.150	6.04

From Table 1 it can be seen that the deposited mass and film thickness are both proportional to pulse frequency. It is assumed that the flux density at the combiner is uniform. The film thickness is about 1% of the wavelength ($t/\lambda = 0.01$). Future work may be able to interpret this information in regards to a reflectance loss and develop a more accurate model for the visibility budget available for this or similar types of interferometers ^[14].

Testing & Experimentation

Typical investigation of PPT contamination utilizes a high vacuum facility with pressure ranges of 10^{-6} to 10^{-9} Torr. Baffles used to protect the inner tank surfaces from contamination are common practice. Section 3.2 provides information about the specific baffle design used for this project. Contamination “rakes” are used to support arrays of quartz witness plates (deposition monitors), and these setups utilize semi-circular arrays of these witness plates aligned with the

PPT electrodes in parallel or orthogonally. The mutual perpendicularity of these rakes allows the investigation of the off-axis thrust vector, which is canted towards the cathode electrode. Multiple studies describe the use of collimators with quartz witness plates and an example is shown below in Figure 18. This prevents unnecessary sputtering of the sample surfaces from random collisions during PPT firing ^{[15][16]}.

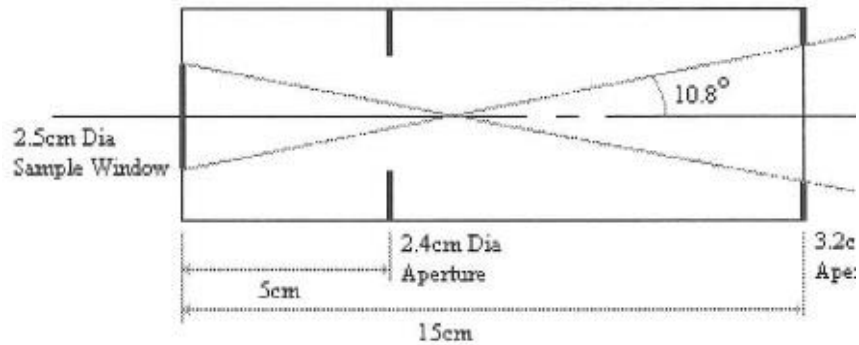


Figure 18: Example collimator with Quartz Sample (far left) ^[16]. Copyright 2000 AIAA.

In one example of such a study, contamination rakes with quartz sample witness plates housed inside collimators were used to investigate the symmetric and asymmetric mass deposition (or ablation) and film characteristics of a PPT plume on said samples. This study describes an experimental method which uses 24 two inch by two inch quartz squares comprised of 3 control and 21 testing samples. Samples 1-11 are fixed into collimators spaced 20 degrees apart along the rake array in the plane orthogonal to PPT electrodes, and samples 12 through 21 are similarly set up in the parallel plane. Both of these setups can be seen in Figure 19. In this experiment all quartz witness plates were cleaned with ethanol and dried prior to testing. Pre-test measurements of surface roughness for the samples were also taken. The collimator centerlines are aligned with the Teflon fuel bar centerline. All 21 of these samples were exposed to over one

million pulses at constant energy level within a cryogenically pumped vacuum tank capable of pumping down to a pressure range of 10^{-7} Torr [16].

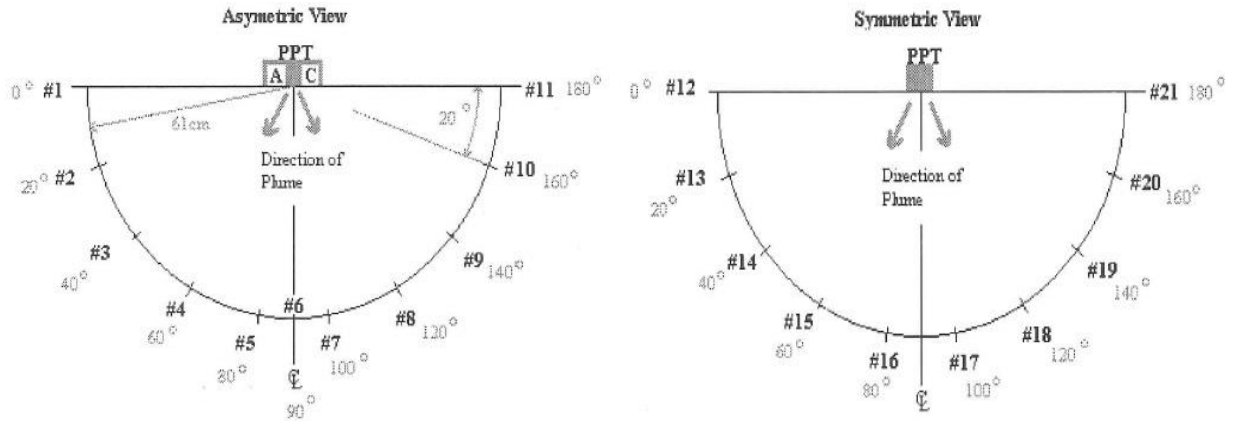


Figure 19: Orthogonal (left) and Parallel (right) Planes [16]. Copyright 2000 AIAA.

Measurements

Characterization of the film deposited onto spacecraft surfaces is an integral part of measuring the contamination effects of PPTs. The major characteristics of the film are thickness, composition, transmittance and reflectance. Measurements of film mass can also be taken. The use of spectrometers to measure the transmittance and reflectance of deposited films is common practice [14] [15]. Scanning Electron Microscopy is a well-documented method for measuring both composition and thickness of contaminant films [15] [16].

In order to understand the effects of plume contamination on optical surfaces used in multiple spacecraft interferometry missions a model for overall visibility “budget” is developed. The deposition of material from the plume can impact instrument visibility in three ways. The first is a decrease in transmissivity, which lowers the receiving signal intensity. Second is an increase in reflectivity, which increases background noise of the received signal. Finally, wave

front phase distortions can result in a given frequency spectrum. The visibility model describes an ideal visibility, Γ_{Ideal} of 1, and a total visibility, Γ_{Total} , which is the product of source visibility, Γ_{Source} , and instrument visibility, $\Gamma_{Instrument}$. The relationships between these visibility terms are described by ^[16]:

$$\Gamma_{Instrument} = \Gamma_{Phasing}\Gamma_{Pointing}\Gamma_{Dispersion}\Gamma_{Wavefront}\Gamma_{Intensity}\Gamma_{Area}$$

$$\Gamma_{Wavefront} = e^{-\left(\frac{2\pi^2(t_{RMS})^2}{\lambda^2}\right)}$$

$$\Gamma_{Intensity} = \frac{2\sqrt{K}}{1 + K}$$

The phasing visibility is reduced when two source signals are received out of phase, due to a difference in path length. Pointing visibility is effected by misalignment of the source and receiver. Phasing and pointing visibility are not affected by plume contamination. The dispersion visibility term is a frequency dependent phase shift introduced by adjacent electronics and instrumentation. Film thickness can inhibit this mode of visibility by altering the index of refraction of the receiver. Non-uniform film thicknesses, t_{RMS} , greater in size than the observing wavelength, λ , contribute to wave front visibility reductions, and this can be seen in the $\Gamma_{Wavefront}$ equation ^[16].

The equation for $\Gamma_{Intensity}$ is only a function of K which is the ratio of electric field strengths of the two beams before combination, which is defined by $K = \left(\frac{E_2}{E_1}\right)^2$. Signal intensities decrease with increasing film absorption and decreasing transmittance, both of which are frequency dependent.

The signal area is defined by the available area which can collect a transmitted signal, and on ST-3 this value is 144 cm^2 and corresponds to siderostats with a diameter of 12 cm . Area visibility is reduced by the percentage of the signal area being covered by contaminant film or particulates. This parameter can be determined by measuring the size and density distribution of totally reflecting or absorbing particles ^[16].

It has been shown that Auger Electron Spectroscopy is suitable for the measurement of film thickness and film composition on samples with net deposits. In this case each sample is installed in the spectrometer at 10^{-9} Torr and backfilled with argon to 10^{-5} Torr. The sample surface is sputtered with an ion gun at 1-2kV and then analyzed by rastering an area of 0.01 mm^2 with a 5 kV electron beam. Film composition was monitored during sputtering. Film thickness was measured by sputtering the film until the percent of contaminants drop to 50 percent of the initial level, using a known sputtering rate. For this experiment the sputtering rate was found to be 140 angstroms per minute, by sputtering an aluminum foil of known thickness over a given time. A profilometer was used to measure etch depths on samples with net ablation since AES could not be used in those cases due to severe charging ^[16].

The reflectance and transmittance for this same experiment were measured using a type of spectrometer that fits the requirements described previously. For samples 4 through 8 where net ablation occurred, it was found that transmittance was significantly reduced and this can be seen in Figure 20. This may be due to the presence of totally reflecting or absorbing particles houses on an uneven, sputtered quartz witness plate. Correspondingly the film thicknesses on samples 1-3 and 9-11 cause a reduction in transmittance ^[16].

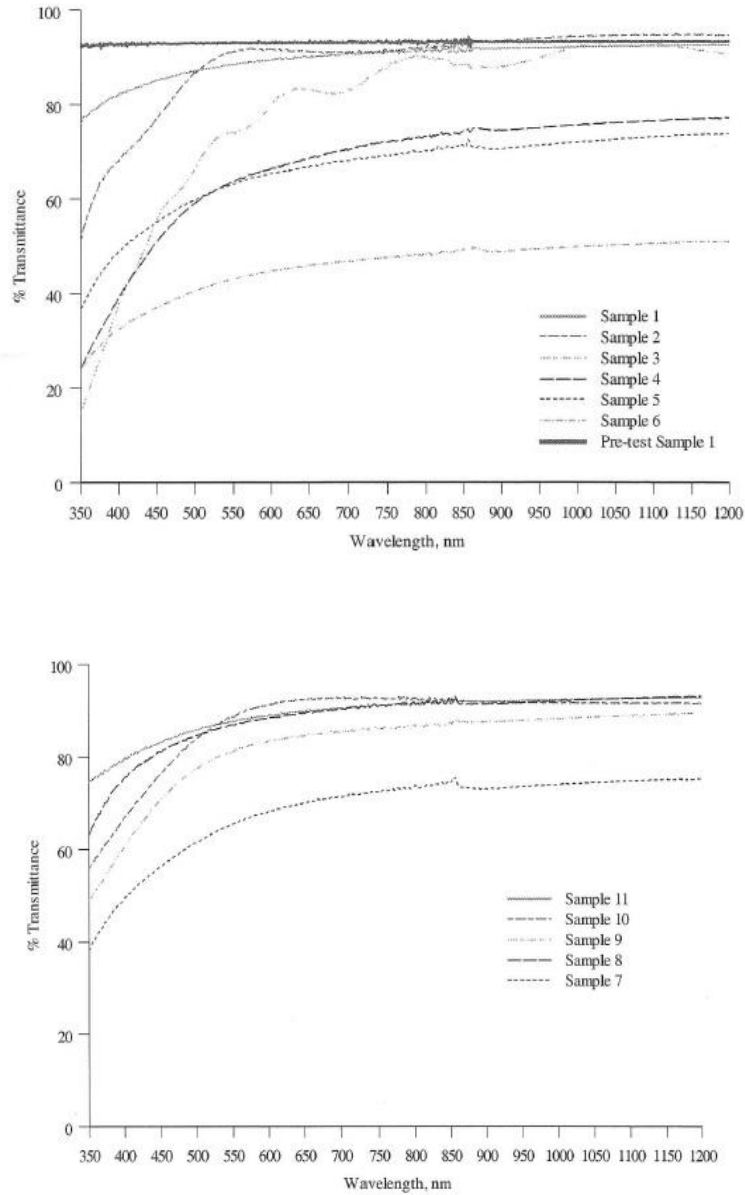


Figure 20: Orthogonal Plane Transmittance ^[16]. Copyright 2000 AIAA.

Reflectance is affected much less than transmittance as a result of deposition. The orthogonal plane samples show wider variation while parallel plane samples show tighter grouping, as seen in Figure 21. The most predominant effects of film contaminants on transmittance and reflectance occur below the threshold wavelength of 550 nm and this is seen in Figure 21 ^[16].

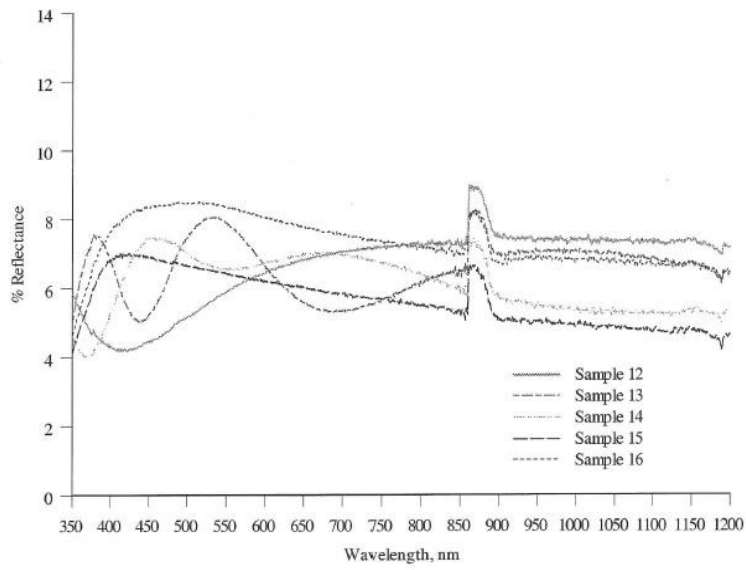
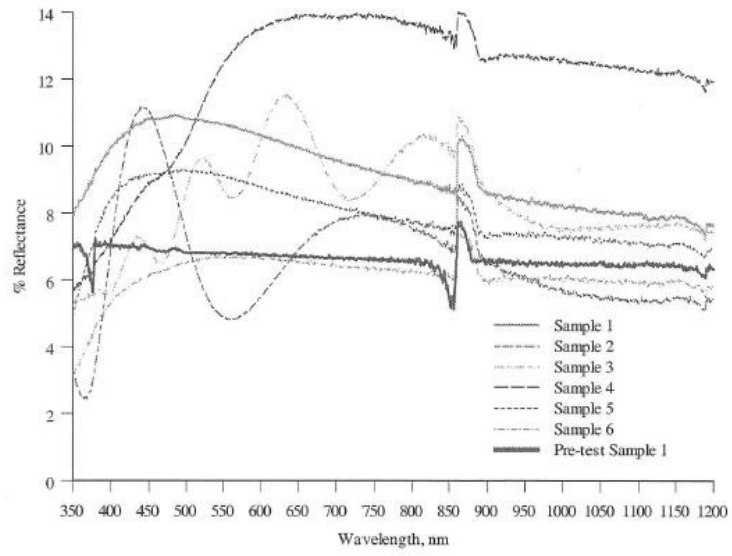


Figure 21: Orthogonal (top) and Parallel (bottom) Reflectance ^[16]. Copyright 2000 AIAA.

2.1.5 Toxicity Reports and Precautions

Some of the constituents in the PPT plume could be toxic to operators of T4 if they remain in the gas phase and are pumped into the lab. A review of the literature shows that chlorine and fluorine could be present in PPT emissions. Although the neutral forms of both elements have been found to deposit as films on surfaces within the chamber ^[16], thereby reducing the risk of the gases being pumped out into atmosphere, there is no data on whether the ionized forms of fluorine share the same properties. Thus, calculations were made on the potential toxicity of the plume constituents.

However, previous spectroscopy research shows that the ionized forms of fluorine from the Teflon fuel neutralizes rapidly after ablation ^[19]. That fact combined with the very small amounts of Teflon being ablated per pulse by the MTU (will be on the order of micrograms per pulse), implies a negligible risk of toxicity to the operators for any limited tests anticipated. Table 2 shows each ion species previously documented to be present in PPT plumes, and whether or not there is data regarding the constituent leaving deposits on surfaces.

Table 2: Ion Present in the PPT Plumes and their Contamination Risk ^{[16] [19] [20]}

SPECIES PRESENT	CONTAMINATION RISK
Cl	Forms deposits
C	Forms deposits
C ⁺	Inconclusive
C ⁺⁺	Inconclusive
C ⁺⁺⁺	Inconclusive

C ₂	Forms deposits
F	Forms deposits
F ⁺	Inconclusive
F ⁺⁺	Inconclusive
F ⁺⁺⁺	Inconclusive
O	Forms deposits
Fe	Forms deposits
Si	Forms deposits
Ni	Forms deposits

2.2 Vacuum System Technology

2.2.1 Vacuum Pumps

In this project there are three kinds of vacuum pumps being used to lower the pressure in the vacuum chamber from atmospheric to the micro Torr range where optical measurements are performed. The three pumps are a rotary mechanical pump, a turbomolecular pump and an ion pump. When pumping down from atmospheric pressure, the first pump to be activated is a Leybold Trivac D16B rotary-vane dual-stage mechanical pump, shown in Figure 22.

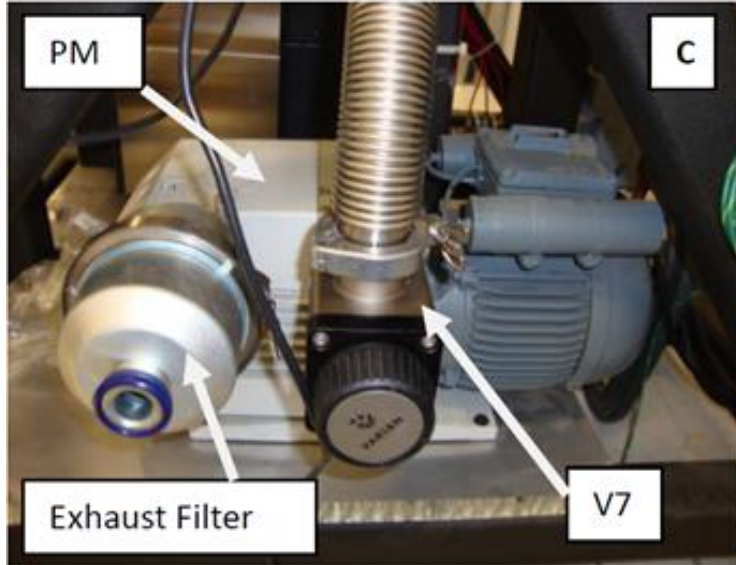
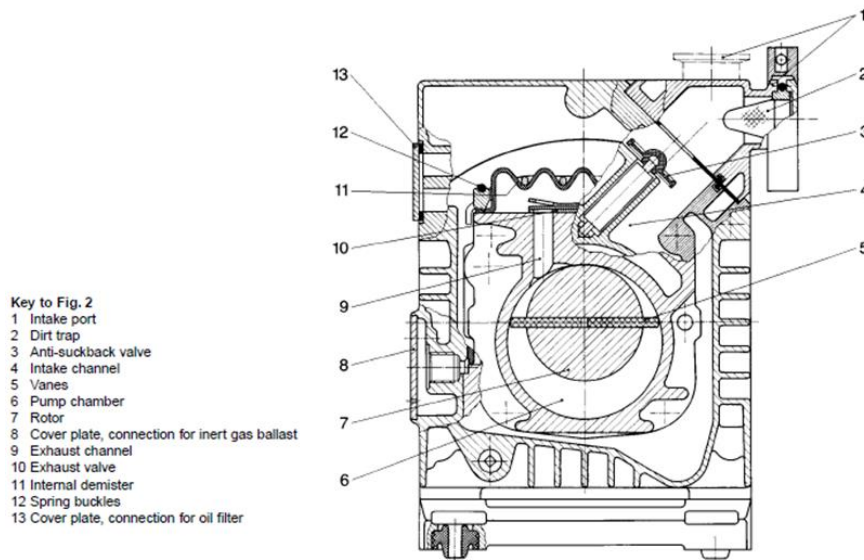


Figure 22: Mechanical Pump ^[2]. Copyright 2011 Sebastian Ryan.

The rotor of the pump is mounted off-center with a cylindrical stator with two radially sliding vanes, which divide the pump chamber into different compartments, and changes the size of the compartments with the rotation of the rotor as shown in the schematic shown in Figure 23.



- Key to Fig. 2
- 1 Intake port
 - 2 Dirt trap
 - 3 Anti-suckback valve
 - 4 Intake channel
 - 5 Vanes
 - 6 Pump chamber
 - 7 Rotor
 - 8 Cover plate, connection for inert gas ballast
 - 9 Exhaust channel
 - 10 Exhaust valve
 - 11 Internal demister
 - 12 Spring buckles
 - 13 Cover plate, connection for oil filter

Figure 23: Diagram of Mechanical Pump ^[21]. Copyright 2001 Ideal Vacuum Products.

As a result of the volume changes gas is sucked in at the intake port and compressed ^[21]. Oil is injected into the pump chamber to create a seal between the rotors and stator and to provide lubrication. The pumping speed of the mechanical pump is highly dependent on the pressure at the inlet, with the pumping speed dropping quickly to near zero when approaching pressures on the order of millitorr ^[21]. This is shown in the pumping speed curve in Figure 24.

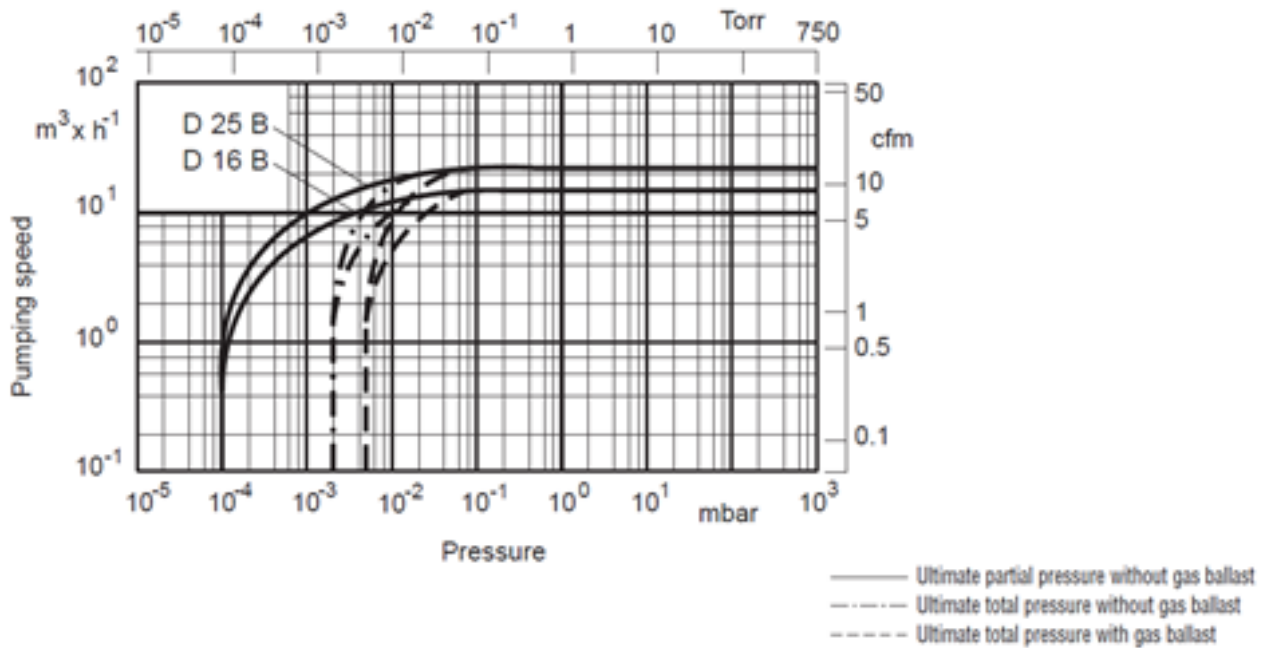


Figure 24: Pumping Speed vs. Pressure of Mechanical Pump ^[21]. Copyright 2001 Ideal Vacuum Products.

The pressure range of the pump is listed as 760-0.0015 Torr and the pumping speed is listed as 6.36 L/s; however, the team planned to switch to the second stage using the turbomolecular pump when the pressure reaches 0.375 Torr ^[2]. T4 operation procedure can be found in Appendix A.1. The second pump being used is a Leybold TurboVac 361 turbomolecular pump, shown in Figure 25.

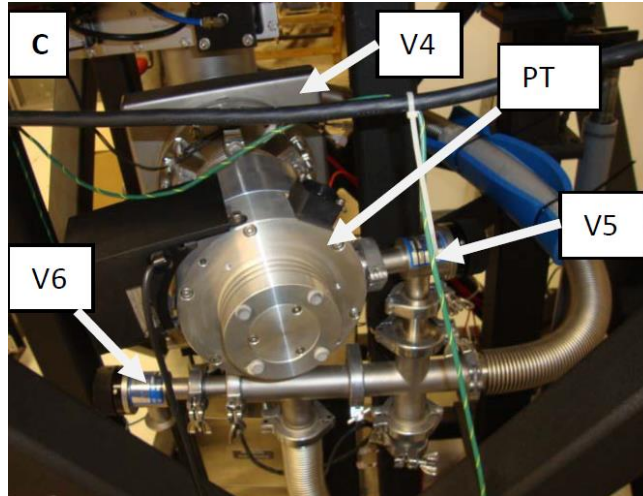


Figure 25: Turbomolecular Pump ^[2]. Copyright 2011 Sebastian Ryan.

Turbomolecular pumps operate in the molecular flow regime with a bladed turbine rotor turning within a slotted stator as shown in Figure 26.

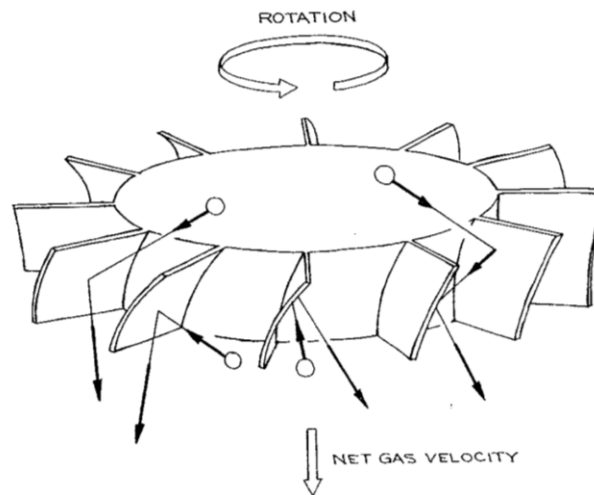


Figure 26: Turbine of a Turbomolecular Pump ^[22]. Copyright 2009 Cambridge University Press.

The tips of the blades approach molecular speeds which allow the vacuum system to be pumped from the millitorr to nano Torr range. The turbomolecular pump is rated for a pump speed of 350 L/s on air and has an operating pressure of down to 75×10^{-10} Torr. Roughing the chamber down and back pumping the turbomolecular pump with the mechanical pump lengthens

the lifespan of the turbopump, and the maximum pressure at which the pump can operate depends on the size of the chamber and the roughing pump. For this project, the turbopump should not be switched on until the pressure reaches approximately 0.375 Torr ^[2]. The pump is run with a Turbotronik's controller shown in Figure 27.



Figure 27: Turbotronik Controller ^[2]. Copyright 2011 Sebastian Ryan.

The final stage of pumping, if needed, uses a Physical Electronics 640 I/s Ion Pump shown in Figure 28.



Figure 28: Physical Electronics 640 I/s Ion Pump

The ion pump is only turned on when the pressure has reached one millitorr or lower ^[23], and is capable of pumping the chamber down to a pressure as low as 10^{-9} Torr ^[2]. Rather than remove gas from the system like the previously described pumps, it adsorbs gas particles on pump surfaces or combines them with active metals by ionizing gas present in the system and then accelerating them towards traps. The ion pump speed is dependent on the gases present, and inert gases are not pumped as efficiently.

2.2.2 Vacuum Measurement

Pressure Gauges

There are currently three operational pressure gauges associated with the pumping system, labeled G1, G2 and G4 on Figure 29.

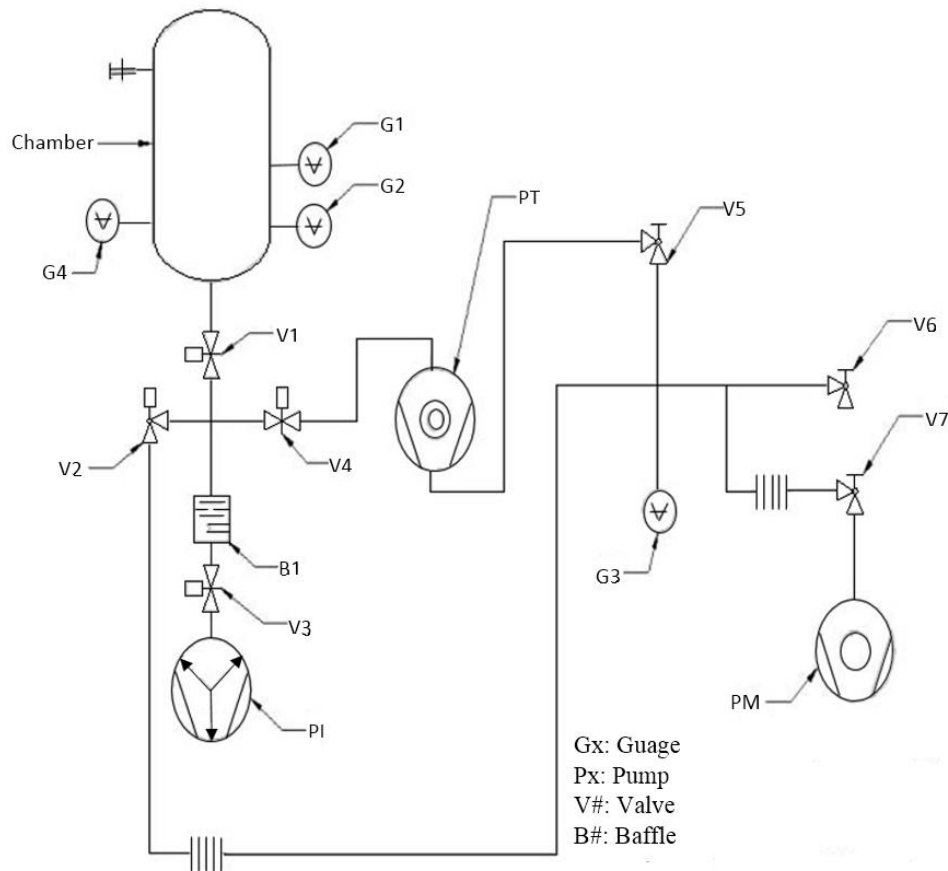


Figure 29: Schematic of T4 Vacuum System ^[2]. Copyright 2011 Sebastian Ryan.

G1 is located on the collar for measurement of the chamber pressure. It is a Leybold Thermovac T221 thermocouple gauge that measures the pressure of a gas by measuring its thermal conductivity. The thermal conductivity of a gas decreases from some constant value above 1 Torr to near zero at about one millitorr ^[17]. A filament is heated by a constant current so the temperature of the filament depends on the rate of heat loss to the surrounding gas. G3 is located on the foreline for measurement of the foreline pressure, and it is also a thermocouple gauge. G2 was removed from T4 and attached to T2. G4 is a 572 Ionization gauge and is used for measuring the chamber pressure below the milli Torr range.

State of Vacuum System

Originally, the T4 vacuum system was only able to reach a pressure as low as 40 Torr due to a leak in the system. This was not low enough to proceed to the second stage of the pumping down process using the turbomolecular pump. The first approach used to find the leak involved removing and cleaning the O-ring which provides the seal between the chamber bell and collar, and re-applying vacuum grease to this O-ring to insure an airtight seal. After that was unsuccessful, the team ordered replacements for all the blank flanges encircling the bell jar. Instead of the method that the previous blanks used, where an aluminum knife edge provides a mechanical seal, the new blanks ordered are outfitted with rubber O-rings. This solved the leak problem and the team was able to bring the chamber down to a low enough pressure that allows the use of the turbopump.

2.2.3 WPI Vacuum Test Facility (VTF) Tank 4 (T4)

T4 itself consists of a bell that is 29.75 inches in diameter and 34.25 inches tall. The chamber bell is lowered by a hoist onto a 5.25 inch tall collar. Figure 30 shows a diagram of T4's chamber bell with the collar.

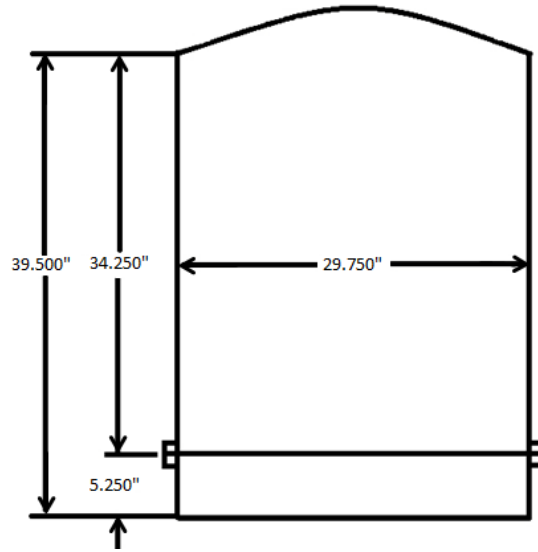


Figure 30: T4 Internal Dimensions ^[2]. Copyright 2011 Sebastian Ryan.

The collar is ringed with electrical feedthroughs and blank flanges. The chamber is lowered onto the collar and the surface between the two is lined with an O-ring to provide a seal as previously mentioned. Figure 31 shows T4 with its collar and hoist assembly, and Table 3 provides a description of T4's collar ports. The ports on the chamber are numbered using labels.

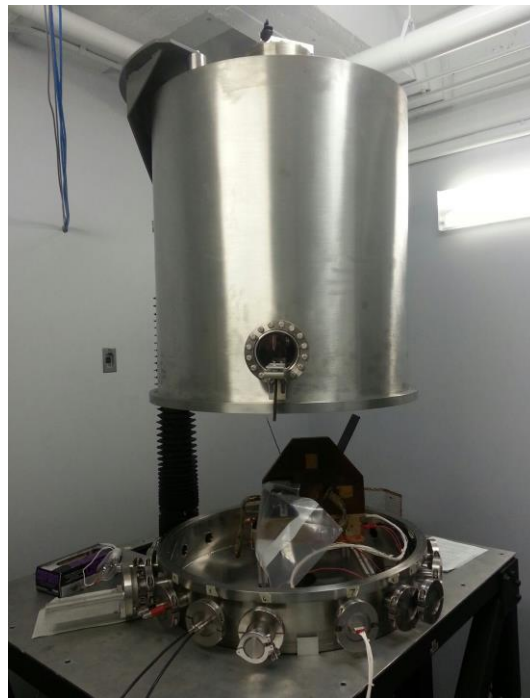


Figure 31: T4's Collar and Hoist Assembly

Table 3: Description of T4's Collar Ports

Port Number	Description
1	NW50 Feedthrough with NW40 Adapter and Blank
2	572 Ionization Gauge
3	Window Port
4	Single Ended, Large Grounded Shield Coaxial Feedthrough
5	Single Ended, Grounded Shield Coaxial Feedthrough
6	NW50 Feedthrough with NW40 Adapter and Blank
7	15-Pin Double Sided Sub-D Feedthrough
8	NW50 Blank
9	NW50 Blank
10	NW50 Blank
11	NW50 Blank
12	NW50 Blank
13	NW50 Feedthrough with NW25 Adapter and Blank
14	NW50 Blank
15	Gauge 1 Thermocouple for CombiVac
16	High Voltage BNC Feedthrough
17	NW50 Blank
18	NW50 Blank

2.3 Optical Spectroscopy

Optical Spectroscopy is defined as the study of absorption and emission of light by matter. Spectroscopy was originally utilized to observe wavelength dependences of absorption and emission, but has evolved to include time resolved, single-molecule, and non-linear spectroscopy ^[24].

2.3.1 Theory

Optical Spectrometers are used to study optical activity of a medium, which is the ability of a system to modify the propagation velocity and amplitude of a light ^[25]. These observations can then be used to obtain parameters that define the system. For example, spectrometers can measure the fluorescent decay and extract the lifetime of an excited state of a compound ^[24].

There have already been substantial studies on the emission spectra of PPTs, which provides a guideline to what kind of data to expect. A 1971 Teflon PPT emissions study used spectroscopy to determine the ion species present in PPT exhaust, and they identified all intense lines of neutral and singly, doubly, and triply ionized atoms of carbon and fluorine. They also detected numerous weak lines of Iron that apparently came from bombardment of the stainless steel electrodes and spark plug erosion ^[19]. Another study conducted in 1997 identified the species of ions present and then collected data on how the emissions of each species changed with discharge time and energy, as shown in Figure 32. Their plotted data shows that while the intensity of singly ionized atoms remains relatively the same with increasing discharge energy, the amount of doubly charged ions greatly increases ^[20].

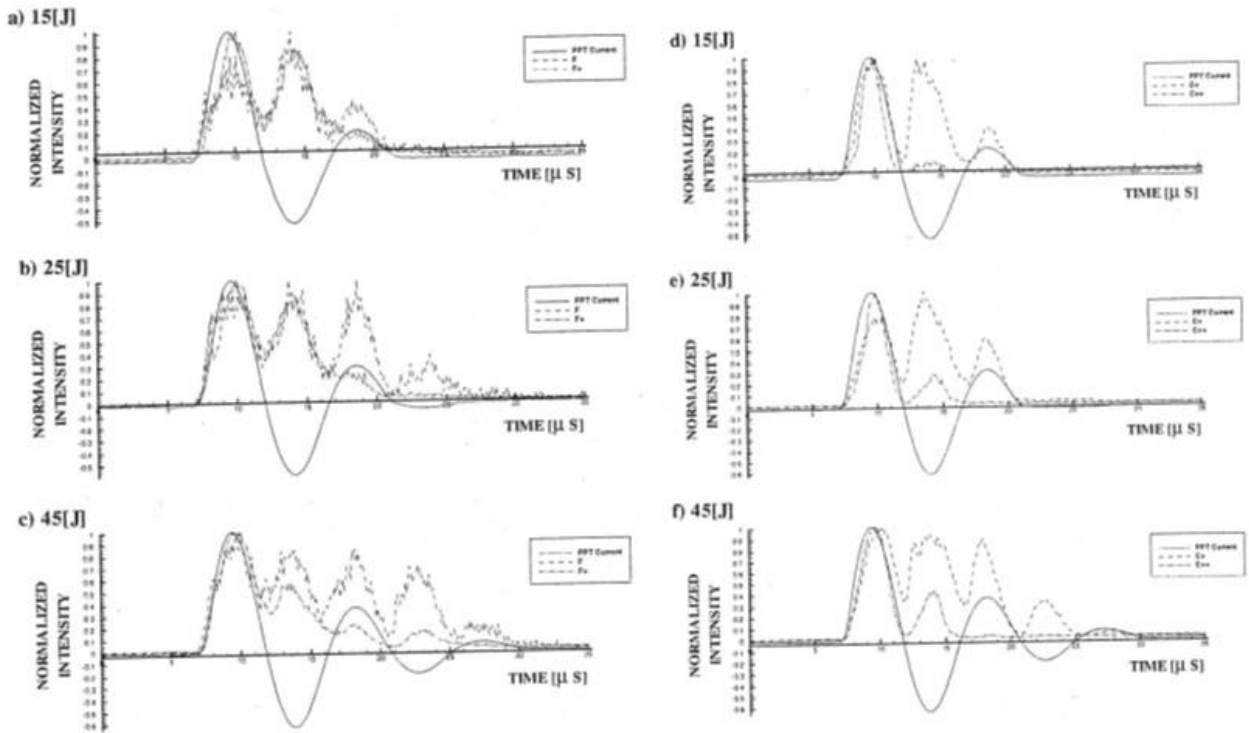


Figure 32: PPT Emission as a Function of Discharge Energy and Time ^[20]. Copyright 1997 AIAA.

2.3.2 Ocean Optics High Resolution Spectrometer HR4000

The Ocean Optics High Resolution Spectrometer HR4000 [HR4000] used for this project uses a grating designed for visible light, from 700–1100 nm with an Optical Resolution of up to 0.025 nm (full width at half maximum). The HR4000 analyzes light carried from the experiment using an optical fiber, which it redirects and aligns until the processing unit obtains the light as shown in Figure 33. Table 4 lists HR4000 parts and description, which are adapted from Ocean Optics’ manual.

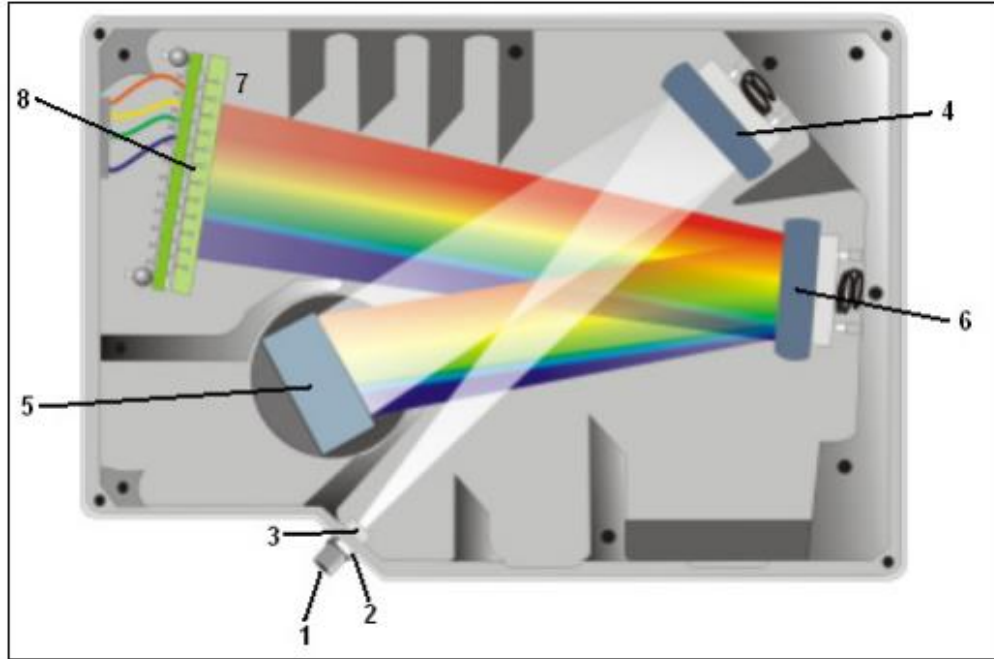


Figure 33: HR4000 Spectrometer with Components ^[26]. Copyright 2008 Ocean Optics.

Table 4: HR4000 Components ^[26]. Copyright 2008 Ocean Optics.

Item	Name	Description
1	SMA Connector	SMA stands for Spectroscopie Moléculaire et Applications, which is French for Molecular Spectroscopy and Applications. It Secures the input fiber to the spectrometer. Light from the input fiber enters the optical bench through this connector.
2	Slit	<p>A dark piece of material containing a rectangular aperture, which is mounted directly behind the SMA Connector. The size of the aperture regulates the amount of light that enters the optical bench and controls spectral resolution.</p> <p>The HR4000 can also be used without a Slit. In this configuration, the diameter of the fiber connected to the HR4000 determines the size of the entrance aperture.</p> <p>NOTE: Only Ocean Optics technicians can change the Slit.</p>

3	Filter	<p>Restricts optical radiation to pre-determined wavelength regions. Light passes through the Filter before entering the optical bench. Both bandpass and longpass filters are available to restrict radiation to certain wavelength regions.</p> <p><u>NOTE:</u> Only Ocean Optics technicians can change the Filter.</p>
4	Collimating Mirror	<p>Focuses light entering the optical bench towards the Grating of the spectrometer.</p> <p>Light enters the spectrometer, passes through the SMA Connector, Slit, and Filter, and then reflects off the Collimating Mirror onto the Grating.</p>
5	Grating	<p>Diffraction light from the Collimating Mirror and directs the diffracted light onto the Focusing Mirror. Gratings are available in different groove densities, allowing you to specify wavelength coverage and resolution in the spectrometer.</p> <p><u>NOTE:</u> Only Ocean Optics technicians can change the Grating.</p>
6	Focusing Mirror	<p>Receives light reflected from the Grating and focuses the light onto the CCD Detector or L2 Detector Collection Lens (depending on the spectrometer configuration).</p>
7	L2 Detector Collection Lens	<p>An optional component that attaches to the CCD Detector. It focuses light from a tall slit onto the shorter CCD Detector elements. The L2 Detector Collection Lens should be used with large diameter slits or in applications with low light levels. It also improves efficiency by reducing the effects of stray light.</p> <p><u>NOTE:</u> Only Ocean Optics technicians can add or remove the L2 Detection Collection Lens.</p>
8	CCD Detector(VIS)	<p>Collects the light received from the Focusing Mirror or L2 Detector Collection Lens and converts the optical signal to a digital signal. Each pixel on the CCD Detector responds to the wavelength of light that strikes it, creating a digital response. The spectrometer then transmits the digital signal to the SpectraSuite or OOIBase32 software of HR4000.</p>

CHAPTER 3. METHODOLOGY

3.1 Vacuum Chamber Leak Detection and Recommissioning

T4 Initial Operating Experience

The project advisor (Prof. Blandino) and laboratory manager (Graduate student Zach Taillefer) for WPI's HL016 vacuum facility both assisted the project team throughout its initial operating experience with the T4 system. The project advisor and laboratory manager conducted a simple pump down of T4, while the project team observed the process and learned how to operate the mechanical roughing pump. The project team was also shown how to make proper laboratory notes in the T4 lab notebook. Whenever a new section of the T4 procedure had to be performed either the project advisor or lab manager was present initially to assist the project team.

Leak Detection and Recommissioning Process

Initially, the team and advisor thought that dust or some other debris might be the cause of the leak in T4; so a plan was implemented to clean and grease T4's main collar and O-ring as shown in Figure 34. Later, the team suspected that the leak was localized to the upper bell chamber and collar with its numerous flanges and port components. In an attempt to isolate the leak, the project team ordered two sets of NW50 blanks and centering rings with Viton O-rings from Nor-Cal. The purpose of ordering these components was to systematically replace the collar flange ports one by one with one of the new NW50 sets, and perform Rate-of-Rise (ROR) time measurements.

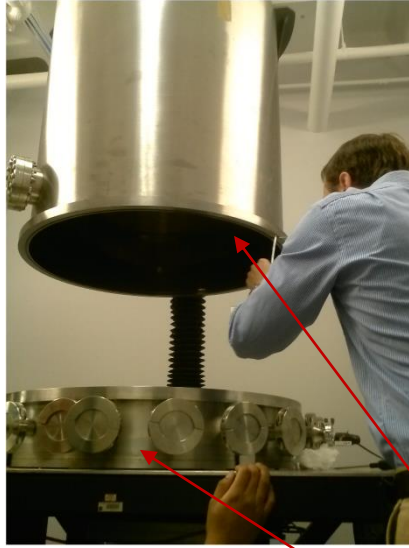


Figure 34: Cleaning and Greasing T4's Collar and O-ring

The ROR time of a vacuum system is a suitable parameter for measuring vacuum integrity and an acceptable value is approximately 5 mTorr per minute. The leak isolation process was to pump down T4 to as low as possible (but never lower than 50 mTorr), using the mechanical pump only, record that pressure, stop the pump, start a stop watch while allowing the system pressure to increase (if there is a leak) or remain the same (if no leak), and then record the final pressure and time when the stop watch is stopped. Initial ROR measurements before any changes to the system were made were on the order of 25.5 Torr per minute, which was much higher than the target values required for a suitable vacuum environment. The project team developed a ROR experimental procedure and data sheet, which can be found in Appendix A.2.

During this leak detection activity the team noticed that the sealing components used on ports #4 and #6 were different from the centering ring and O-ring purchased from Nor-Cal. After initial examination and research it was determined that the sealing components in use were aluminum metal seals, as shown in Figure 35. These types of seals are only good for one time

use in ultra-high vacuum applications. When this was discovered, the leak detection process was put on hold and the project team submitted another order to Nor-Cal for 16 additional NW50 centering rings with Viton O-rings.



Figure 35: Aluminum Metal Seal with T4's Port #4 Electrical Feedthrough

After replacing all of the metal seals with elastomer seals the ROR experimental procedure was resumed. A significant and rapid pressure drop below 40 Torr was noticed, and continued to drop until the 10-20 mTorr range as shown on the CombiVac display in Figure 36. The flange seal replacement appeared to fix the leak, and ROR measurements were taken over the next several days to monitor T4's behavior. The results of those measurements are shown in Table 5 below.

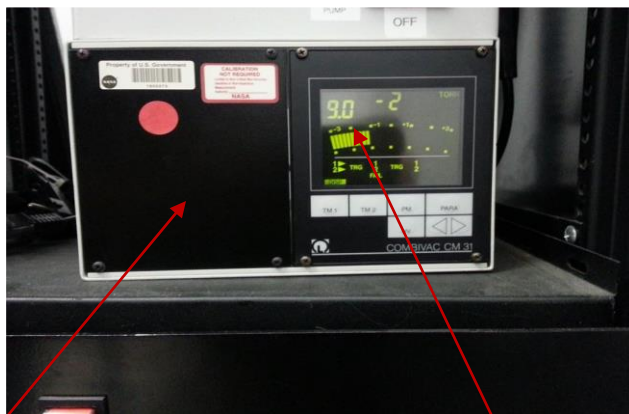


Figure 36: CombiVac Displaying Chamber Pressure of 90 mTorr (11/08/2013 @ 10:40 AM)

Table 5: ROR Measurements after the Initial Leak Fix (11/7/13-11/11/13)

Start Pressure (Torr)	Stop Pressure (Torr)	Duration (min)	Rate-of-Rise (mTorr/min)	ΔROR (mTorr/min) (> 0 is OK) (< 0 is BAD)
17E-3	19E-3	6.5	0.31	4.69
19E-3	63E-3	1080	0.04	4.96
63E-3	70E-3	360	0.02	4.98
70E-3	90E-3	1120	0.02	4.98
90E-3	140E-3	4320	0.01	4.99
17E-3	140E-3	6886.5	0.02	4.98

The last column, Δ ROR, is a measure of the difference between a given ROR measurement and the chosen ideal value of 5 mTorr/min. For example, the last row is an average ROR measurement using the first start pressure of 17 Torr with the final stop pressure of 140 Torr. Here the average ROR is 0.02 mTorr/min and this is subtracted from the ideal value of 5 mTorr/min to obtain the difference. As the system pressure ROR approaches zero the Δ ROR approaches 5 mTorr/min, the ideal ROR. This progression can be seen throughout the last column. This was anticipated due to outgassing in the T4 system as time under vacuum increases and the chamber pressure increases at a decreasing rate.

Since the pressure was low enough, the turbopump could be turned on; however, it had not been operated in several years, so its condition was unknown. Before turning it on an initial ROR measurement was performed. A value of 5.4 mTorr per minute was calculated and it was decided this was low enough to proceed with the turbopump start procedure. During pump down with the turbopump, the chamber pressure drop stalled at roughly 4.8 Torr. This indicated the presence of another leak in the system. After careful inspection of the turbopump under rough vacuum, suction was felt on an open port on the side of the turbopump, which had no seal or

clamp. Therefore, a third component order to Nor-Cal was made. This order was for an NW16 blank and SureSeal Clamp, and an NW 10/16 reducing centering ring (the inner diameter on the valve port for the turbopump is NW10, and the blank size is NW16). These components are shown in Figure 37.



Figure 37: Turbopump Valve with Components from Nor-Cal

Once the NW16 components were attached to the turbopump, the T4 pump-down procedure was restarted. ROR measurements were performed to gauge the performance of the turbopump, because T4 was initially at atmospheric pressure. The Aerojet MTU was present in the T4 chamber during this measurement phase, much like the previous phase from Table 5. Table 6 below shows post turbopump recommissioning ROR measurements.

The first row in Table 6 is for the initial ROR measurement which is influenced by the fact that the system was pumping down from atmospheric pressure, and this can be seen clearly in the last column for ΔROR . The 2nd row was the next iteration and the improvement from the initial measurement is clear to see. The last row was performed the following day after T4 was

shut down and given a chance to outgas, and as was expected the Δ ROR improved even further with time.

Table 6: Post Turbopump Recommissioning ROR Measurements (initial pressure = atmosphere)

Start Pressure (Torr)	Stop Pressure (Torr)	Duration (min)	Rate-of-Rise (mTorr/min) (5 is ideal max)	Δ ROR (mTorr/min) (> 0 is OK) (< 0 is BAD)
73E-3	120E-3	4.9	9.6	-4.60
40E-3	75E-3	5.0	5.0	0
60E-3	140E-3	32.82	2.44	2.56

The lab manager installed a 572 Ionization Gauge (IG) on the T4 collar, replacing the previously installed MBA-200. The IG has an effective pressure range of 1E-3 to 1E-10 Torr. The first measure of T4's lowest pressure while operating the turbopump with the MTU present in the chamber can also be seen in Figure 38, as shown on the Varian BA2 SenTorr Controller front panel. The TC1 pressure readout is from the G3 foreline pressure gauge, which bottoms out at 1.0E-3 Torr. Typical IG values for system pressure with the MTU present were around 4.0-5.0E-5 Torr.

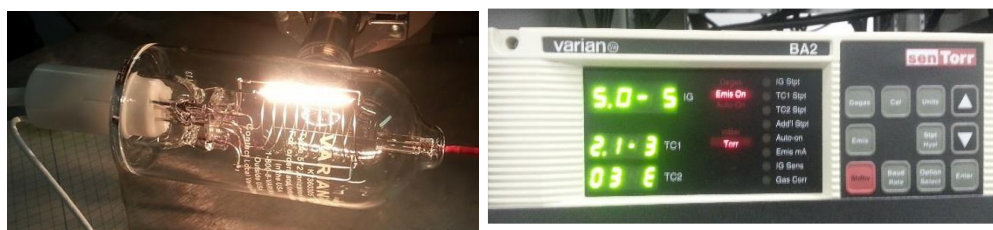


Figure 38: 572 Ion Gauge (left) and BA2 Front Panel with Ion Gauge Pressure Display (right)

To establish a wider understanding of overall T4 system behavior (turbopump specifically) it was necessary to measure the ROR and system pressure with the chamber empty. T4 was back-vented to atmosphere to remove the MTU from the chamber, and then the pump-

down procedure was restarted from the atmospheric pressure state. The first ROR was calculated with start and stop pressures of 29 and 30 mTorr respectively, with a duration of 10 minutes, which resulted in a measured value of 0.1 mTorr/min. When this value is compared to previous ROR measurements of similar magnitude, such as those in Tables 5 and 6, the user can justify taking no further ROR measurements, as the leak rate has essentially become negligible. When the MTU was present in the system it would take several hours if not days for a ROR value of this magnitude to be realized. Another important note is the pump down time, which was much less under these conditions. This is a qualitative observation, but pump down times could be measured and compared for both cases. The lowest system pressures achievable with the empty bell jar range from 1.0-2.0E-6 Torr. This is an order of magnitude lower than the pressures measured when the MTU was inside the chamber. In order to achieve systems pressures on this order with the MTU present T4 must pump down for longer periods of time.

This general measurement was performed to provide a comparison between the performance of the system with and without the presence of the MTU, which leads to an understanding of how much outgassing occurs when the MTU is inside the chamber. This also allows the user allocate enough pump down time prior to when the experiment needs to be performed. This will depend on how long the T4 system was at atmosphere or under vacuum prior to experimentation. The project group pumped down T4 for a week in advance of experimentation in order to account for the outgassing from the MTU and related system integration components, such as wiring, adapters, etc.

Development of the Modified T4 Operational Procedures

The T4 pump-down procedure from Sebastian's report ^[2] provided suitable information to operate the mechanical pump, but did not accurately outline the pump down and back venting

procedures for the TurboVac 361 turbopump. Therefore, a modified procedure specific to this project was prepared and refined throughout the leak detection and recommissioning process. This procedure is available in Appendix A.1. The modified procedure incorporated the mechanical pumping steps and other considerations from Sebastian and also includes warnings and special considerations for the TurboVac 361, including a section on back-venting the turbopump.

In developing the modified procedure there was concern regarding the correct chamber pressure required to turn on the turbopump. The project group contacted Leybold and spoke to a representative who was able to clarify concerns over the starting pressure. Using the graph in Figure 39 below, the pumping speed at the fore vacuum pump S_f was found from the roughing pump manual as $18.9 \frac{m^3}{h}$ [21]. According to Sebastian's report, the volume, V , of the T4 chamber is roughly $0.45 m^3$ [2]. This corresponds to a $\frac{S_f}{V}$ value of $42 h^{-1}$, which gave a rough (max) starting pressure of 20-30 mbar (15.0-22.5 Torr). A more conservative value is the next lowest intersection of the "TurboVac 151 to 1000" line in the graph, namely 10 mbar (7.5 Torr). The Leybold representative suggested the project team use the (even more conservative) maximum foreline pressure for nitrogen, which is 0.5 mbar (0.375 Torr), to reduce bearing forces and increase the service life of the TurboVac 361 [27]. The starting pressure value used in the modified T4 procedure was therefore chosen to be 375 mTorr.

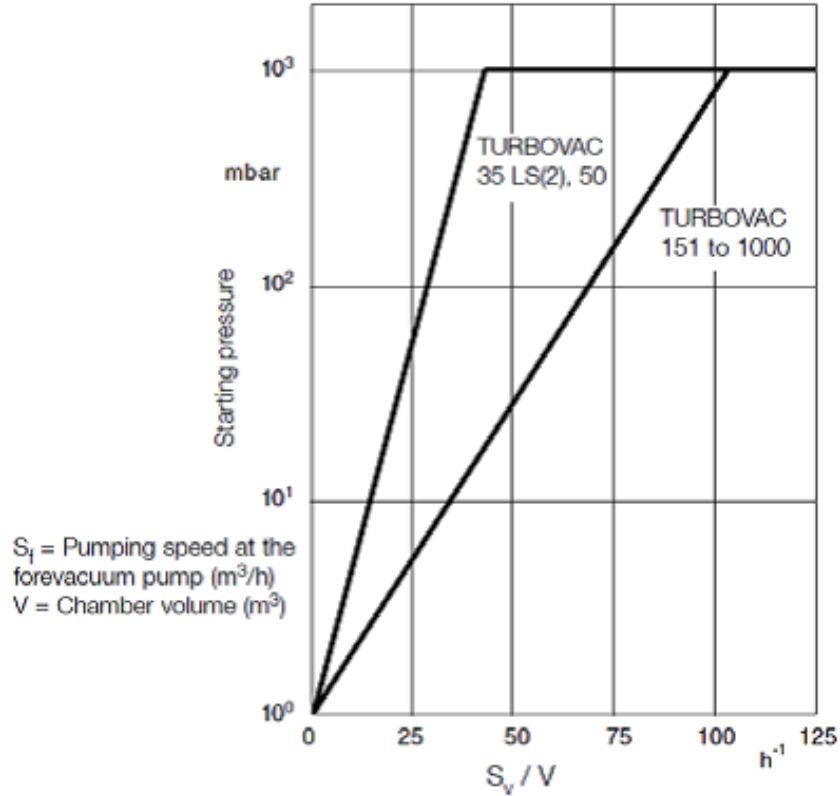


Figure 39: Determining Starting Pressure for TurboVac 361 Graph ^[28]. Copyright 2006 Leybold Vacuum.

The pump-down time t_{pd} required to reach the desired starting pressure was calculated with the following relationship ^[22], $t_{pd} = 2.3 \left(\frac{V}{S_p} \right) \ln \left(\frac{P_1}{P_2} \right)$. Where V is the chamber volume, P_1 is the starting pressure (typically atmosphere), P_2 is the desired chamber pressure and S_p is the nominal pumping speed of the roughing pump. The calculated time required to pump down the chamber from atmosphere to the desired starting pressure for the TurboVac 361 is roughly 25 minutes. The time required to pump down to 50 mTorr from atmosphere is about 32 minutes, and this initial pressure was the one used for performing ROR measurements.

3.2 PPT Mount and Plume Baffle Design and Construction

The bottom of T4's collar has a 13.6 cm hole, which is the main opening for all pumping operations. Because of this hole in the bottom of the chamber, the MTU cannot be directly placed inside the vacuum chamber, and the team had to design and construct a PPT support mount. The PPT mount has to support the MTU's weight, and be a standalone structure that can easily be detached from the MTU when needed.

The PPT mount designed by the team consists of four 3 in. long legs, two 17 in. main runners, and two 10.22 in. crossbars. These parts are all made out of x-channel. The main runners are connected to the four legs using four concealed 90° connectors, while the crossbars are attached to the legs using four adjustable 90° connectors. A constraint arising from the use of adjustable connectors was the need to drill four holes in the crossbars. Figure 40 below shows a detailed image of the PPT mount.

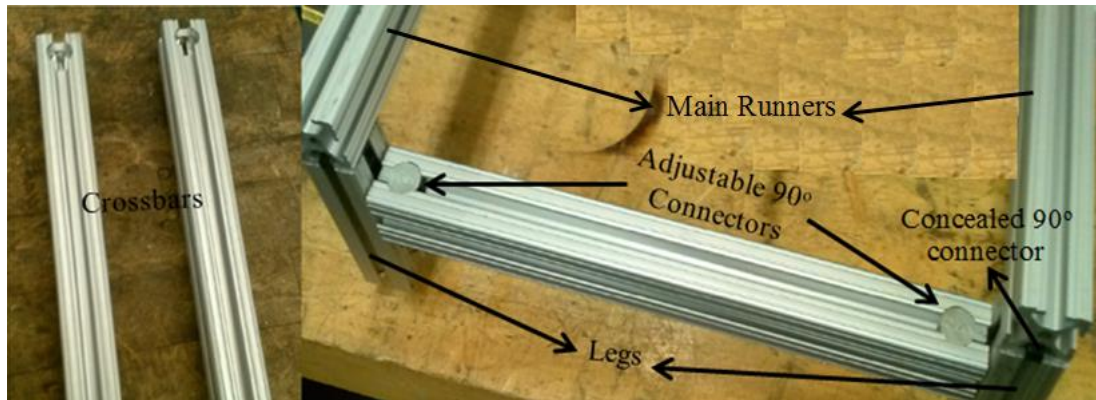


Figure 40: Connection between the Crossbars and the Legs

The MTU sits directly on the main runners, and is attached by four 90° brackets. These brackets are connected to the main runners by four compact head end-feed fasteners and to the MTU's bottom panel by its original screws. All of the parts the team used to build the PPT

mount were bought from McMaster-Carr. Figures 41 and 42 show a detailed solid model of the PPT mount with and without the MTU.

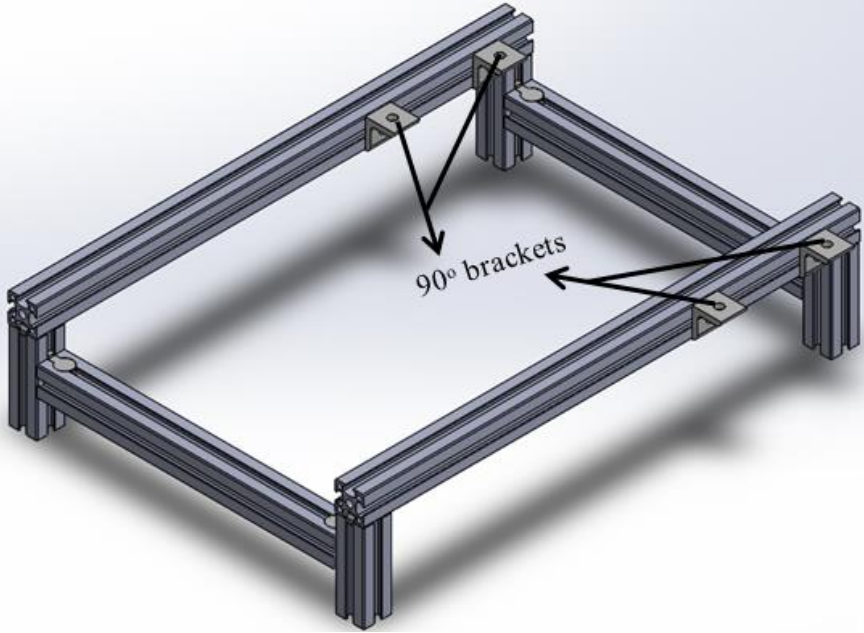


Figure 41: PPT Mount

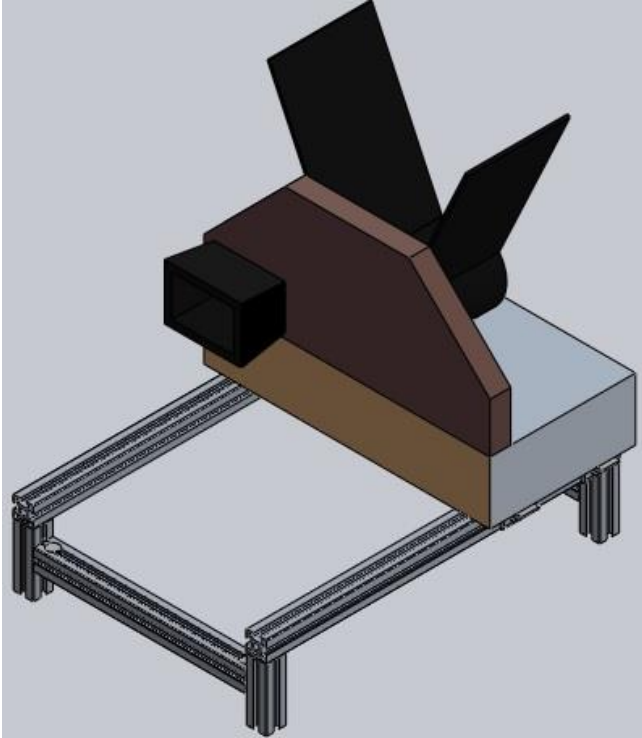


Figure 42: PPT Mount with the MTU

In order to prevent the MTU's emissions from directly impinging on the interior of T4, the team also designed and manufactured a baffle. The baffle was shaped by bending a piece of aluminum sheet metal found in WPI's Manufacturing Lab. The metal sheet was bent to fit squarely around the sides of the main runners and face the MTU's active "thruster head" as shown in Figure 43. The main runners are connected to the baffle through four holes using four compact head end-feed fasteners. The CAD drawing of the PPT mount and Baffle can be found in Appendix A.4

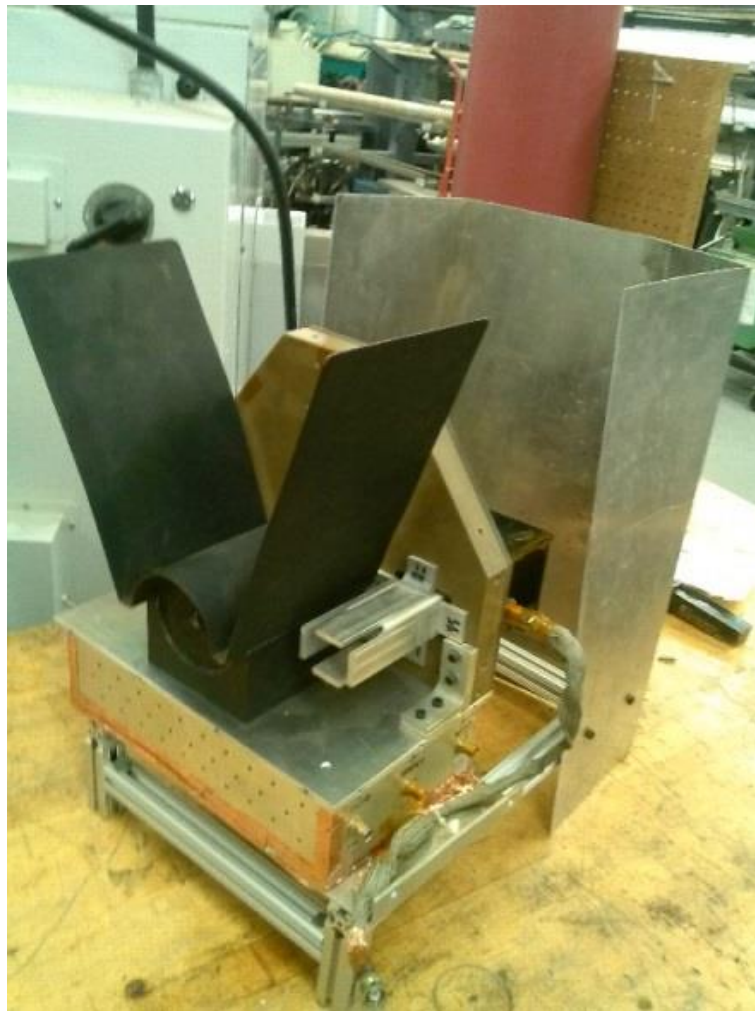


Figure 43: Plume Baffle around the MTU

3.3 MTU Integration

Electrical Wiring

As discussed in Chapter 2, section 2.2, the right side of the MTU has a 25-pin male Sub-D connector which interfaces with the Interface Box. In this project, the MTU is tested inside a vacuum chamber with the Interface Box outside. Thus, an electric connection is needed between their Sub-D connectors, requiring a suitable feedthrough on one of the chamber ports.

After a careful review of Aerojet’s Interface Box pin assignments, the team concluded that full control could be achieved using only 15 of the 25 pins on the connector. This meant control could be achieved using the 15-pin Sub-D electrical feedthrough already on the chamber, eliminating the need to buy a 25-pin Sub-D feedthrough. Therefore, the team took advantage of T4’s 15-pin double sided Sub-D feedthrough shown in Figure 44, and its detailed pin assignments are listed in Table 7.



Figure 44: T4’s 15-Pin Double Sided Sub-D Feedthrough, outside (left) and inside (right)

Table 7: T4’s 15-Pin Double Sided Sub-D Feedthrough Pin Assignments

15-Pin Sub-D Outside (air-side)	15-Pin Sub-D Inside (vacuum-side)
1	8
2	7

3	6
4	5
5	4
6	3
7	2
8	1
9	15
10	14
11	13
12	12
13	11
14	10
15	9

In order to achieve a wiring connection through T4’s feedthrough, the team purchased four, solder-terminal, Sub-D connectors from Newark Element 14. The two 15-pin female (model: 79K5028) connect to the inside (vacuum-side), and outside (air-side) of T4’s feedthrough. While the 25-pin male (model: 93K4294), and 25-pin female (model: 93K4295) connect to the Interface Box and the MTU respectively.

The team soldered 15 American wire gauge (AWG) 20 wire leads, with stranded silver conductor, from pins in the 25-pin Sub-D to the corresponding ones in the 15-pin Sub-D. A detailed pin assignments relation between the four 15-pin and 25-pin Sub-Ds is shown in Table 8, which is adapted from the original Aerojet’s MTU operating procedure [29]. For more information about the assignment of each pin, see Chapter 2, section 2.1.2 and Appendix A.3.

Table 8: 15 to 25 Sub-D Connection Pin Assignments.

25-Pin Sub-D	15-Pin Sub-D	15-Pin Sub-D	25-Pin Sub-D	Assignment
Outside (air-side)		Inside (vacuum-side)		
1	1	8	1	Cap Charge TLM
2	2	7	2	Cap Charge TLM RTN
3	3	6	3	D.I Voltage TLM
4	4	5	4	D.I Voltage TLM RTN
5	5	4	5	D.I #1 Fire TLM

6	6	3	6	D.I #1 Fire TLM RTN
12	7	2	12	Cap Charge Command
13	8	1	13	Cap Charge Command RTN
14	9	15	14	D.I #1 Fire Command
15	10	14	15	D.I #1 Fire Command RTN
21	11	13	21	Bit '0'
22	12	14	22	Bit '1'
23	13	11	23	Bit '2'
24	14	10	24	Bit '3'
25	15	9	25	Bit RTN

Note: TLM: Telemetry, RTN: Return

Once soldered and zip-tied, continuity was checked between each pin in the two 25-pin to 15-pin Sub-D sets using a multimeter. This assures that each pin is only connected to (and only to) the corresponding pin as described in Table 8. The bare wire that extends from the solder cups were sealed using McMaster-Carr's moisture and crack resistant liquid electric tape (model: 76425A51).

The cable that joins the feedthrough's inside Sub-D to the MTU is 3ft long. While the one that connects the outside feedthrough Sub-D to the Interface Box is 6ft long as shown in Figure 45. This allowed the team to move the Interface Box where desired while testing the MTU.

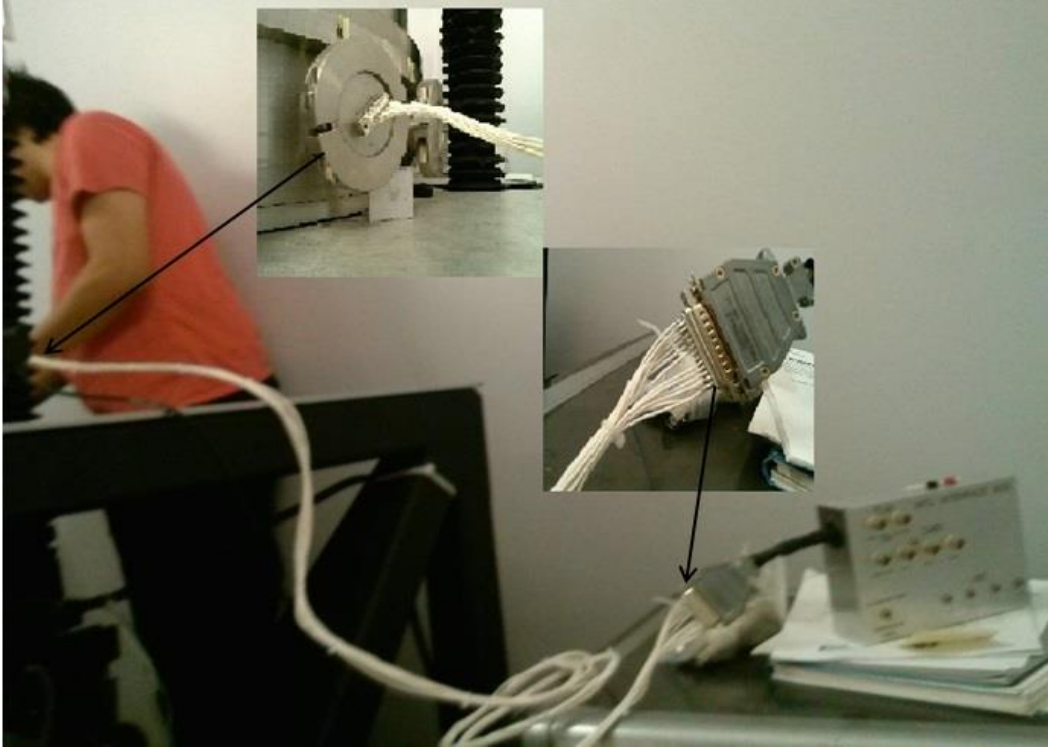


Figure 45: Sub-D Connection between the Interface Box and T4's Feedthrough

The team was able to distinguish the rest of the required connections by referring to Aerojet’s general MTU operation procedure. The most important connection is the one from the MTU to the power supply through the vacuum chamber. Using T4’s single ended, grounded shield coaxial feedthrough shown in Figure 46, the team was able to make the needed connection.



Figure 46: T4's Single Ended, Grounded Shield Coaxial Feedthrough, outside (left) and inside (right)

For the vacuum chamber side, the team designed two connections from two Kurt J. Lesker Be/Cu inline barrel connectors (model: FTAIBC094) to two banana jacks using a 14 AWG (stranded copper conductor) with a 600V rating wire and heat shrink tubing. The two inline barrel connectors connected to the inside of T4's coaxial feedthrough while the banana jacks connected to the side of the MTU.

For the air-side, the team designed two connections from two Newark 4.92ft RG59/U male to male BNC cables (model: 18J2365). One BNC connector end was cut off each cable, creating two single ended BNC cables, and then, the bottom of each cable was stripped and connected to two banana jacks. The banana jacks connected directly to the power supply.

Another connection the team prepared was from the DAQ to the Interface Box, which was achieved using two Newark 6.56ft RG59/U male to male BNC patch cords (model: 18J2366). The two cables were cut in half making four single ended BNC cables, and then, the bottom of each cable was stripped in order to connect to the appropriate DAQ pin. The four male BNCs connected to the corresponding female BNCs in the Interface Box. Table 9 shows a detailed relation between the DAQ pins and Interface Box BNCs. The BNC cables are grounded through the Interface Box, which is grounded through the negative end of the power supply.

Table 9: Assignment List of DAQ Pins to Interface Box BNC Connections

DAQ Pin	Interface Box BNC
2	Charge Cap Telemetry
5	D.I Voltage Telemetry
14	Cap Charge Command
14	D.I #1 Fire Command

3	Ground
6	Ground
16	Ground

3.4 Spectrometer Integration and Data Acquisition

In order to collect emission data (spectra) while the MTU is firing in the vacuum chamber, the team used SpectraSuite (Ocean Optics, Dunedin, Florida), which is a software package that is included with the Ocean Optics High Resolution Spectrometer HR4000. In order to test the integration of the spectrometer with SpectraSuite, the team pointed the fiber optic probe to light in real time and received the display of spectra shown in Figure 47.

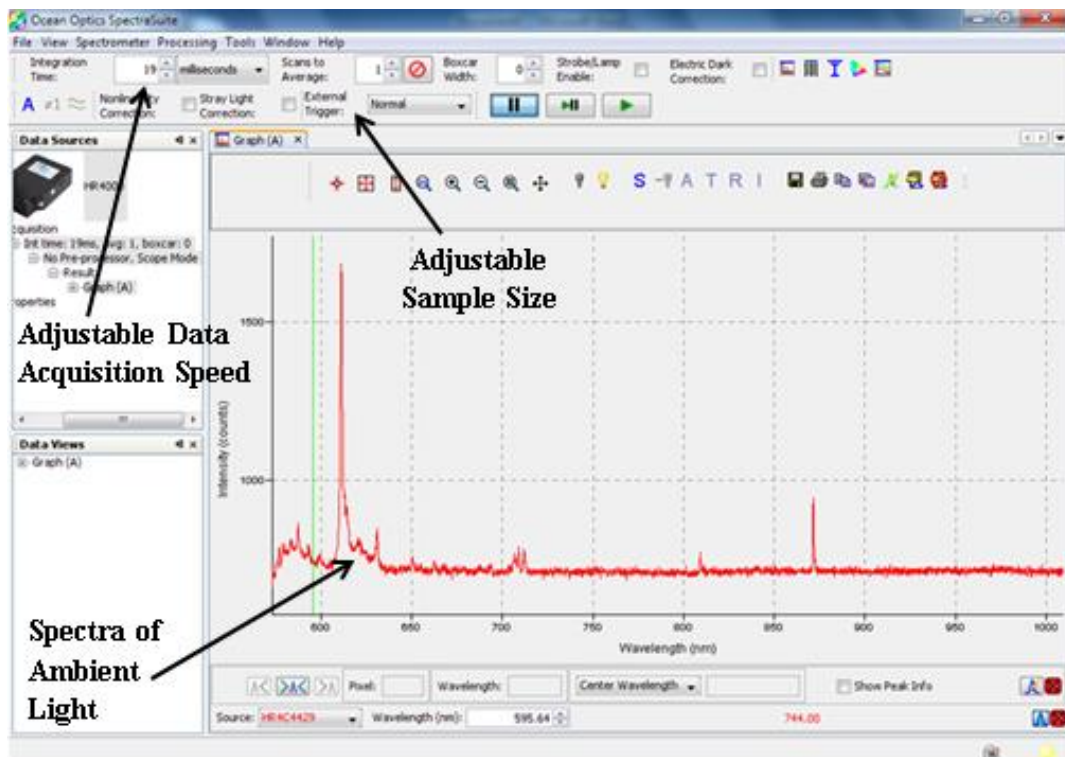


Figure 47: Screenshot of SpectraSuite Software User Interface

The software allows for an adjustable integration time, allowing for adjustment of the light collection (photon counting) time, and also allows one to select the number of scans to

average for each refresh of the plot. A useful feature is the ability to save the spectra at a given time and compare it to the current live feed ^[30]. This will be useful in order to compare the makeup of the PPT emissions corresponding to different energy levels in the capacitor (and hence pulse energy). After we identify the peak wavelengths present in the spectra, we can specify a particular wavelength and track and display the intensity of that wavelength over time. We hope this will allow us to draw some conclusions about how the operational parameters such as energy, pulse rate, and duty cycle, affect the makeup of the “light pollution” from a spacecraft firing a PPT. Such information could help in the design of optical filters for spacecraft flying in formation near another spacecraft using a PPT

3.5 LabVIEW Integration and Implementation

In order for an operator to have full control of the MTU, a LabVIEW Virtual Instrument (VI) was developed to send commands to, and receive telemetry from, the MTU. Segments of the VI were developed separately. The team created the Binary Calculator first; then worked on developing buttons and other user interfaces for the abort command, experiment time, pulses per second, signal display, and pulses-on-demand. To communicate with the MTU Interface Box, LabVIEW uses a data card I/O device (DAQ). In this project, a DAQ model NI USB-6009 is used ^[31]. For the VI instructions referred to Appendix A.5.

Goals

The desired goals for the VI were to:

- Control the number of command pulses sent to the MTU per second.
 - The maximum number of command pulses per second was limited by a minimum command signal length of 0.5 seconds as specified by Aerojet ^[29].

- To ensure that the MTU consistently and correctly interprets a command to fire, each command pulse was set to have a duration of 0.6 seconds (instead of the minimum of 0.5 sec). With this value, the frequency was limited to approximately 1.5 command pulses per second (or 1.5 Hz pulse rate). These are controlled via a knob on the VI Front Panel as shown in Figure 48, part A.
- Set a range of time for the MTU firing experiment, i.e. a duration of time over which command pulses would be sent at the specified rate.
 - This allowed the command pulses per second to continue for a desired time only.
 - The maximum firing duration was set to 20 seconds, an arbitrary value set as a safety precaution. This is controlled via a slider shown in Figure 48, part B.
- Allow the user to fire command pulses on demand, i.e. “single-shot” operation.
 - This allowed the team to observe individual PPT pulse flashes, in addition to a set pattern of PPT pulse flashes.
 - The length of the individual command pulses was determined to be 0.928 seconds, as specified by Aerojet ^[29].
 - The single-shot button is shown in Figure 48, part C.
- Provide a visual indication of the command pulse signal, capacitor charge state, and Discharge Initiator (DI) charge state.
 - The telemetry (TLM) from the MTU Interface Box, shown in Figure 49, output two signals ranging from 0-5V, which corresponded to 0-2000V for the capacitor (approximately 400 V on main capacitor per V from telemetry) charge and 0-800V for the DI charge (approximately 160 V on DI capacitor per V from telemetry).

- The VI received the voltage levels from the MTU Interface Box via an external, USB connected, DAQ and scaled them to the actual voltage levels of the capacitor and DI, as shown in Figure 48, part D.
- Provide a means for the operator to stop the command pulses to the MTU in an emergency.
 - This was accomplished with the abort button shown in Figure 48, part E, which overrides the pulse rate and single-shot button to ensure that the MTU ends any firing sequence in progress.
- Translate desired voltage levels into a binary bit position.
 - The Binary Calculator shown in Figure 48, part F, took the binary level desired (1-16) and translated it into the bits required to be ON.
 - The calculator gave a visual display of which switches on the MTU Interface Box needed to be pushed on. The switches are shown in Figure 49 along the bottom.

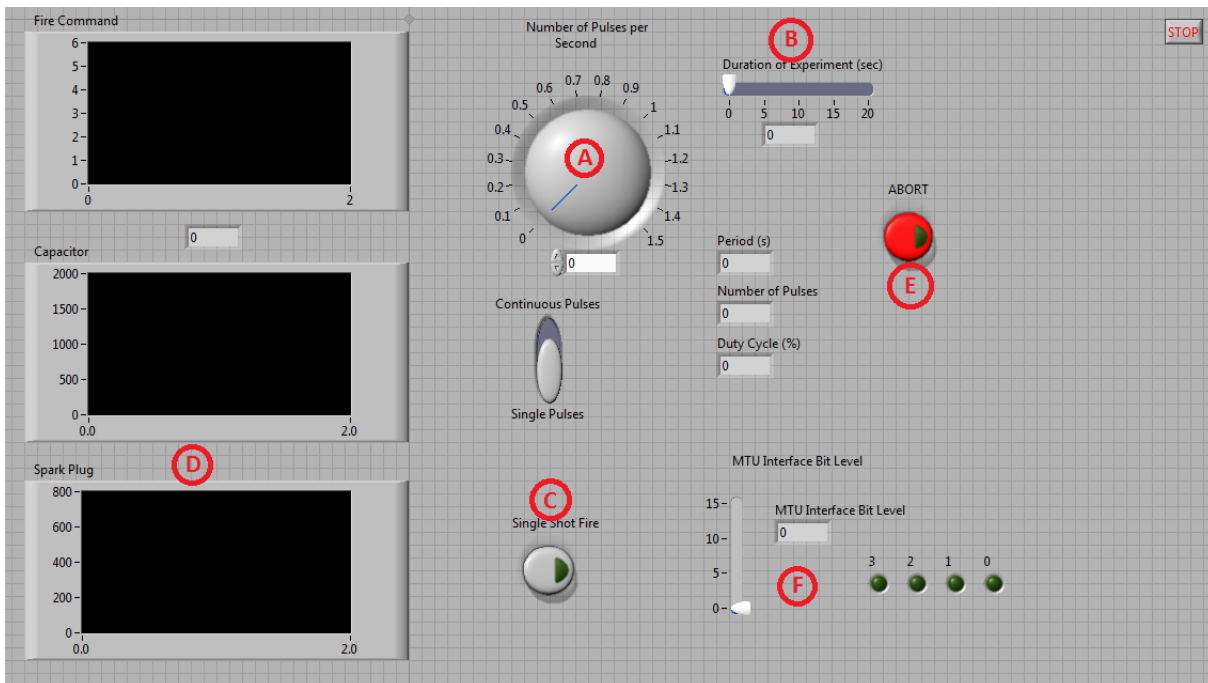


Figure 48: LabVIEW VI Front Panel



Figure 49: MTU Interface Box

Construction Problems

Throughout the development of the VI, the team ran into issues with the specific length of the command pulses, the single-shot button, and the VI not creating a signal in real time.

LabVIEW was extremely helpful in that it has pre-created modules that can act as various devices, including a signal generator of various kinds, including triangle, sine, and square waves. The team used the latter to create their command pulses, which when combined with the frequency and duration knob, it created the desired command pulses per second. LabVIEW also includes a “DAQ Assistant,” a module for communicating with the outside world through the various connections on the DAQ itself.

The frequency value, set by the knob on the control panel, would be used by the Square Wave generator to create the appropriate frequency and report the calculated Duty Cycle. Duty Cycle is the percentage of time within a cycle that a particular signal is considered “on,” or in this case, producing an output of 5V.

By default, the Square Wave generator module of LabVIEW has a set Duty Cycle of 50%. For a frequency of 1, this would mean that there would be 500 ms of a 5V signal, and 500 ms of 0V, resulting in a total Cycle Time of 1 second. Cycle Time is defined as the total time from beginning of pulse to beginning of next pulse. Table 10 shows how the Duty Cycle of 50% relates to the command pulse time. The 0.83 Hertz was included to show the one case where a 50% Duty Cycle does coincide with 0.6 s of 5V.

Table 10: 50% Duty Cycle

Frequency (Hz)	Cycle Time (s)	Duty Cycle (%)	5V time on (s)
0.25	4	50	2
0.5	2	50	1
0.83	1.2	50	0.6
1	1	50	0.5

The team modified the Duty Cycle within the VI so that it would always create an on time of 0.6 seconds, the desired command pulse time. To achieve this, the frequency (in Hz) would be multiplied by 0.6, and then further multiplied by 100%, resulting in a final Duty Cycle unique to that particular frequency. Table 11 shows how this method produced the desired effect.

Table 11: Variable Duty Cycle

Frequency (Hz)	Cycle Time (s)	Duty Cycle (%)	5V time on (s)
0.25	4	15	0.6
0.5	2	30	0.6
0.83	1.2	50	0.6
1	1	60	0.6

The single-shot button was supposed to, as described above, create a single command pulse for the MTU. The team realized that the Frequency Knob was altering the length of the command pulse, because the Square Wave generator in the VI was still adjusting the duty cycle according to the frequency. The desired outcome was a set length of the single command pulses, and thus, to resolve this problem the team set the single-shot button to also correspond to a frequency of 1, which would set the Duty Cycle to the correct percentage and consequently the single command pulses to 928 ms.

Once the DAQ was connected to the VI, the team attempted preliminary tests by connecting the DAQ to itself. This was done by creating a command pulse of 5V for a set frequency, and observing if the DAQ was reading the signal correctly. The team quickly realized that the VI was generating the pulses at a fraction of the frequency that it was originally set to. This was caused partly by the Square Wave generator's signal generation speed and partly by the DAQ Assistants, described below. Thus, the team slowed down the Square Wave generator to 50 data points per second, and removed the DAQ Assistants.

The DAQ Assistants are designed to connect with the outside world and are used for a wide variety of applications, so they have a lot of prepackaged programming that simply was not being used in this particular VI. To hopefully reduce the complexity of the VI, the team replaced the DAQ Assistants with "task managers," simpler modules that have only one function, and should therefore be less complex.

In order to test these final changes, the DAQ was connected to an oscilloscope and run for both single-shot and continuous modes. Figure 50 shows the result of this test. In the end,

these changes and corrections resulted in a successful communication between the VI and the MTU Interface Box.

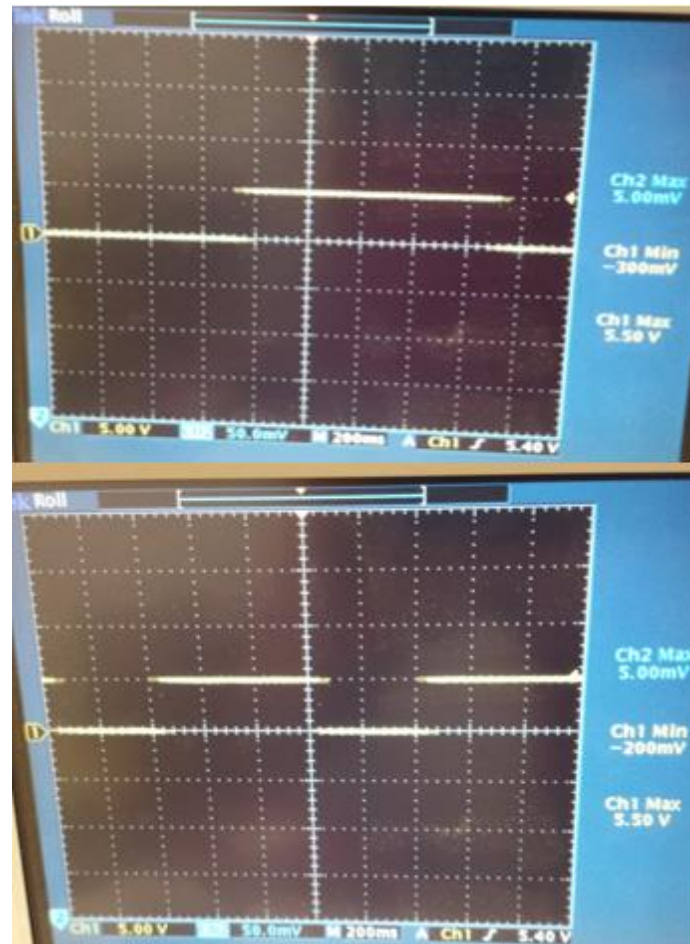


Figure 50: Test of VI with Oscilloscope, single pulse (above) and pulse train (below)

LabVIEW Flowchart

Figure 51 shows the basic flow of how the user inputs result in command pulses and Binary Bit Levels, and also shows how the VI does very little to TLM inputs from the Interface Box, which are displayed in the VI with an oscilloscope style interface.

1. Setting the Pulse per second knob and the Duration slider (Figure 51, A and B respectively) determines the total pulses over the duration of the experiment and the period directly, as shown in Figure 51A.
2. The Duty Cycle percentage is determined by the VI with additional values for how long each particular pulse has to be, in Figure 51B.
3. With the combination of the internal values for the amplitude and phase with the Period of the pulses (total on+off time for a full cycle), the Square Wave Generator, Figure 51C, creates the command pulses at the desired frequency. This also corrects the signal length in order for the Interface Box to interpret the command pulses as firing commands. This train of command pulses is then sent to the Interface Box, Figure 51D.

In addition to creating the MTU command pulses, the VI acts as a Binary Calculator for the Interface Box switch positions as well as a scope for the Interface Box TLM inputs, pictured in Figure 51E. More information about the wiring of the VI can be found on Appendix A.6.

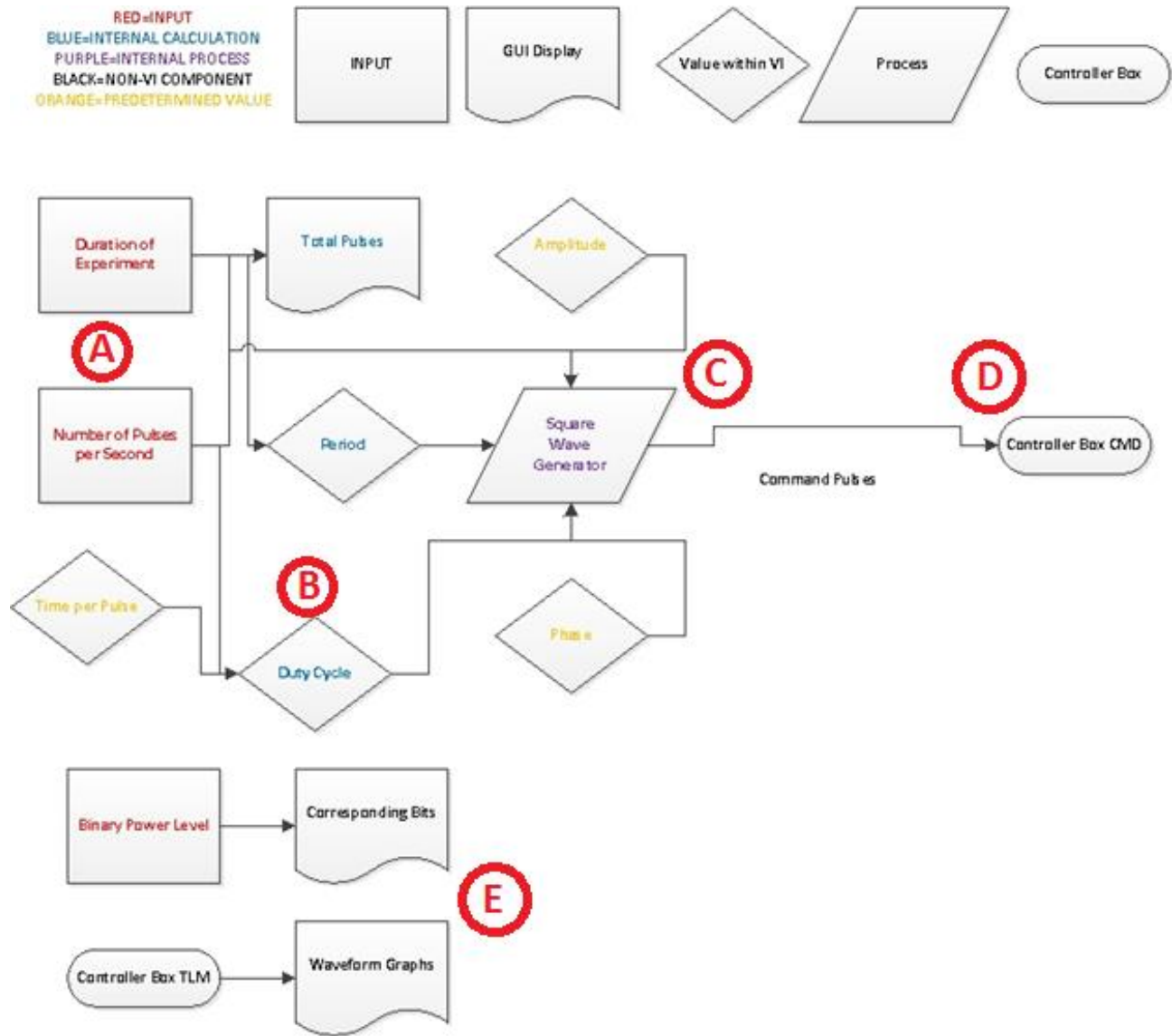


Figure 51: LabVIEW Flowchart

CHAPTER 4. EXPERIMENTAL RESULTS AND DISCUSSION

4.1 Test Plan

There were many considerations and challenges the project team addressed to integrate all system components into an effective experimental setup. The project team identified power supplies available in the project advisor's laboratory and which could be used for testing. The main 28VDC power supply for the MTU required fabrication of custom cables for connection to both the outside and inside of the T4 collar. Custom connections for communication between the DAQ and Interface Box were also fabricated. Fixtures for the MTU and fiber optic probe were also designed and integrated. Software for the fiber optic probe was installed on the laboratory PC. A LabVIEW VI was developed for enhanced control of the Interface Box and ease of use for the operator. A basic block diagram of the experimental setup can be seen in Figure 52.

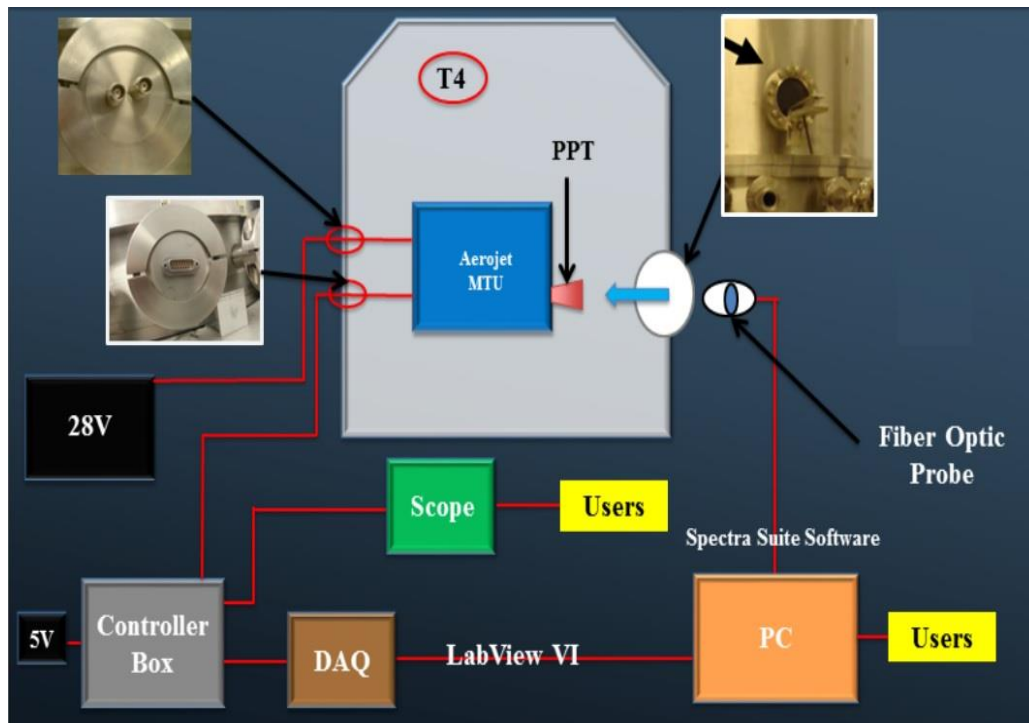


Figure 52: Block Diagram of the Experimental Setup

Power Supplies

A total of two power supplies were acquired for the experimental setup. A dual power supply, capable of providing 28VDC as well as the 5 VDC used to power the Interface Box, with adjustable voltage and current control, was selected for integration with the MTU. This power supply was obtained from one of WPIs labs for the project team.

NW50 Custom Adapters

The collar flange ports on T4 are listed in Table 3 in Chapter 2, section 2.2.3. Port #05 is a double BNC feedthrough adapter which is the access point for the 28VDC MTU power supply. The NW40-NW50 feedthrough adapters on ports #01 and #06 interface with the fiber optic probe, which uses an NW40 feedthrough. On port #07 there is an NW50 15-pin Sub-D double-sided feedthrough which interfaces with the custom cabling designed for communication between the Interface Box and the MTU.

Wiring

The Interface Box and MTU are connected with a 25-pin Sub-D connection, but since the NW50 feedthrough adapters for 25-pin access are too expensive, the team used T4's 15-pin Sub-D double-sided feedthrough. The team fabricated custom cables with adapters for 25-pin to 15-pin connection. This was made possible by the pin assignments in the MTU system which allowed the project team to choose only the functions which were ultimately necessary for firing the PPT at discrete energy levels. In order to connect the DAQ and Interface Box, stock BNC to BNC patch cables were modified. One end of the BNC connects to standard female BNC jacks on the Interface Box, and the other end was stripped and the leads connected to specific DAQ pin assignments shown in Table 9. The DAQ interfaces with the PC via a standard plug and play USB connection. The 5VDC power supply for the Interface Box uses standard banana connectors.

Connecting the 28VDC power supply to the MTU requires two different sets of custom cables. The first set connects the power supply on the outside of the chamber to the female BNCs on port #05. These cables are custom made from BNC-BNC stock. One end connects directly to port #05, and the other end is stripped with the leads attached to banana jacks for connection to the 28VDC power supply. The second set connects the inside of port #05 to the power input on the MTU. Two inline shaft connectors connect the inside of port #05 to two banana jack inputs on the MTU.

The fiber optic probe was taped to T4's bell jar window instead of being attached to the plume baffle due to time constraint and manufacturing difficulties. The fiber optic probe was also covered by a black cloth in order to reduce interference of the plume's spectral response by ambient light. During testing, the team did not use the plume baffle since the MTU was only firing under single-shot option. Figure 53 below shows the single-shot MTU emission light during a main discharge firing. This was done after going through all of the checkout and set-up procedures listed in Appendix A.3.



Figure 53: Single-Shot MTU Emission Light

Software - User Control

The Interface Box and DAQ allow an operator to control firing of the MTU remotely with the LabVIEW VI. The VI is also capable of sustaining autonomous firing of the MTU to obtain larger string of data. The operator is also able to collect data from the fiber optic probe through the SpectraSuite software. For example, the user may save the ambient light level present in the T4 chamber prior to performing the experiment, and then subtract that from the spectral response during firing of the PPT. The probe may also be used for spectral identification of plume constituents which are deposited on the plume baffle as a result of PPT firing.

4.2 Sensitivity of Spectra to Pulse Energy and Repetition Rate

When attempting to adjust the energy level transferred to the MTU using the Interface Box, the voltage across the capacitor dropped. Initially, the team suspected that there was a short inside the MTU causing the malfunction; however, once they closely reviewed the Aerojet MTU procedure, they remembered that the adjustable energy level function had been disabled by Aerojet before the unit was sent to WPI. The existing default setting permanently set the energy level to the maximum of approximately 40 Joules. Since enabling the adjustable energy level function would require extensive knowledge of the MTU circuitry, the team decided to only observe the emission spectra at the maximum energy level.

4.3 Discussion of Results

LabVIEW VI

The LabVIEW VI was used to fire the MTU at a frequency of 1 command pulse per second. The Capacitor and Spark Plug graphs shown in Figure 54 indicated charging as expected. These plots were also compared with the oscilloscope traces during testing and appeared correct.

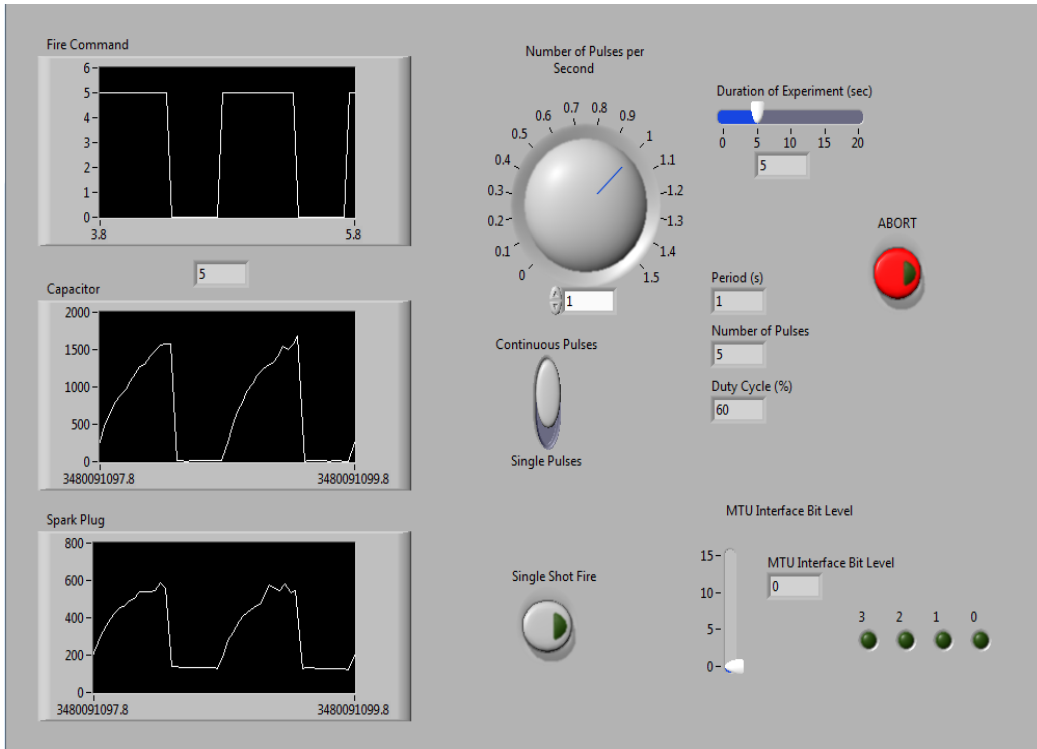


Figure 54: LabVIEW VI Results

The LabVIEW VI performed as needed and performed all the required functions as intended for the completion of the project.

Spectrometer

The experiment was conducted by setting all of the energy level bit switches on the MTU Interface Box to zero. The SpectraSuite software was then set to gather data continuously for a period of three seconds, with an integration time of 3800 microseconds. During this time, a single pulse was fired using the LabVIEW VI, and then the frames during which the pulse took place were examined. The frequencies at which the intensity of the photon count peaked were compared to emission lines that the background research claimed to indicate the presence of certain ions ^[16] ^[19] ^[20]. The conditions and SpectraSuite settings used in all of the tests are listed in Table 12.

Table 12: Test Conditions and SpectraSuite Settings

Vacuum chamber pressure	4.5E-5 Torr
Spectrometer range	500nm-1000nm
Integration time	3800 microseconds
Boxcar width	0
External trigger mode	Normal
Capture period	3 seconds
Scans to average	1
Correct for electrical dark	No
Correct for detector non-linearity	No
Correct for stray light	No
Energy level switch positions	0000

Since each frame was taken 3800 microseconds apart, no individual test was able to form a complete timeline of the pulse cycle. Therefore, the team conducted three tests, each capturing a different moment of the discharge. During the first test pulse, the spectrometer collected data, which was plotted on the graph shown in Figure 55. The graph has intensity on its y-axis, measured by photon count, and wavelength measured in nanometers on its x-axis.

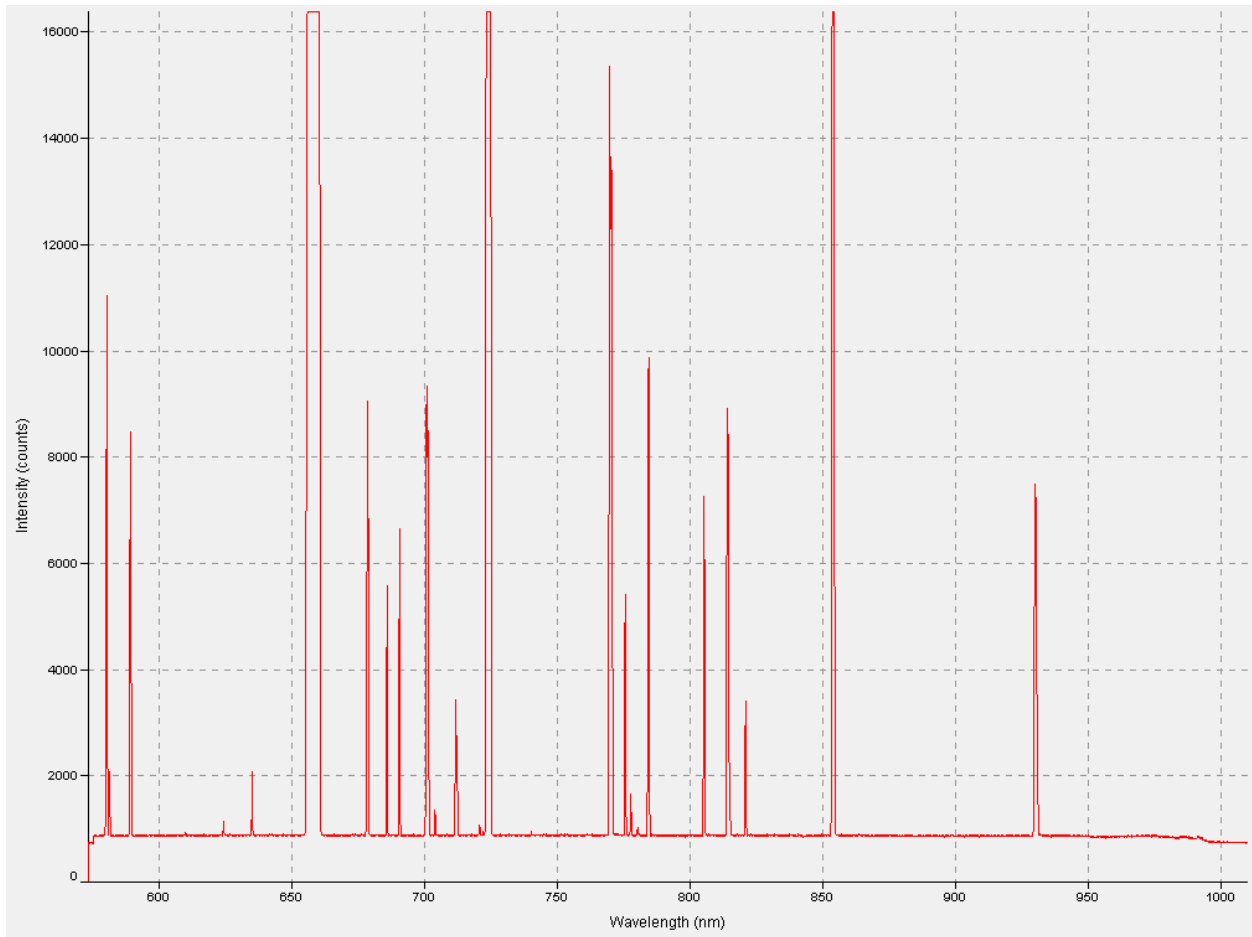


Figure 55: Spectra from Test 1

The second test pulse yielded two spectra with detected emissions. The first spectra is shown in Figure 56 and it does not appear to have discernable peaks at specific emission lines, rather it seems to have saturated the detector across the entire spectral range. This may be the result of the initial flash from the thruster overloading the spectrometer, since the spectrometer has a maximum measurable intensity of 16000 photons, meaning the readable data that was recorded by SpectraSuite in Test 1 was actually the emissions at a time a few milliseconds after discharge.

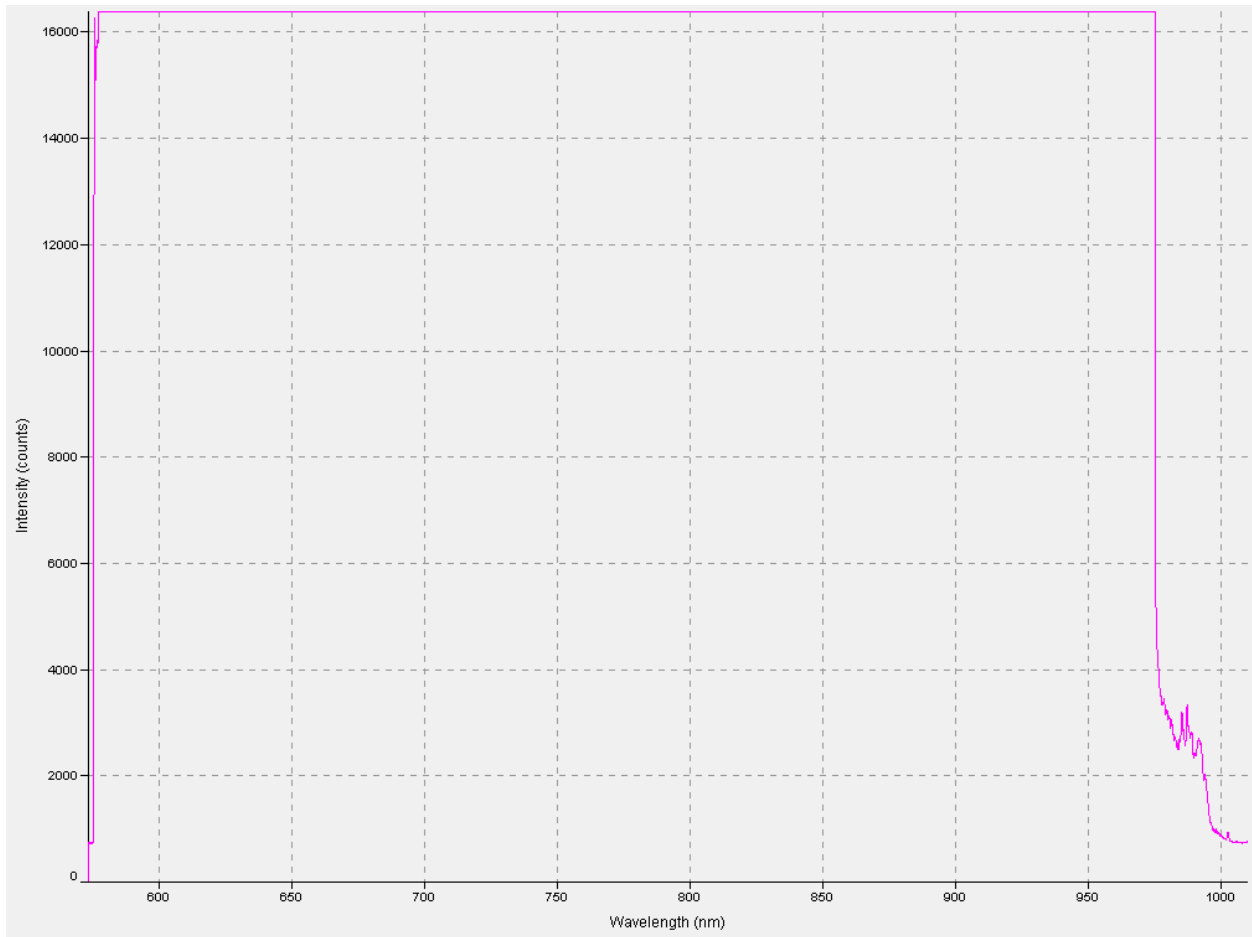


Figure 56: Spectra from Test 2.1

The next spectrum recorded by SpectraSuite reveals the specific emission peaks that remain after the initial discharge. Since the data is not identical to the first test, it illustrates how quickly the emissions dissipate after discharge, reducing from saturation of the entire spectrum range to much lower in intensity than Test 1 during the spectrometer's short integration time, as shown in Figure 57.

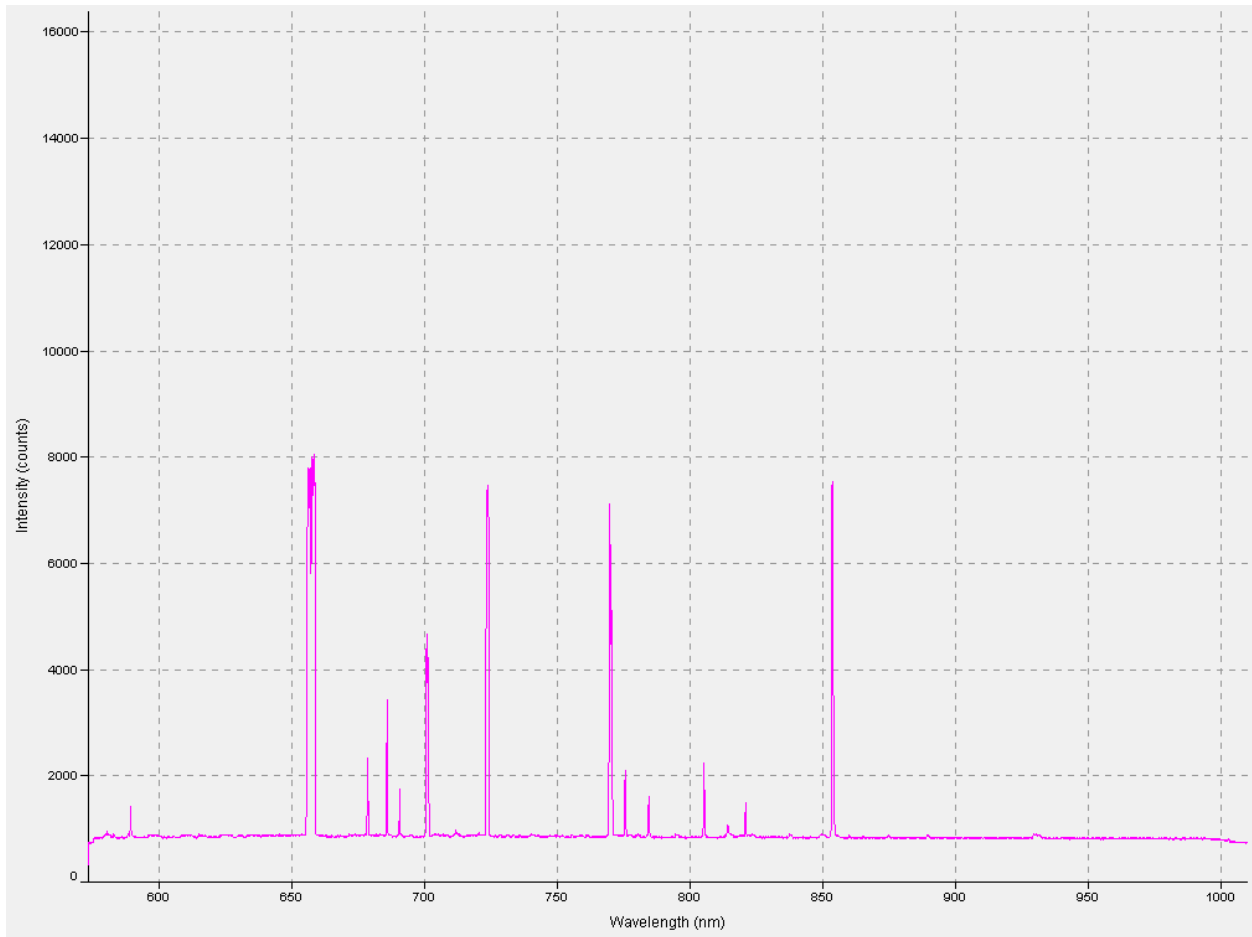


Figure 57: Spectra from Test 2.2

The first spectrum taken from test 3 also appears to be the result of activity other than the main discharge of the thruster. A small peak that does not collaborate with the peaks from the second spectrum from Test 3 seems indicative of the spark plug firing before the ablation of the Teflon, as seen in Figure 58.

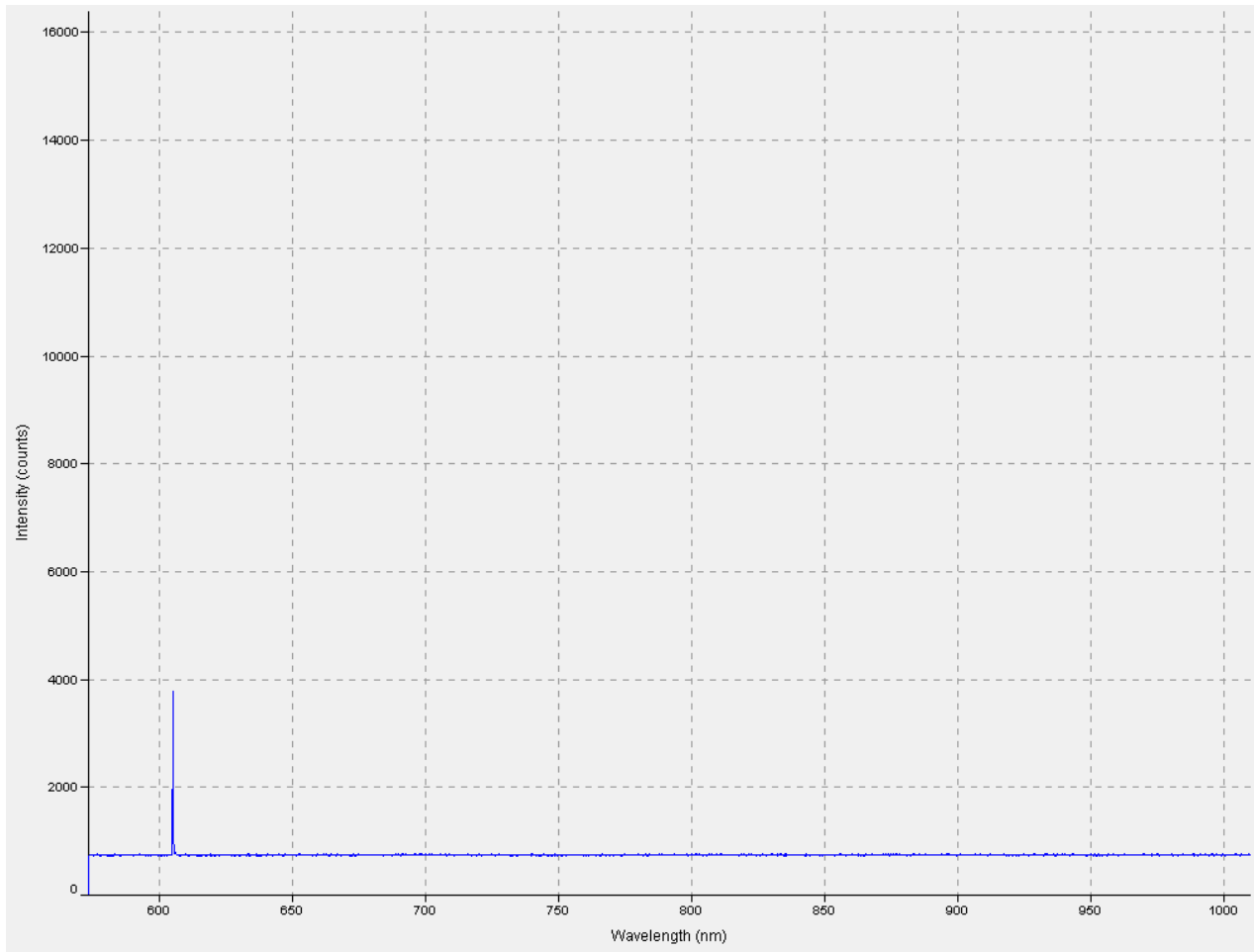


Figure 58: Spectra from Test 3.1

The next spectrum recorded during Test 3 again displays a very different level of intensity at all peaks compared with the other two tests. This demonstrates how much the emissions dissipate during even the spectrometer's minimum integration time, as shown in Figure 59.

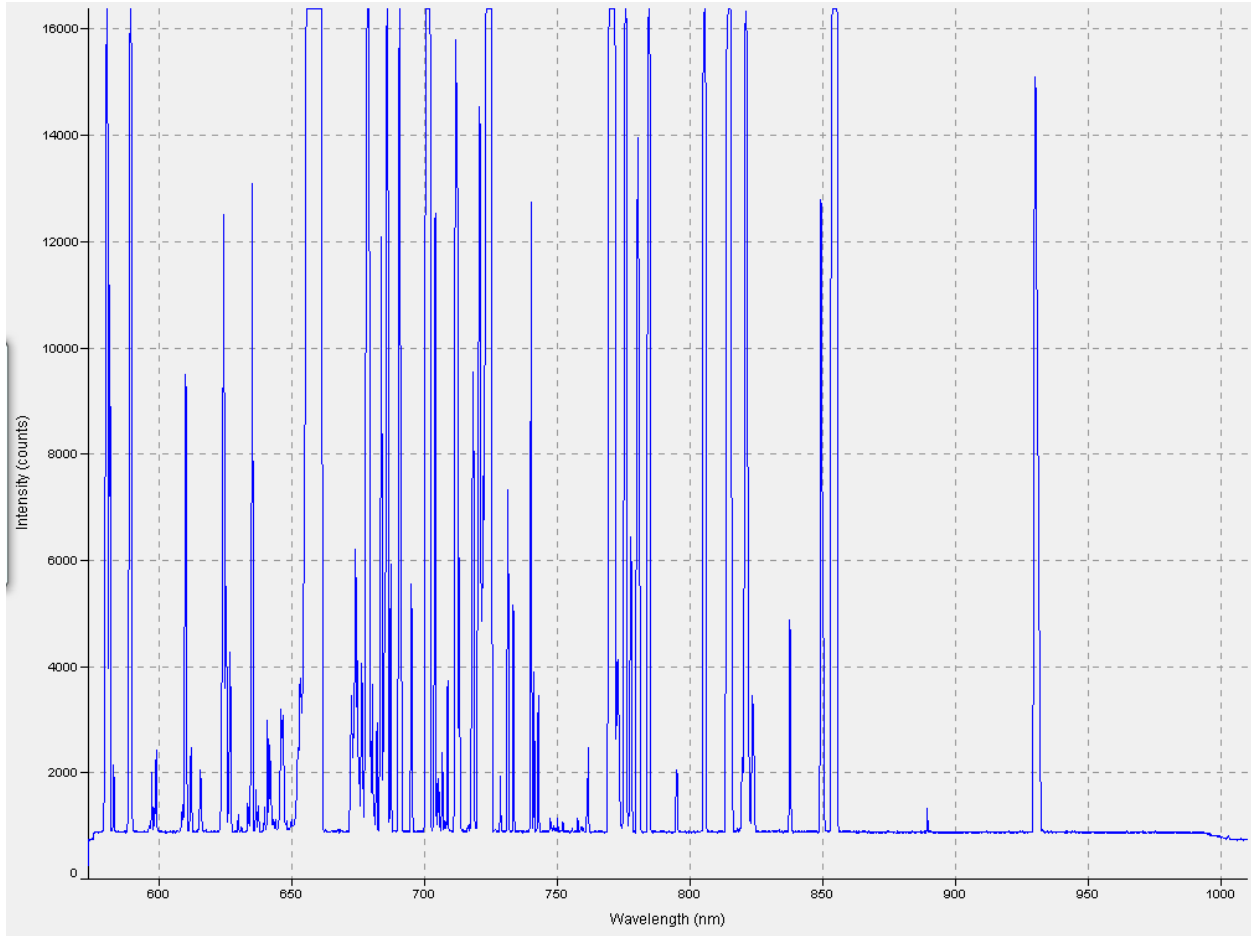


Figure 59: Spectra from Test 3.2

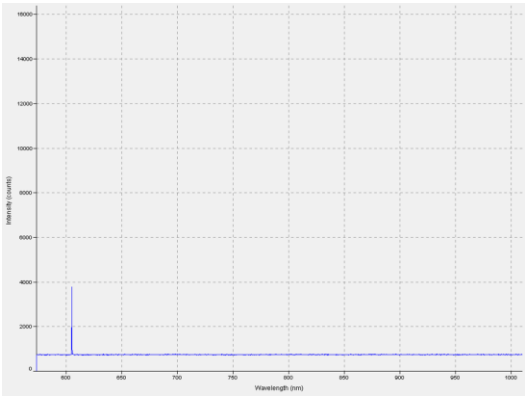
A full timeline of the pulse cycle is presented in Table 13. Since all of the tests besides Test 3.1 form a continuous decrease in intensity while maintaining the same peak locations, it can be concluded that Test 3.1 takes place before the main discharge.

Table 13: A Full timeline of the Pulse Cycle

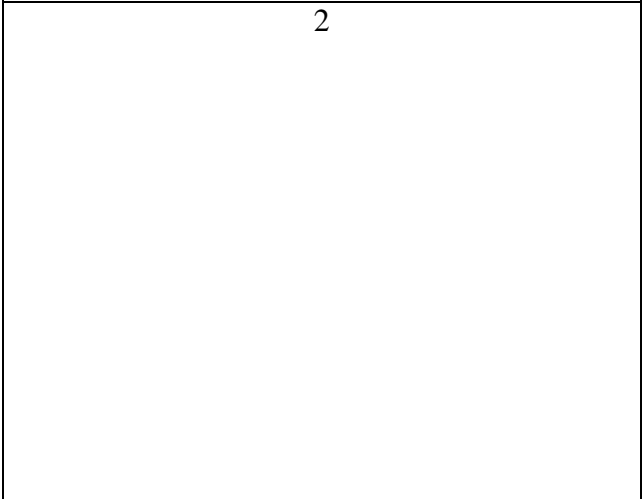
Test Chronological Order	Plot
1	3.1



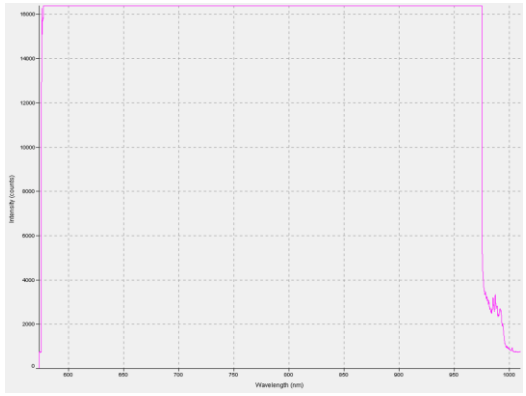
2



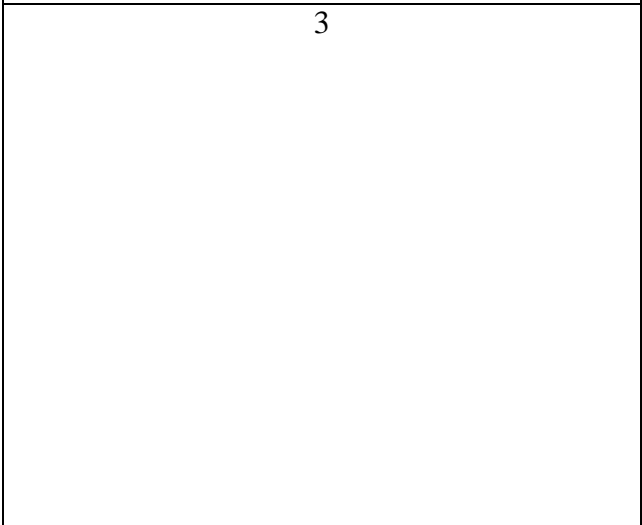
2.1



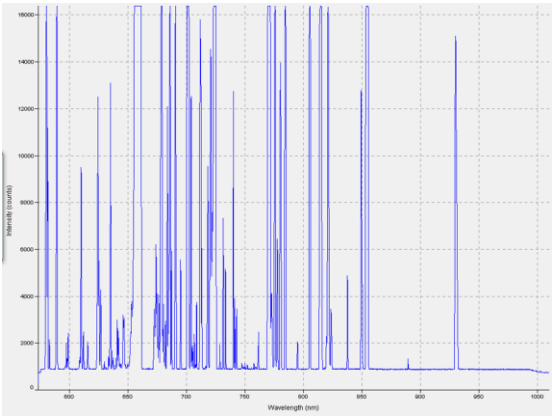
3



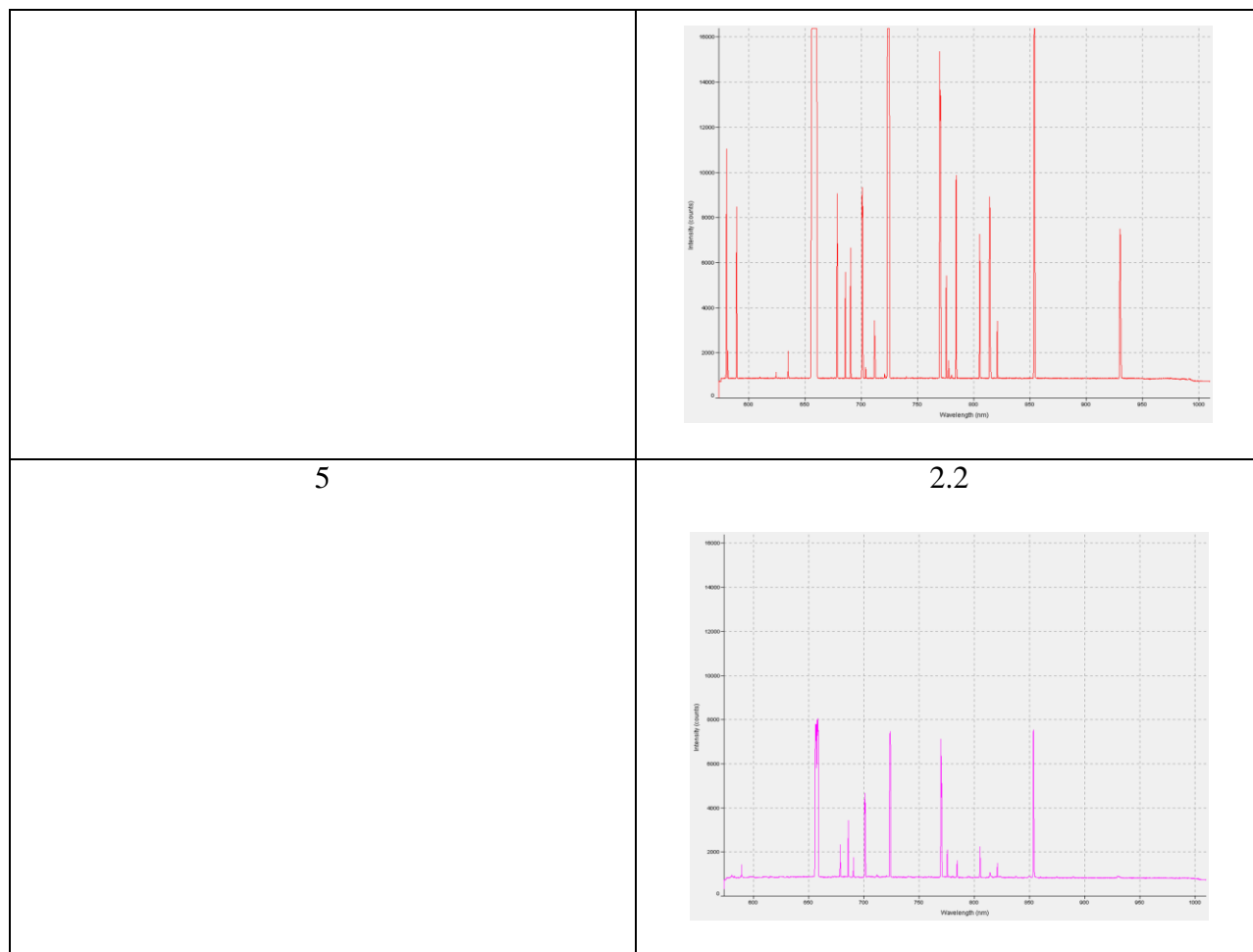
3.2



4



1



Many of the recorded emission peaks correspond to the ion species previously found to be contained in emissions of Teflon PPTs. Table 14 relates some of the peaks in the test spectra to ions expected to be present [20].

Table 14: Plume Species Identified by Spectral Peak [20]

Test	Emission Line (nm)	Species
1, 2.2, 3.2	589.17	C+
1	634.8	F
1, 3.2	658	C+

1, 2.2	685.6	F
1, 3.2	704	F
3.2	712.8	F
1, 2.2, 3.2	723.1	C+
1, 2.2, 3.2	723.6	C+
1, 2.2, 3.2	775.4	F

Since some of the tests were cut off at the spectrometer's peak intensity of 1600 and a few of the peaks are closely clustered, there is an ambiguity in the exact positions of the maximum peaks; however, all the peaks that can be identified after the intensity drops to manageable levels correlates within one nanometer to the emission lines of the ions presented in Table 14. Some ions reported in the background research were not detected, but the reported corresponding emission lines were less than 500 nanometers, so they would be invisible to this spectrometer ^{[16] [19] [20]}.

CHAPTER 5. CONCLUSIONS AND RECOMMENDATIONS

5.1 Conclusions

Based on WPI's MQP learning objectives, the team achieved the following:

- *Apply fundamental and disciplinary concepts and methods in ways appropriate to their principal area of study.*

A LabVIEW VI was developed to remotely control the firing of the MTU inside T4. This required optimization of the VI, and troubleshooting of any problems that occurred through the initial checkout and set-up operations. The VI successfully controlled single-shot and autonomous operation of the MTU.

SpectraSuite software was installed on Fluids Lab HL016 computer in order to analyze the data from the MTU. The spectral response of the MTU plume was analyzed effectively using this software.

A PPT mount and plume baffle were designed and constructed by the project team. The construction of the stand and baffle were completed with the assistance of the Washburn Shops' staff and tools.

A budget was meticulously kept throughout the course of the project in order to track expenditures. The team members were required to complete purchase orders for all of the products ordered. The team was able to meet the project goals while remaining under budget.

A timeline (Gantt Chart) was used during the first two-thirds of the project. The purpose of this chart was to keep the project group organized and on task to meet sub-objectives and minor milestones that were required for meeting the overall project goals.

- *Demonstrate Skill and knowledge of current information and technological tools and*

techniques specific to the professional field of study.

The integration of the MTU with the T4 vacuum system and the Interface Box required substantive construction of wire assemblies, components and custom connections. Due to this requirement, the team was given the opportunity to gain experience soldering and ordering components from vendors. Also, the team had to complete checkout and set-up of these connections for various procedures in order to verify and complete total system integration.

The team developed a Rate-of-Rise time experiment, complete with data sheet, for the T4 vacuum chamber leak detection and recommissioning process. The rate of rise is an effective metric for characterizing vacuum system technology performance. This experiment led to the discovery of the first major leak source, which in turn led to the discovery of the second leak source, and ultimately the T4 system was recommissioned to a usable state for experimentation both during this project and for the future.

The team designed a PPT mount and plume baffle using 1 inch x-channel and related x-channel fasteners and components. Before the PPT mount and plume baffle were constructed, they were modeled in SolidWorks.

The team developed a modified safety and operational procedure for the MTU, which is based on the original documentation provided by Aerojet Corp. This gave the team ample experience developing a procedure where safety was the primary concern. The MTU procedure was the only procedure that all of the group members were expected to be familiar with due to the high voltage and current present in the charging capacitor of the MTU. The initial checkout and setup procedures were performed with the project advisor, laboratory manager, and some of the team members. In contrast, the single-shot firing of the MTU was performed with all of the MQP team members as well as the project advisor and lab manager. Autonomous operation to

continuously fire the MTU was performed similarly through the use of the LabVIEW VI.

- *Use effectively oral, written and visual communication.*

The team presented nine bi-weekly updates to their aerospace colleagues and professors. The team also presented at one of the closer-look open house events hosted by WPI in D term. In addition, the team presented their final results to their aerospace colleagues, professors and members of industry at the end of the senior year on MQP presentation day. The project team participated in weekly meetings with the project advisor, and also scheduled group meetings of their own throughout the course of the project. Meetings were also schedule between the project team and representatives in WPI's Washburn Laboratory. Furthermore, the team compiled the project information in the form of a professional-quality, MQP report.

- *Identify, analyze and solve problems creatively through sustained critical investigation.*

The project team solved a major problem through the T4 leak detection and recommissioning process. The first minor milestone related to this was the discovery and subsequent replacement of aluminum metal seals with elastomer seals in the T4 collar ports. A second milestone was the discovery of an uncovered valve port on the turbopump, which required a simple component order from Norcal. The pump-down procedure, modified from Ryan Sebastian's original version, was revised several times before it was complete enough for T4 operations to proceed. This required contacting a representative at Leybold for clarification on what pressures were required before the turbopump could be turned on.

Another problem related to the MTU integration was with the NW15 Sub-D feedthrough. Initially the team did not realize the pins on either side of this feedthrough were mirrored, so the wires in the custom -made cable running from the inside (vacuum-side) of the NW15 Sub-D

feedthrough to the 25-pin Sub-D connector on the MTU were reversed. This was discovered during the final stages of MTU integration when the team attempted to fire the PPT through all of the custom connections. Repairing this component resulted in proper response of the MTU.

The LabVIEW VI also presented the team with a few minor challenges. Some of the hard-wired equations in the program required some troubleshooting. WPI's Academic Computing Applications Scientist, Adriana Hera, assisted the team in solving the VI problems.

The PPT mount and plume baffle required custom machining and fasteners in order to attach the spectrometer lens. This was required in order to get a rigid connection for the lens on the baffle in the T4 chamber during experimentation. For final testing in this project, which did not involve many pulses (< 10), the probe was just fixed to the outside of one of the windows on the outside of T4.

- *Integrate information from multiple sources.*

The overall literature review and collection of background information provided multiple sources of information for the team to draw on. Some related areas of research were: PPT Technology, PPT Contamination, Optical Spectroscopy and Vacuum Chamber Leak Detection Methods. In addition to these broad categories, the following specific documents were instrumental in meeting the project goals: The Aerojet Laboratory PPT General Operating Procedure and Ryan Sebastian's directed research study on T4.

- *Demonstrate an awareness and application of appropriate personal, societal and professional ethical standards.*

The team attended weekly MQP presentation meetings, were attentive, and asked questions to their peers when appropriate. This demonstrates effective personal ethical standards.

The team participated in the closer look open house event hosted by WPI for high school students. The team presented information on their MQP that was both exciting and relevant in the real world. This is an example of demonstrating an effective societal ethical standard.

All members of the team thoroughly prepared and rehearsed their final MQP presentation for project presentation day. The team effectively delivered a high impact and professional presentation utilizing effective visual and oral techniques developed throughout the course of the project. This example demonstrates effective professional ethical standards.

- *Practice the skill, diligence and commitment to excellence needed to engage in lifelong learning.*

Consistent and constructive feedback was provided to the team by its own members, the project advisor, laboratory manager, and fellow aerospace seniors and faculty. The team was able to meet the majority of the project goals under budget and in a timely fashion. The recommissioning work performed on the T4 vacuum chamber and the Aerojet MTU will have a lasting impact on WPI's future research and potential student MQP groups. The team also analyzed the results of the PPT plume study in an effort to draw conclusions with substantive real world applications, such as implications for spacecraft integration.

5.2 Recommendations for Future Work

For future projects that require the use of T4's ion pump, the team recommends testing it ahead of time. This is due to the fact that its operation status is unknown since it was not used in this project. For more information about the ion pump and its operation refer to Ryan Sebastian's directed research report on T4 ^[2].

Since the team did not attach the fiber optic lens to the plume baffle and did not perform long term testing (with thousands of pulses), there was no need for the plume baffle as part of this work. The team however recommends that future teams who will be running multiple tests on the MTU to use the plume baffle and attach the lens to it. This could be done by using the existing holes in the plume baffle and the part already bought from McMaster (18 and 12 inches flexible positioning arms (models: 50035A673 and 50035A672, respectively) and 1 inch spring clamp (model: 5107A1).

Currently, the Interface Box is configured to provide operation only at the maximum energy level, 40 J, on the main capacitor. Thus, the team was not able to examine the PPT plume's spectral response as a function of energy level. The Interface Box has the capability to provide 16 discrete energy levels for the main charging capacitor; however, future teams will have to consult with Aerojet, and perhaps reverse engineer pin assignments 21-25 in accordance with the Aerojet Laboratory PPT – General Operating Procedure and the MTU Operational and Safety Procedures in order to realize these capabilities.

REFERENCES

- [1] Cassady, R Joseph, W Andrew Hoskins, Mark Campbell and Christopher Rayburn. *A Micro Pulsed Plasma Thruster (PPT) for the “Dawgstar” Spacecraft*. American Institute of Aeronautics and Astronautics, 2000.
- [2] Sebastian, Ryan. *Vacuum Chamber/Spectrometer: Directed Research Project Report*, 2011.
- [3] Goebel, Dan M and Ira Katz. *Fundamentals of Electric Propulsion*. Hoboken: John Wiley, 2008.
- [4] Nawaz, Anusheh, Riccardo Albertoni and Monika Auweter-Kurtz. *Thrust efficiency optimization of the pulsed plasma thruster SIMP-LEX*. *Acta Astronautica*, 2010.
- [5] [Anonymous]. *PPT Operation Sequence* [online] 2013. Available from: http://www.al.t.u-tokyo.ac.jp/ppt/English/PPT_anime/Solid_PPT.GIF. Accessed 10/1/2013.
- [6] Sutton, George P and Oscar Biblarz. *Rocket Propulsion Elements*, ch. 2. Hoboken: John Wiley & Sons, 2011.
- [7] Kramer, H. J and H. J Kramer. *Observation of the earth and its environment*. Berlin: Springer-Verlag, 1994.
- [8] [Anonymous]. *LES 4 (Lincoln Experimental Satellite 4)* [online] 2013. Available from: http://space.skyrocket.de/img_sat/les-4__1.jpg. Accessed 10/1/2013.
- [9] [Anonymous]. *ETS 4 (Kiku 3)* [online] 2013. Available from: http://space.skyrocket.de/img_sat/ets-4__1.jpg. Accessed 10/1/2013.

- [10] Charles Z. and Benson S. *Pulsed Plasma Thruster (PPT)*. NASA Mission Technology Forum, 2001.
- [11] [Anonymous]. *CubeSat Design Specification (CDS)*. The CubeSat Program, California Polytechnic State University, 2012.
- [12] [Anonymous]. *Delfi-C3 - eoPortal Directory - Satellite Mission* [online] 2013. Available from: http://www.dk3wn.info/images/delfi_c3.gif. Accessed 10/1/2013.
- [13] Horisawa, Hideyuki, Masatoshi Kawakami and Itsuro Kimura. *Laser-assisted pulsed plasma thruster for space propulsion applications*. *Applied Physics A*, 2005.
- [14] J. J. Blandino, Cassady R. J. and Peterson T. T. *Pulsed Plasma Thrusters for the New Millennium Interferometer (DS-3) Mission*. American Institute of Aeronautics and Astronautics, 1997.
- [15] R.M. Mayers, L. A. Arrington, E. J. Pencil, J. Carter, J. Heminger and N. Gatsonis. *Pulsed Plasma Thruster Contamination*. American Institute of Aeronautics and Astronautics, 1996.
- [16] Lynn A. Arrington, Collen M. Marrese, John J. Blandino and R. J. Cassady. *Pulsed Plasma Thruster Plume Study: Symmetry and Impact on Spacecraft Surfaces*. American Institute of Aeronautics and Astronautics, 2000.
- [17] Gregory G. Spanjers, Jason S. Lotspeich, Keight A. McFall and Ronald A. Spores. *Propellant Inefficiency Due to Particulates in a Pulsed Plasma Thruster*. Air Force Research Laboratory (AFMC), 1997.

- [18] Nesmeyanov, A.N. *Vapour Pressure of the Elements*. Academic Press, New York. 1963.
- [19] Thomassen, Keith I. and Vondra, Robert J. *Exhaust Velocity Studies of a Solid Teflon Pulsed Plasma Thruster*. American Institute of Aeronautics and Astronautics, 1971.
- [20] Markusic, Thomas E and Spores, Ronald A. *Spectroscopic Emission Measurements of a Pulsed Plasma Thruster Plume*. American Institute of Aeronautics and Astronautics, 1997.
- [21] Ideal Vacuum Products. *TRIVAC B Rotary Vane Vacuum Pump Operating Instructions*, Leybold Vacuum [online] 2001. Available from: http://www.idealvac.com/files/manuals/Leybold_TRIVAC_D16B-D25B_Operating_Instruction_Manual_2.PDF. Accessed 10/10/2013.
- [22] Moore, J.H., Davis, C.C., Coplan, M.A. and Greer, S.C. *Building Scientific Apparatus*, ch. 3. Cambridge University Press, 2009.
- [23] Physical Electronics. *Technician's Low Profile Ion Pumps Component Manual* [online] 2000. Available from: http://uhv.cheme.cmu.edu/manuals/phi_ion_pump.pdf. Accessed 10/10/2013.
- [24] Tkachenko, Nikolai V. *Optical Spectroscopy Methods and Instrumentations*. Elsevier Science, 2006.
- [25] Lalane, J.R. François Carmona and Laurent Servant. *Optical Spectroscopies of Electronic Absorption*. World Scientific, 1999.

- [26] Ocean Optics. *HR4000 Installation and Operation Manual* [online] 2008. Available from:
<http://www.oceanoptics.com/technical/hr4000.pdf>. Accessed 10/10/2013.
- [27] Leybold Vacuum. TurboVac 361 Technical Data Sheet [online] 2006. Available from:
https://leyboldproducts.oerlikon.com/products/pics/FileResources/Orig/TD_Technische%20Daten/TD_85670_EN.pdf. Accessed 12/19/2013.
- [28] Leybold Vacuum. *TURBOVAC Operating Instructions* [online] 2006. Available from:
<http://www.idealvac.com/files/brochures/LeyboldTubo361OperatingInstructions.pdf>.
Accessed 12/19/2013.
- [29] Aerojet Engineers. *Aerojet Laboratory PPT-General Operating Procedure*, Aerojet Company, 2005.
- [30] Ocean Optics. *SpectraSuite Spectrometer Operating Software Installation and Operation Manual*, 2009.
- [31] National Instruments. *Bus-Powered USB Multifunction I/O Device NI USB-6008/6009* [online] 2012. Available from: <http://www.ni.com/pdf/manuals/375553a.pdf>. Accessed 01/19/2014.

APPENDICES

A.1 T4 System Modified Pump Down and Back Venting Procedure

Procedure A - T4 Pump-down Procedure

Step	Description
A1	Verify all sections of the T4 system are at atmosphere then close all valves.
A2	Ensure the system and all monitoring devices are powered. Ensure the CombiVac display is lit. If it is the switch box is also powered. Check that the VA2 display for G3 is powered and working.
A3	Check the oil level and cleanliness in the mechanical pump using the window on the front face of the Trivac D 16 B. (Should be between the top and bottom lines)
A4	Verify the compressed air supply is connected to the valve manifold and pressurized to 80psi.
A5	Make sure the following valves are closed: V3 (Ion Gate Valve), V4 (PT Turbo Gate Valve) and V6 (Back Venting Valve). Open the following valves: V1 (Main Gate Valve), V2 (PM Roughing Gate Valve), V5 (PT Foreline Valve) and V7 (PM Manual Block Valve).
A6	Using the switch panel start the mechanical pump by turning the rotary switch to the "Roughing Pump" position. All positions ahead of this will maintain power to the roughing pump.
A7	Monitor the chamber pressure using G1 and G4; monitor the foreline pressure with G3.
A8	When the chamber pressure is 375 mTorr or lower the TurboVac 361 can be turned on. If a ROR measurement is desired continue to step A9, else skip to step A10. If the user is familiar with operating the TurboVac 361, skip to step A11.
A9	ROR Procedure I. Continue pumping the chamber down to 50-100 mTorr. II. Close V1 (Main Gate Valve), record start pressure and start stop watch. III. Close V7 (PM Manual Block Valve). IV. Turn off the mechanical pump. V. After 5-15 minutes record the stop pressure and the duration. VI. Turn on the mechanical pump. VII. Open V7 (PM Manual Block Valve). VIII. Open V1 (Main Gate Valve). Once the ROR measurement is completed continue to step A10.
A10	<u>WARNING:</u> The TurboVac 361 requires careful consideration during pumping and back venting. Please bear the following in mind before continuing with this procedure. <ul style="list-style-type: none"> • Avoid impacts and vibrations while the TurboVac 361 is in operation (resonance). • Do NOT touch any part of the TurboVac 361 during operation, the temperatures on the surface of the pump can reach 120 deg C (248 deg F). • Longer back venting prolongs bearing service life and reduces dust/particulate

	<p>interaction with the rotors/stators in the TurboVac 361.</p> <ul style="list-style-type: none"> • Even though the Trivac D 16 B is equip with an anti-suck back valve, it is prudent to close V7 while back venting the TurboVac 361, or whenever the TurboVac 361 is being pumped on by the mechanical pump and the mechanical pump needs to be turned off, i.e. for a ROR measurement (See step 9). <p>Continue to step 11 once this step has carefully been reviewed.</p>
A11	Open V4 (PT Gate Valve).
A12	Close V2 (PM Roughing Gate Valve).
A13	Plug the PT cooling unit into the power strip located below the hoist side of the T4 system. Confirm that the cooling unit is functioning before proceeding to step 14.
A14	<p>Turn the rotary switch on the switch panel to the “Turbo” position.</p> <p>This provides power to the TurboTroniks controller as well as the roughing pump. Confirm that all LEDs turn on and then off after a few seconds, with the exception of the green “POWER” LED and the yellow “ACCEL” LED, both of which should remain lit. After the pump has reached 80% of its acceleration (couple minutes) the green “NORMAL” LED will light up and the yellow “ACCEL” LED with turn off. (For some reason the TurboVac 361 starts accelerating when the rotary switch is turned to the “Turbo” position, instead of after pressing the “START” button on the TurboTroniks controller)</p> <p><u>WARNING:</u> The acceleration period of the TurboVac 361 cannot exceed 30 minutes without being subjected to a 25 minute cool-down period. This is not an issue as long as the TurboVac 361 is turned on at pressures at or below the conservative estimate of 375 mTorr.</p>
A15	Once the pressure on the CombiVac display drops to 5E-4 Torr the 572 Ionization Gauge must be turned on to continue measuring the chamber pressure. To turn on the 572 IG press “Enter” than “Emis” on the VA2 senTorr Gauge Controller.
A16	<p>Once the desired chamber pressure is achieved the system is ready for experimentation.</p> <p>Please refer to Procedure B if the user desires to keep the chamber under pressure.</p> <p>Please refer to Procedure D if the user desires to vent the T4 system to atmosphere.</p>

Procedure B – Shut Down (T4 under Vacuum)

Step	Description
B1	Press “STOP” on the TurboTroniks Controller to power down the TurboVac 361.
B2	Unplug the cooling unit for the TurboVac 361.
B3	Close V7 (PM Manual Block Valve).
B4	Turn off the PM and power to the TurboTroniks Controller by moving the rotary switch to the “OFF” position.
B5	Turn off the 572 IG by pressing “emis” on the VA2 senTorr Gauge Controller.
B6	Follow Procedure C when reinitiating pump down of T4 from the shutdown state.

Procedure C – Start Up (from shut down state)

Step	Description
C1	Turn on the PM and power to the TurboTroniks Controller by moving the rotary switch to the “Roughing Pump” position.
C2	If the CombiVac Display Pressure is > 375 mTorr, return to step A5 .
C3	If the CombiVac Display Pressure is < 375 mTorr, Open V7 (PM Manual Block Valve) and return to step A13 .

Procedure D – T4 Back Venting

Step	Description
D1	If T4 is in a vacuum state with pumps operating, continue to step D2. If T4 is in the shutdown state, skip to step D6.
D2	Press “STOP” on the TurboTroniks Controller to power down the TurboVac 361.
D3	Unplug the cooling unit for the TurboVac 361.
D4	Close V7 (PM Manual Block Valve).
D5	Turn off the PM and power to the TurboTroniks Controller by moving the rotary switch to the “OFF” position.
D6	Open V6 (Back Venting Valve) one half turn.
D7	Using G3 to monitor the pressure in the foreline, back vent the system such that the pressure rises from about 7.5 mTorr to 760 Torr over 1 minute, or longer. Prolonging the back venting of the TurboVac 361 will increase bearing service life.
D8	Once the TurboVac 361 is vented to atmosphere close valves V4 (PT Valve) and V5 (PT Foreline Valve).
D9	Close V1 (Main Gate Valve)
D10	Close V6 (Back Venting Valve)

EMERGENCY: If an emergency shutdown is required, refer to steps D1-D5. If back venting is also required as a result of an emergency, continue through steps D6-D8.

A.2 T4 Leak Detection Procedure and Data Sheet

T4 Leak Detection and ROR Measurement Procedure

- 1) Measure the initial Rate-of-Rise (ROR) time for the T4 system and record this on the “0th” line of the T4 Leak Detection Data Sheet. Refer to steps 10 through 12 of this procedure if the user is unfamiliar with the ROR measurement process.
- 2) Verify new NW-50 blank and NW50 Centering Ring w/ Viton O-ring sets are available. Verify ample supply of KimWipes and alcohol for cleaning port flange equipment.
- 3) Confirm there are no pressure differentials present in the T4 system.
- 4) Remove the flange and equipment from port #01 on the collar.
- 5) Make sure the replacement blank and O-ring pair, and the port #01 face are wiped down using KimWipes moistened with alcohol. Apply vacuum grease to the O-ring. Vacuum grease must be used sparingly so that the replacement O-ring is covered with a tacky film.
- 6) Attach primed blank and O-ring to port #01 with the flange and confirm a secure connection.
- 7) Begin pumping T4 as outlined in the T4 Pump Down, Shut Down, and Back Venting procedure (Appendix A.1).
- 8) Clean and reapply vacuum grease to the original equipment from port #01 while the T4 system is roughing down. Record observations for each of the old flange/O-ring pieces, i.e. "In regards to port #13 there is a tear in the O-ring and that's one source of leaking in the system".
- 9) Rough down T4 until the pressure stops decreasing.
- 10) Record “Start Pressure” on the data sheet.

- 11) Close the Main Gate Valve and start the stop watch.
- 12) Wait 2 minutes, or longer if ROR time is slowing down, and record the stop pressure and duration on the data sheet.
- 13) Calculate the ROR, enter it on the data sheet and compare to the previous value.
- 14) Vent T4 to atmosphere.
- 15) If the ROR decreases continue to step 16. If the ROR is unchanged skip to step 17.
- 16) Make a note of the decreased ROR in the T4 lab notebook and repeat steps 9-14 with the original port #01 equipment. Compare this ROR from the original equipment to the ROR from the replacement parts. If the replacement ROR is lower than the original equipment ROR it may be necessary to permanently replace the original equipment with 1 of the 2 NW50 replacement sets.
- 17) Repeat the entire procedure for port #02, until all ports have been tested or the ROR time falls to an ideal level of 5 mTorr/min averaged over 5 minutes.

Date: _____

ROR Measurement Data Sheet

Flange Position #	Start Pressure (Torr)	Stop Pressure (Torr)	Duration (s)	Rate-of-Rise (Torr/s)	Performed By:
0					
1					
1a					
2					
2a					
3					
3a					
4					
4a					
5					
5a					
6					
6a					
7					
7a					
8					
8a					
9					
9a					
10					

10a					
11					
11a					
12					
12a					
13					
13a					
14					
14a					
15					
15a					
16					
16a					
17					
17a					
18					
18a					

A.3 MTU Operational and Safety Procedures

WARNINGS:

- Upon application of >22 V to the main input and 5 V to the main CMD inputs, there will up to 2KV on the anode electrode of the PPT
- While the DI circuits can be charged and fired in air, do not fire the PPT in air (anode electrode is at lethal voltage, discharge has currents ~ 20 kA – basically incompatible with humans)
- It is critical that the polarity of the input power be correct!!! Reverse polarity can cause PPU damage! There is a reverse polarity diode that will allow current to flow in reverse until the diode fuses. When applying input voltage initially, watch for current greater than 100 mA. If noted, shut off immediately and check input power polarity!

Procedure

The procedure below includes several sections (highlighted in yellow) which should be performed in order to assess functionality and detect faults before proceeding to the next section of the procedure. The figures below correspond to the power supply (PS), the modular test unit, pulsed plasma thruster (PPT), the user Interface Box (IBOX), and laboratory facility (earth) ground (FGND).

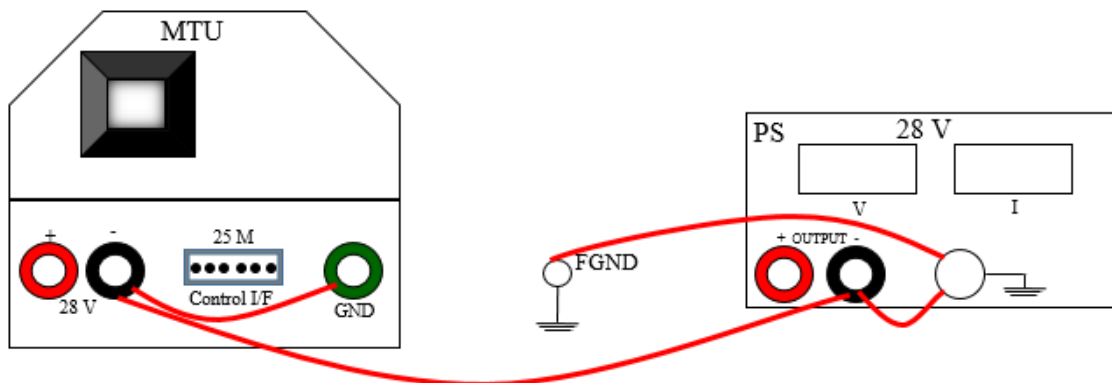
Steps that involve making or breaking electrical connections are also illustrated with simplified icons. The convention in these figures is that any connections made in that step are shown as solid red lines. Connections broken in that step are shown as dashed red lines, and connections existing from a previous step are shown as solid black lines.

The power supply being used should have capability of voltage and current control (with either an analog or digital readout), and have a maximum voltage of at least 28 V and a maximum current of at least 100 mA.

It is also assumed that the user has verified that the primary capacitor is installed in the PPT and that the high current lead lines on the PPT (banana jacks with braided shield) are connected.

Checkout/Set-Up (either bell jar or on bench top)

- 1) Verify that the power supply (PS) is floating or at least floatable – i.e. the negative side should be isolated from power ground. (Check for strap between facility (earth) ground (FGND) and the power supply (PS) ground terminals; if found, this grounding strap should be disconnected)
- 2) Make some sort of direct connection from the (28V) power supply negative to the PPT chassis ground. Either provide a jumper with a banana plug cable from the negative power input on the PPT to the PPT chassis ground, or provide a jumper from the power supply (ground or negative) to the PPT chassis ground. Then ground the power system in (only) one location, by connecting to a facility (earth) ground (FGND) point such as a bus bar if available. The point here is to have a single connection to earth ground that is connected to both the PPT chassis and the negative side of the PPT power input.

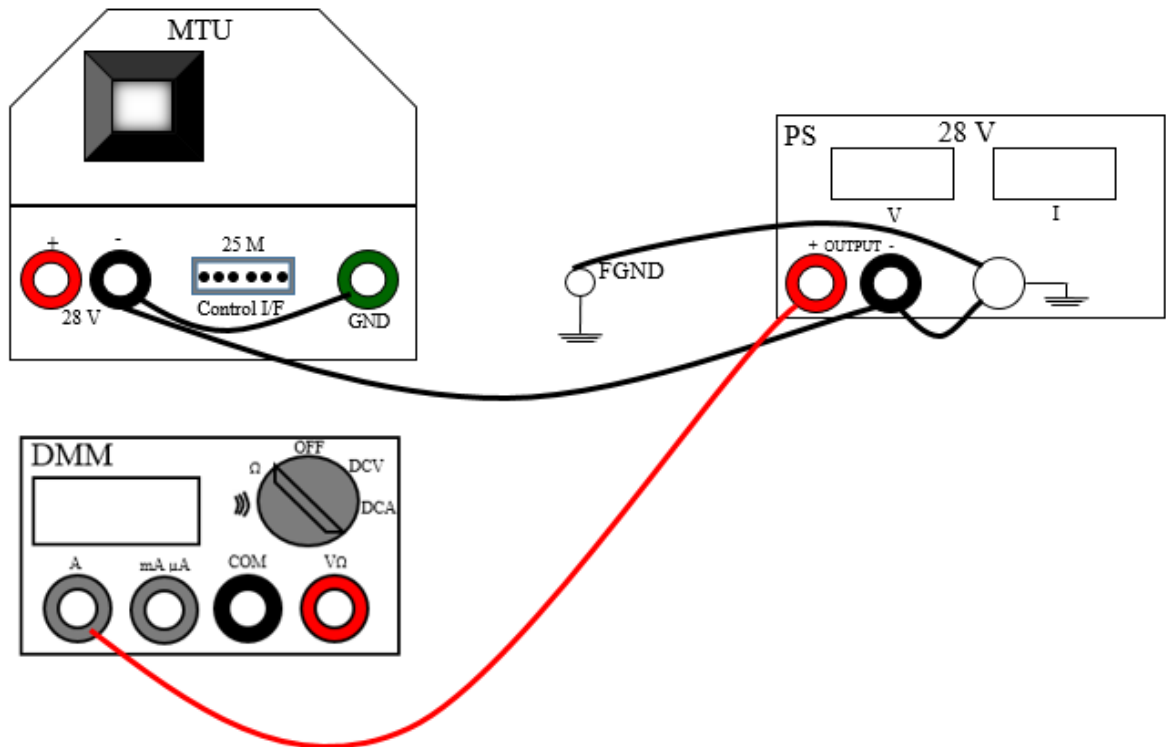


- 3) Ensure that the chassis of the PPT is grounded. (see step 2)
- 4) ~~Snap a suitable split core EMI bead around the customer control cable to the D-sub connection. Verify that the EMI beads are on the cap charging cable and the spark plug cable.~~

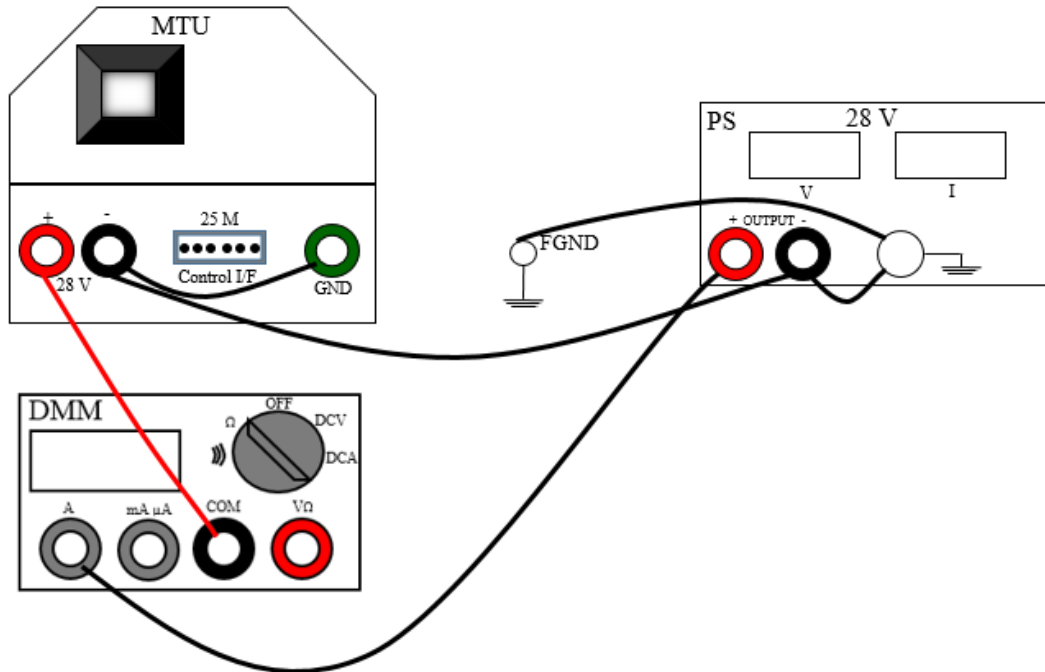
5) Connect a lead from the negative of the power supply to the negative input to the Interface Box (IBOX).

6) Check the standby current:

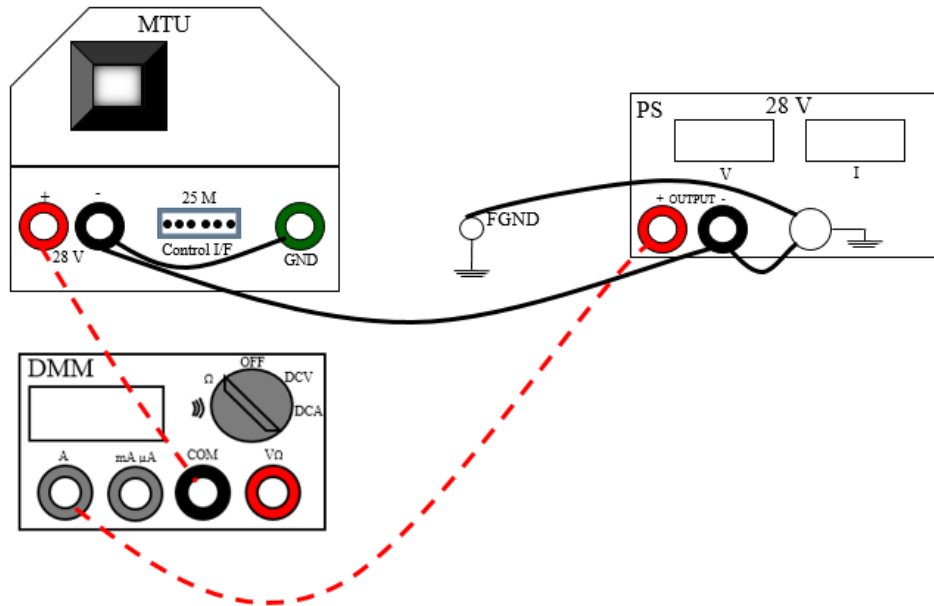
a) Connect a banana lead from the positive of the power supply to the 10 A input of the handheld digital multimeter (DMM).



b) Connect a banana lead from the com (or negative) jack of the handheld DMM to the positive input of the PPT. This arrangement puts a current meter (ammeter) in series between the power supply and the PPT. set the DMM to read DC Amps.



- c) Turn the PS voltage limit all the way down and turn on the power supply.
 - d) Turn the power supply current limit setting to ~ 0.1 A or greater.
 - e) Turn the power supply voltage limit up to 28 V ± 1 V.
 - f) The current being drawn by the PPT should be 40 mA ± 5 mA. If it significantly different, there may be a fault in the PPT electronics – disconnect if current is greater than 100 mA.
 - g) Turn down the voltage limit to zero.
- 7) Disconnect the leads to the DMM.



8) Turn off the power supply

Spark Plug Checkout

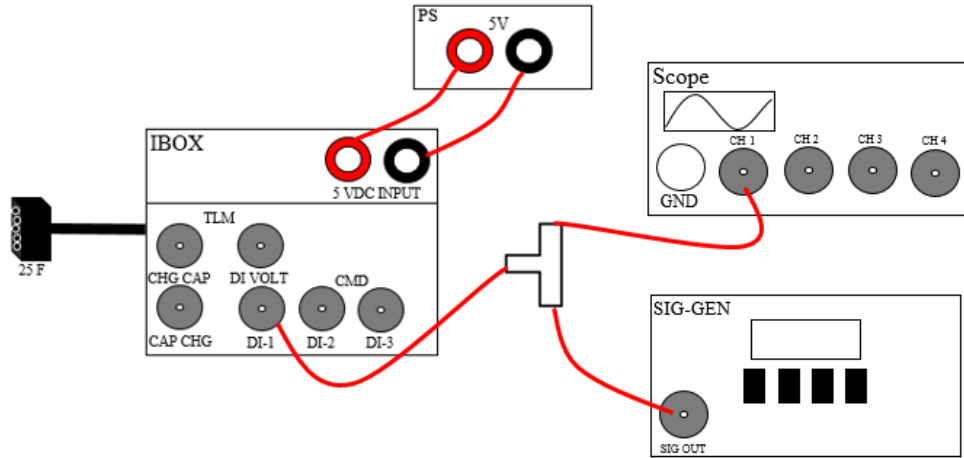
9) Verify installation of input power lines on the PPT. Note that the Red banana jack socket is positive. Be careful to assure that the polarity of the input power lines is correct.

If EMI protection is going to be used for the “control” cables, snap a suitable split core EMI bead around the control cable to the D-sub connection, the cap charging cable, and the spark plug cable.

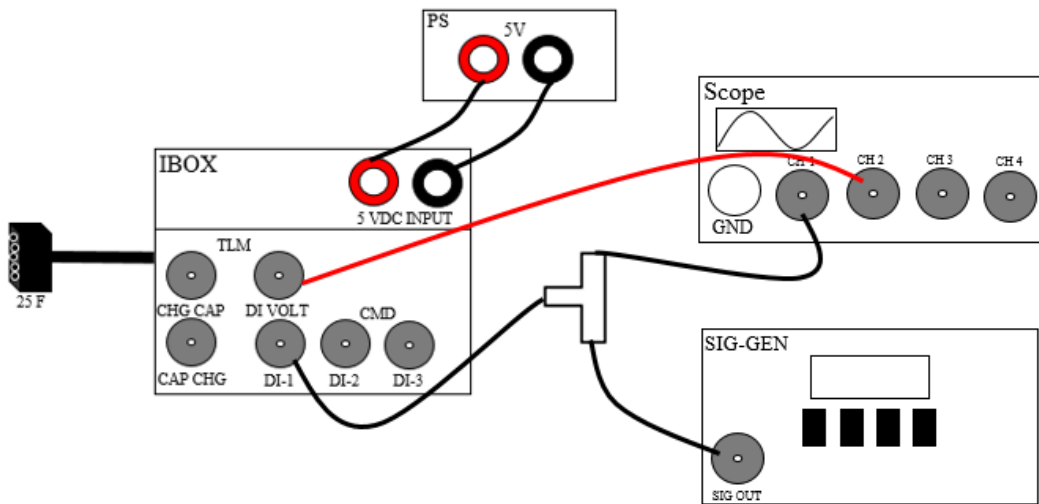
Provide power to the Interface Box (IBOX) using any standard, 5V DC power supply.

10) If the PPT is not in the vacuum chamber, connect a voltage probe (at least 100:1) across the main capacitor and monitor on a scope, along with the input of the command signal.

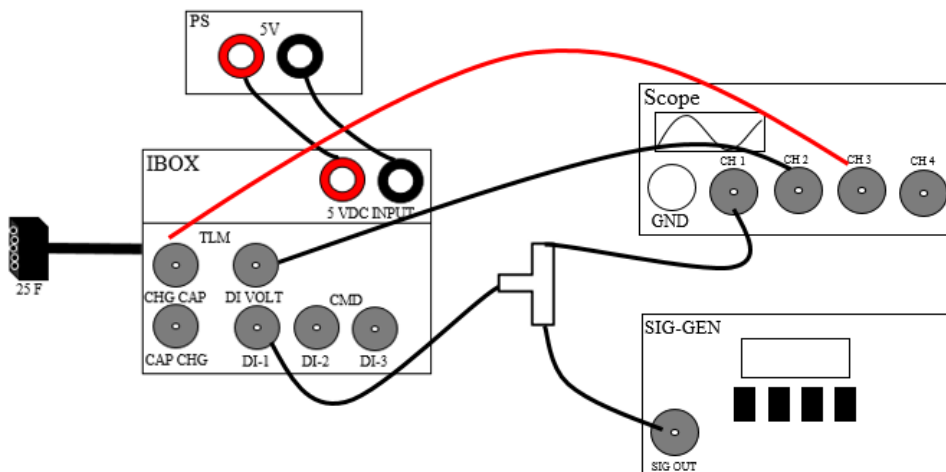
11) Connect signal generator with a BNC “Tee” connector to channel one of a scope and to the DI#1 CMD connector on the IBOX.



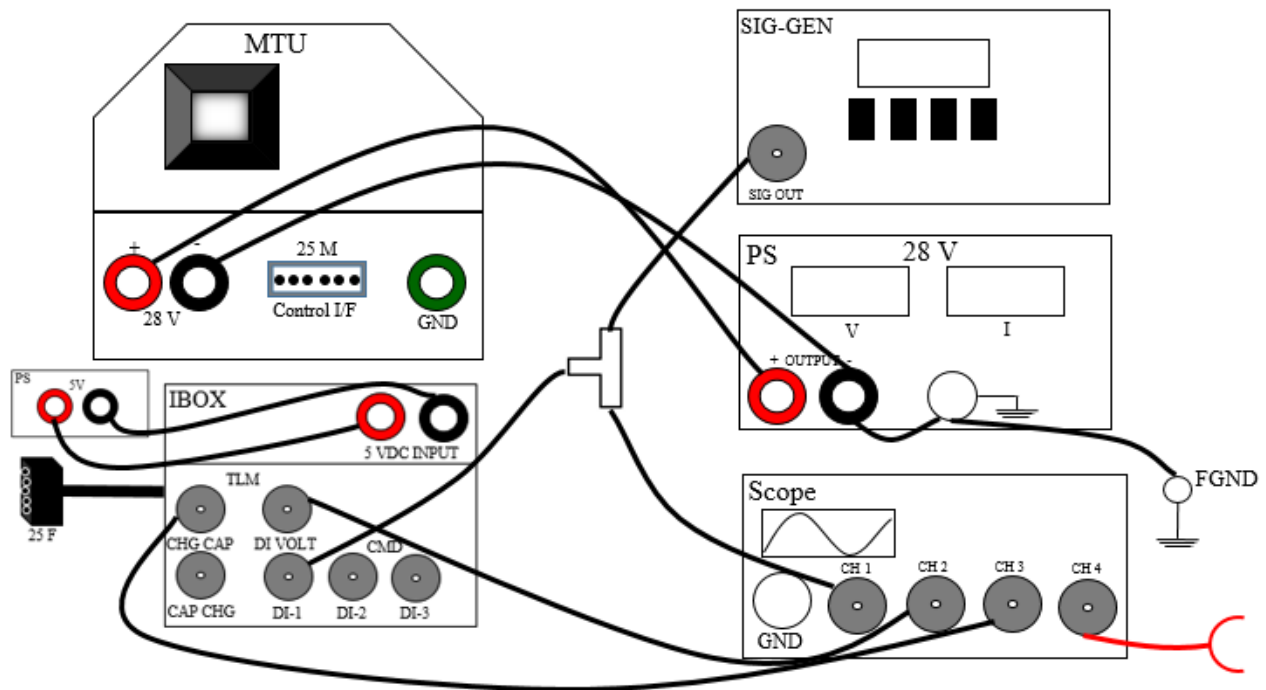
12) Connect DI V TLM to channel two of the scope (0-5 V expected).



13) Connect Cap V TLM to Channel three of the scope (0-5 V expected).



14) Connect a current probe around the positive lead from the power supply to the PPT and monitor on a scope.



15) If using the PPT Interface Box (IBOX), ensure that the box is set to “Independent commands”. Otherwise, connect a command line (from signal generator) only the DI circuit command (choose DI#1).

16) Verify connection of BNC cable from signal/pulse generator to the DI-1 jack (Step 11). The pulse generator should be able to put out 5 V for 920 ms in a single pulse mode.

17) Turn the voltage limit back up to 28 V. Turn the current limit up to ~1 A.

18) Trigger a single pulse and observe the spark at the spark plug. The spark should be blue white.

If it is orange, something is not right. The input current draw is relatively small (i.e. <math><0.25\text{ A}</math>), but easily measurable. You should observe:

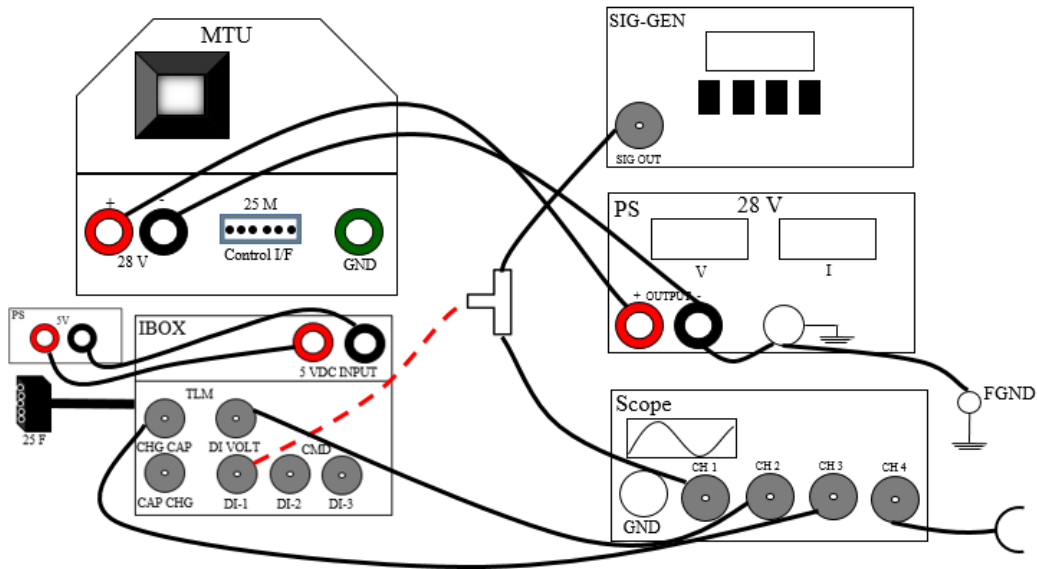
- DI V TLM rising to >4 V within ~600 ms of beginning of pulse and failing to zero at the end of the pulse

- A pulse on the sparkplug (likely will not be visible from the outside of the chamber)
- NO voltage on the main capacitor

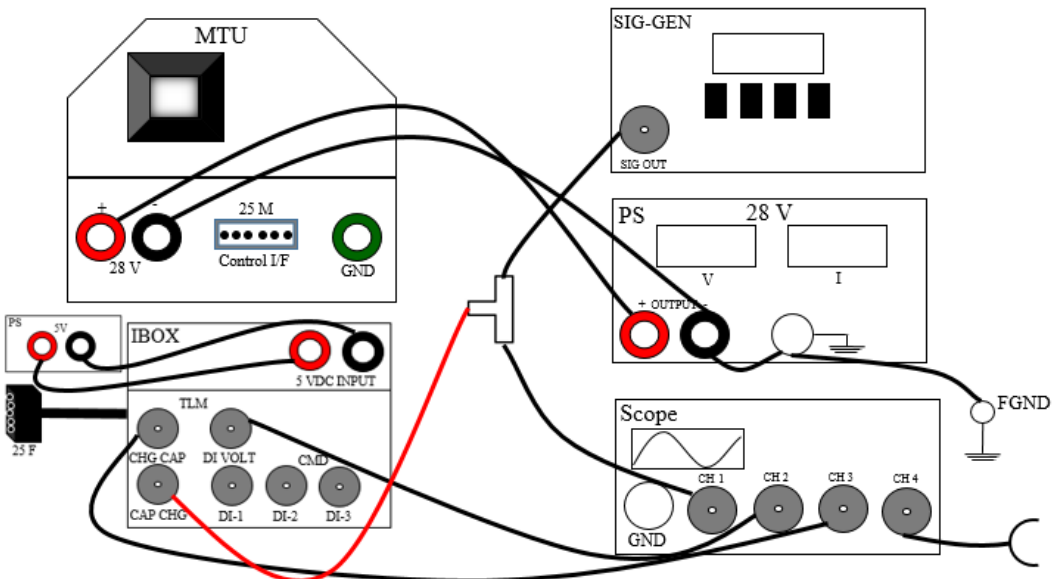
19) Turn off the power supply

Capacitor Charge

20) Disconnect the BNC cable from the DI-1 jack



21) Connect the BNC cable (from the signal generator) to the Capacitor charge BNC on the Interface Box (IBOX).



- 22) Turn on the power supply, set the current limit to 4 A.
- 23) Trigger a single pulse and observe the main discharge capacitor voltage. The appropriate voltage at the end of the charging command pulse is 1530 V (1 V TLM = 402 Cap V ...so TLM V should be 3.8V).
- 24) Remove any residual charge on the main capacitor. Either allow the voltage to bleed off over ~ 10 minutes (bleeds through the 5 M Ohm internal feedback resistor) or use an external resistive load.

Main Discharge

- 25) If not already connected, with another BNC Tee connector, connect the signal generator to the Cap Charge CMD
- 26) Try firing pulse. Should see:
 - 1530 V (3.8 V on the cap V TLM) on the capacitor prior to discharge
 - DI V TLM risking to >4 V within ~600 ms of the beginning of the pulse and failing to zero at the end of the pulse.
 - PPT discharge! Typically plume color is bluish-purple.

Autonomous Operation

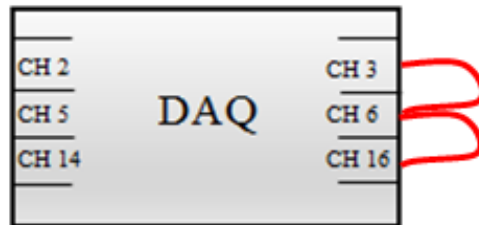
- 27) Turn off power supply
- 28) Set signal generator to provide a periodic square wave pulse of 920 ms (+/- 50 ms) 5V on, and off as long as desired to achieve the desired pulsing frequency.
- 29) Turn on power supply – verify limits at 22V, 4 A
- 30) Start square wave from signal generator.
- 31) Run as long as desired

While running, monitor:

- Main transformer temp. (should be less than 125 deg. C)
- IGBT temp (should be less than 125 deg. C)
- Main capacitor temp. (should be less than 50 deg. C)

Operation Using LabVIEW Interface

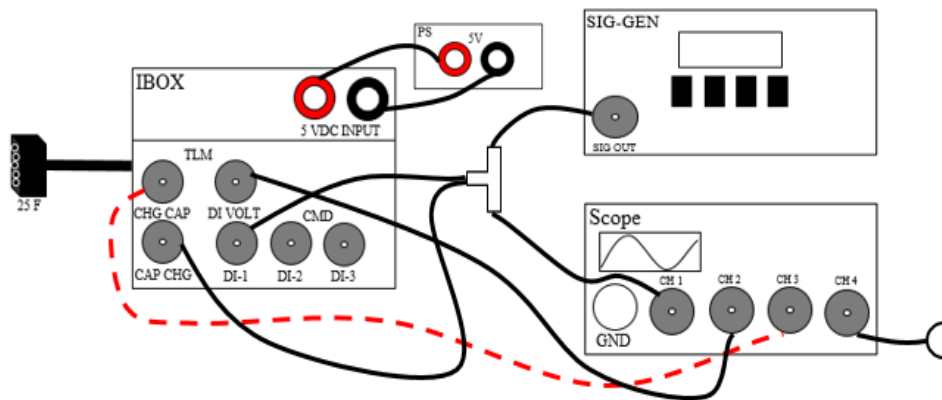
32) Alternatively to step 27, the MTU can be run with the LabVIEW VI. To have the DAQ ready for operation, Connect Pins 3 and 6 to Pin 16 (GND).



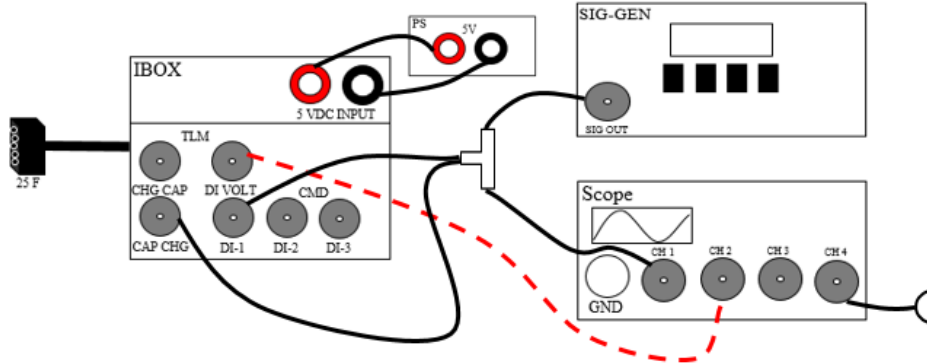
33) Turn off the Scope, Power Supply, and Signal Generator

34) Disconnect the following IBOX connections:

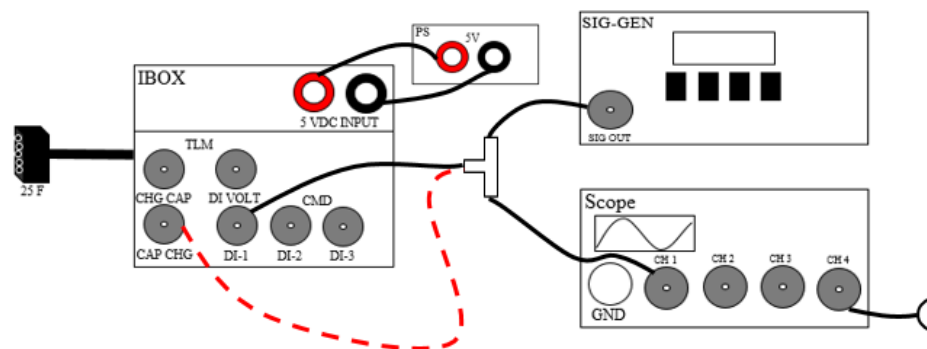
- TLM Chg Cap



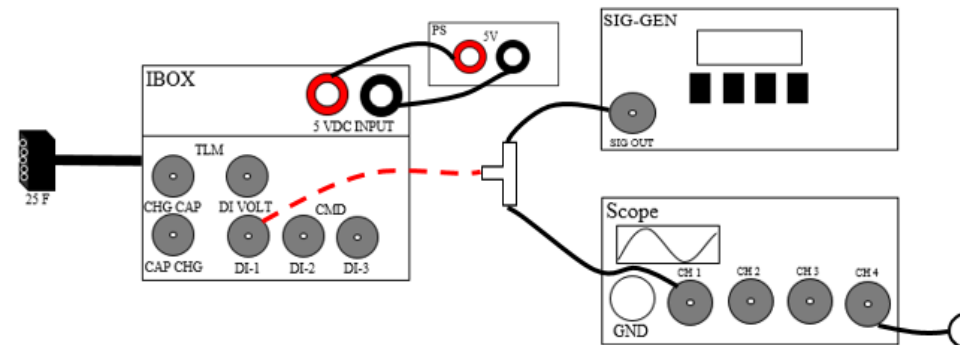
- TLM DI Volt



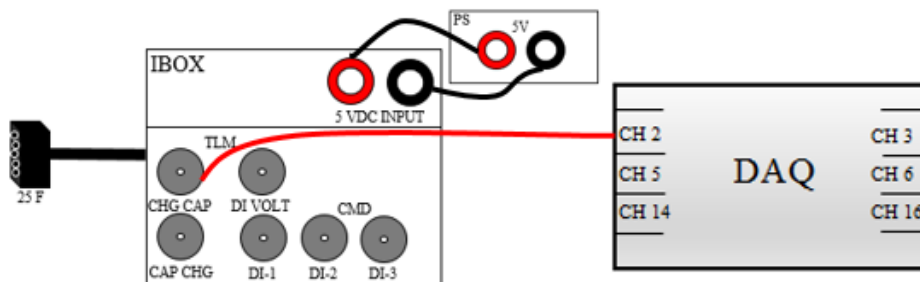
c. CMD Cap Chg



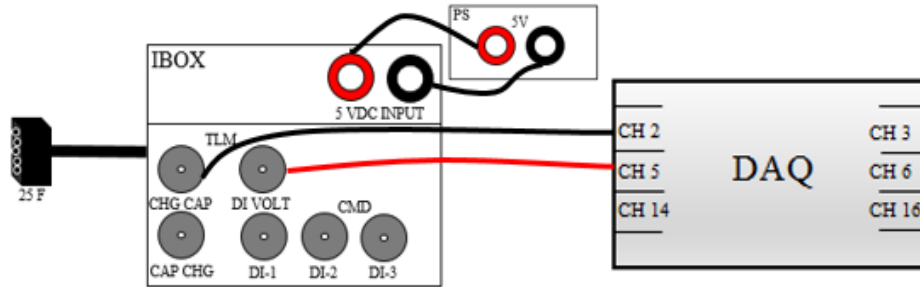
d. CMD DI-1



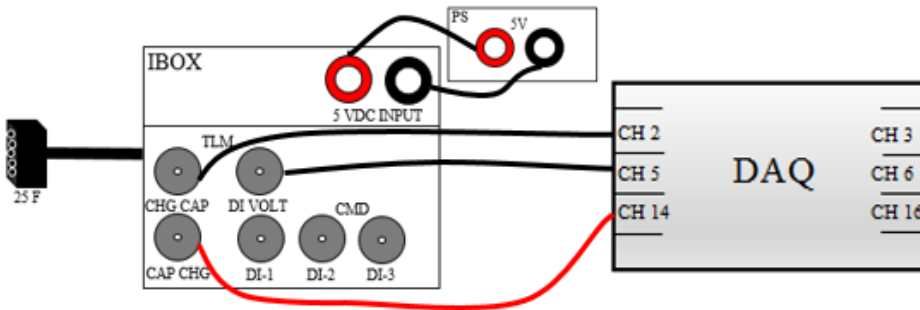
35) Connect TLM Chg Cap to DAQ Pin 2



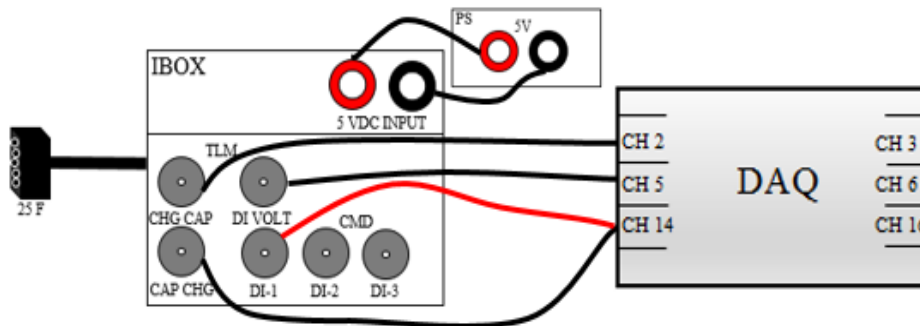
36) Connect TLM DI Volt to DAQ Pin 5



37) Connect CMD Cap Chg to DAQ Pin 14



38) Connect CMD DI-1 to DAQ Pin 14



39) Set the slider (H) to the desired bit level

40) Flip the bit switches on the MTU interface according to which lights turn on (I) to the UP position.

41) Turn on power supply-verify limits at 22V, 4A

42) Set the slider shown in the figure below (part A) to the desired continuous firing duration.

Alternatively, the number of seconds (20 sec max) can be entered in the text field located below the slider.

43) Start the VI by pressing the arrow button (B)

- 44) Set the knob (C) to the desired pulse rate (number of pulses per second), or 0 for single shot operation (skip to step 5). Alternatively, the value can be entered underneath the knob, with accuracy up to 0.01 Hz.
- 45) Activate the switch (D) to start firing at the pulse rate entered in step 3 for the duration set in step 1. Once the firing duration has been reached, the VI will cease sending signals to the MTU.
- 46) For single shot operation, press the single shot button (E) to send a signal to the capacitor to fire.
- 47) In case of emergency, hit the ABORT button (F).
- 48) When done using the VI press the STOP button (G).

15pt Application Font

B. Arrow Button

G. Stop button

C. Knob

A. Slider

F. Abort Button

E. Single-Shot Button

H. Bit Slider

I. Bit Switch Lights

Spark Plug

Capacitor Charge

Fire Command

Number of Pulses per Second

Duration of Experiment (sec)

Period (s)

Number of Pulses

Duty Cycle (%)

MTU Interface Bit Level

MTU Interface Bit Level

ABORT

Single Pulses

Single Shot Fire

3 2 1 0

Aerojet Lab PPT Electrical Interface

Power In: 28 ± 6 V DC banana jack sockets, RED is positive, BLACK is negative

NOTE: IT IS CRITICAL THAT THE POLARITY OF THE INPUT POWER BE CORRECT!!!

REVERSE POLARITY CAN CAUSE DAMAGE! THERE IS A REVERSE POLARITY
DIODE WHICH WILL ALLOW CURRENT TO FLOW IN REVERSE UNTIL THE DIODE
FUSES. WHEN APPLYING INPUT VOLTAGE INITIALLY, WATCH FOR CURRENT
GREATER THAN 100 MA. IF NOTED, SHUT OFF IMMEDIATELY AND CHECK INPUT
POWER POLARITY!

Command/Telemetry: 15 to 25 Sub-D Connection Pin Assignments, adapted from Aerojet Corp.

25-Pin Sub-D	15-Pin Sub-D	15-Pin Sub-D	25-Pin Sub-D	Assignment	Comment
Outside (air-side)		Inside (vacuum-side)			
1	1	8	1	Cap Charge TLM	Scale 0-5 V, 1V TLM= 402 Cap V
2	2	7	2	Cap Charge TLM RTN	
3	3	6	3	D.I Voltage TLM	Scale 0-5 V, 1V TLM= 159 SP V
4	4	5	4	D.I Voltage TLM RTN	
5	5	4	5	D.I #1 Fire TLM	Scale 0-5 V, 1V TLM= 159 SP V
6	6	3	6	D.I #1 Fire TLM RTN	
12	7	2	12	Cap Charge Command	+5 V square wave (500 mS minimum duration) - leading edge starts charge - can be combines with pin 14 (to synchronize cap and D.I. charging/firing)
13	8	1	13	Cap Charge Command RTN	
14	9	15	14	D.I #1 Fire Command	+5 V square wave - starts charging sparkplug cap on leading edge - fires on trailing edge - can be combines with pin 12 (to synchronize cap and

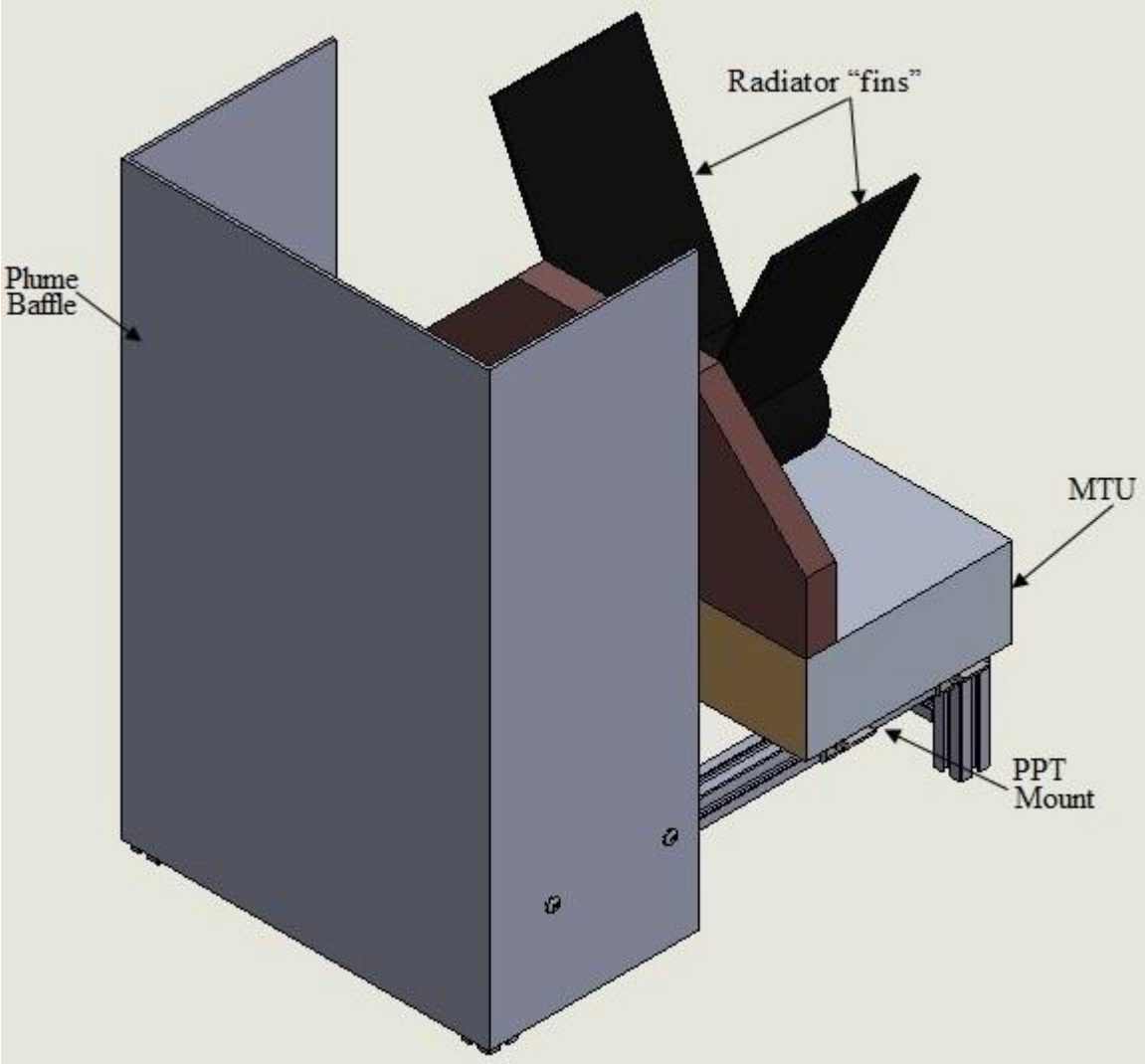
					D.I. charging/firing)
15	10	14	15	D.I #1 Fire Command RTN	
21	11	13	21	Bit '0'	These bits were used to set the logic to set the capacitor charge voltage. They were hard wired in order to provide 40-Joule operation. So, these pins were not used.
22	12	14	22	Bit '1'	
23	13	11	23	Bit '2'	
24	14	10	24	Bit '3'	
25	15	9	25	Bit RTN	

Other Interfaces:

Capacitor current Rogowski coil: BNC connector (socket side). This Rogowski coil is mounted around the center conductor of the main capacitor to monitor capacitor current. This has been calibrated – I still need to dig up the notes on this calibration – this is still coming.

Four type K thermocouples: These monitor transformer, MOSFET, main capacitor and other electronics. More information coming on thermocouple assignments and temperature limits.

A.4 CAD Drawing of PPT Mount and Plume Baffle



A.5 LabVIEW VI Instructions to Control PPT Pulse Energy and Repetition Rate

LabVIEW VI Instructions

1. Set the slider shown in the figure below (part A) to the desired continuous firing duration. Alternatively, the number of seconds (20 sec max) can be entered in the text field located below the slider.
2. Start the VI by pressing the arrow button (B)
3. Set the knob (C) to the desired pulse rate (number of pulses per second), or 0 for single shot operation (skip to step 5). Alternatively, the value can be entered underneath the knob, with accuracy up to 0.01 Hz.
4. Activate the switch (D) to start firing at the pulse rate entered in step 3 for the duration set in step 1. Once the firing duration has been reached, the VI will cease sending signals to the MTU.
5. For single shot operation, press the single shot button (E) to send a signal to the capacitor to fire.
6. In case of emergency, hit the ABORT button (F).
7. When done using the VI press the STOP button (G).

Binary Calculator Instructions

1. Set the slider (H) to the desired bit level
2. Flip the bit switches on the MTU Interface Box according to which lights turn on (I) to the UP position.

15pt Application Font

B. Arrow Button

G. Stop button

C. Knob

A. Slider

F. Abort Button

E. Single-Shot Button

H. Bit Slider

I. Bit Switch Lights

Spark Plug

Capacitor Charge

Fire Command

Number of Pulses per Second

Duration of Experiment (sec)

ABORT

Continuous Pulses

Single Pulses

Single Shot Fire

MTU Interface Bit Level

MTU Interface Bit Level

Bit Switch Lights

A.6 Wiring Diagram for the LabVIEW VI

